Characterization of HIV-1 Proviral Latency Induced Through APOBEC3 Mutagenesis and Reverse Transcriptase Error

Matthew Greig

A Thesis Submitted in Partial Fulfillment of the Requirements for the Master's Degree in Microbiology and Immunology.

Dr Marc-André Langlois

Microbiology and Immunology Graduate Program
Faculty of Science
University of Ottawa

Abstract

Human Immunodeficiency Virus 1 (HIV-1) is a lentivirus that forms persistent latently infected reservoirs that are the remaining major hurdle for current HIV-1 treatments. APOBEC3 (A3) proteins are intrinsic retroviral restriction factors that introduce G→A mutations during reverse transcription, while Reverse Transcriptase (RT) introduces on average 2-3 mutations every reverse transcription cycle due to a lack of proofreading ability. The goal of this research is to characterize the infectivity and activation of mutated HIV-1 viruses that display reduced transcription upon infection, viruses that we term latency prone viruses (LPVs). We hypothesize that G→A transition mutations in the HIV-1 Long Terminal Repeat (LTR) region of the LPVs introduced through Reverse Transcriptase and low levels of A3 protein activity can create HIV-1 sequences that display a reversible, latency-like phenotype. Variable levels of transcription and promoter activation were seen among the LPVs when tested against four classes of Latency Reversing Agents (LRAs). Subsequently, three tested LPVs demonstrated an initial latency-like phenotype before rebounding in infectivity. This project demonstrates for the first time that HIV-1 latency is not simply a byproduct of the infection timing and cellular conditions, but that replication-competent HIV-1 latent viruses can also be created through sublethal mutagenesis of their viral promoter sequence introduced through A3 and RT exposure. The characterization of the complete mechanism of HIV-1 latency induction, maintenance, and reversal is critical in the development of sterilizing and functional cures for HIV-1 infection.

Acknowledgements

I would like to personally thank Dr. Marc-André Langlois for offering me the opportunity to work in his laboratory during the past three years and always being available for troubleshooting, recommendations, and advice. Thank you to Dr. Tyler Renner for the supervision and patience with my constant questions and guidance. Thank you to Anna Fritzsche and Dr. Vera Tang specifically for their expertise in flow cytometry analyses, as well as Dr. Joanne McBane for conducting the majority of the early experimental troubleshooting. Thank you to Tasneem Abbas for assistance on cloning preparation, and to Mariam Maltseva and Andrew Norrie for making every day in the lab more enjoyable than the last. Finally, this project would not have been possible if not for the tireless work of Cindy Lam who provided all the hard work in the development of the LPV library.

Table of Contents

List of Figures

List of Tables

List of Abbreviations

AIDS: Acquired Immunodeficiency Syndrome

AP-1: Activator protein 1

APOBEC3/A3: Apolipoprotein B mRNA editing enzyme, catalytic protein-like 3

CA: Capsid protein

cART: Combinatorial anti-retroviral therapy

CD4: Cluster of differentiation 4

CCR5: C-C chemokine receptor type 5

CTL: Cytotoxic T lymphocyte

CXCR4: C-X-C chemokine receptor type 4

Env: Envelope protein

Gag: Group-specific antigen

HAT: Histone acetyltransferase

HDAC: Histone deacetylase

HMT: Histone methyltransferase

HIV-1: Human Immunodeficiency Virus Type 1

IN: Integrase enzyme

LPV: Latency prone virus

LRA: Latency reversing agent

LTR: Long terminal repeat

MA: Matrix protein

MFI: Mean fluorescence intensity

mRNA: Messenger ribonucleic acid

NC: Nucleocapsid protein

Nef: Negative regulatory factor

NFAT: Nuclear factor of activated T-cells

NF-κB: Nuclear factor kappa-light-chain enhancer of activated B cells

PIC: Pre-integration complex

PKA: Protein kinase A

PKC: Protein kinase C

Pol: Polymerase

PR: Protease enzyme

PTB: Polypyrimidine tract binding protein

Rev: Regulator of expression of virion proteins

RNA Pol II: RNA Polymerase II

RT: Reverse Transcriptase

SIV: Simian Immunodeficiency Virus

Sp-1: Specificity protein 1

STAT5: Signal transducer and activator of transcription 5

SU: Surface protein

TAR: Trans-activation response element

Tat: Trans-activator of transcription

TM: Transmembrane protein

TSS: Transcription start site

Vif: Viral infectivity factor

Vpr: Viral protein R

Vpu: Viral protein U

+ssRNA: Positive sense, single stranded RNA

Introduction

Discovery of HIV-1

Acquired Immunodeficiency Syndrome (AIDS) was first identified as a novel disease in 1981 when increasing numbers of men in the gay community began dying from opportunistic infections (1). Human Immunodeficiency Virus-1 (HIV-1) was identified two years later as the causative pathogen behind this quickly spreading disease (2). HIV-1 spread through sexual, perinatal, or percutaneous routes, however 80% of new infections were through mucosal surfaces and thus HIV-1 was subsequently classified as primarily a sexual disease (3, 4). Since the original isolation of HIV-1, four groups have since been identified: M, N, O, and P. M is the 'major' pandemic viral group, responsible for more than 75 million infections and 32 million deaths since the beginning of the pandemic (4, 5).

HIV-1: The Physical Virus

Structure of Virus

Genome

HIV-1 is a 9.7 kilobase long, positive sense, single-stranded RNA (+ssRNA) virus of the Retroviridae family and Lentivirus genus (6, 7). HIV-1 consists of a nucleocapsid (NC) containing two identical copies of its viral genome which code for nine genes, surrounded by a bullet-shaped capsid core, and finally a spherical bilipid envelope containing viral envelope (Env) proteins (8, 9).

Protein Encoding

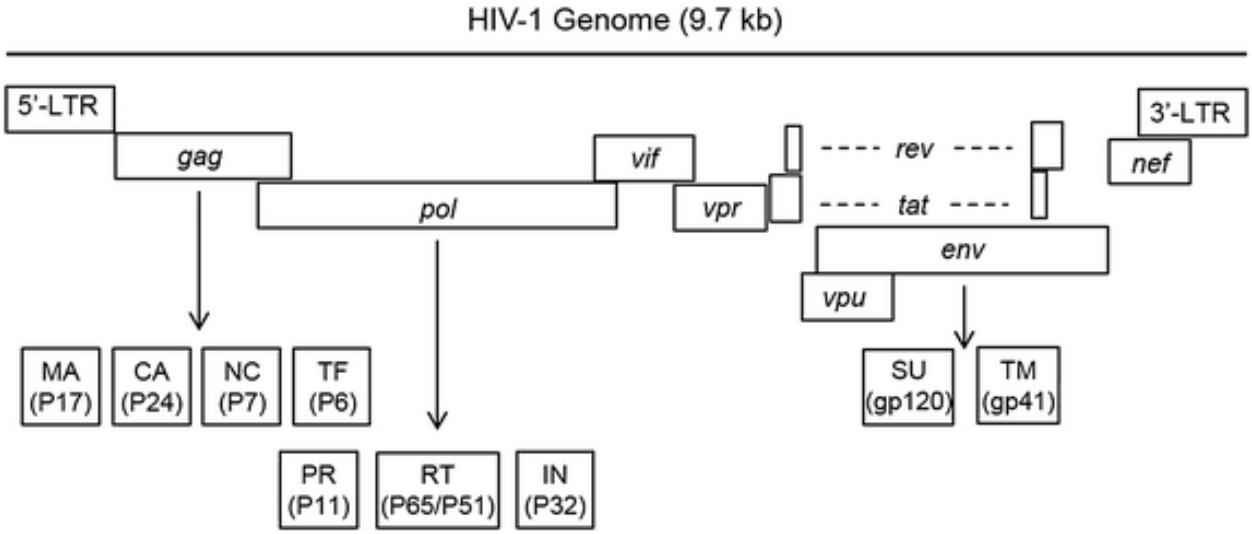

Figure 1. Schematic of the HIV-1 Genome. *Figure reproduced from (10) through Open Access.*

Although the genome of HIV-1 contains nine open reading frames, the virus actually codes for 15 proteins due to polyprotein splicing and alternative splicing of RNAs (11, 12). The three open reading frames of group-specific antigen (Gag), polymerase (Pol), and Envelope (Env), code for polyproteins which are proteolyzed into nine individual proteins (12–15). Of the remaining six proteins, only Vif, Vpr, and Nef are found within the viral particle. Tat and Rev play intracellular roles in regulating gene expression during viral transcription and replication, while Vpu aids in viral release and avoiding co-infection in a single cell (12, 16, 17).

HIV-1 LTR

Location, Duplicity, Equality and Length

Although the genome of HIV-1 encodes for 15 proteins, the most often-transcribed regions of the viral genome are the long terminal repeat (LTR) regions. The HIV-1 LTRs are identical 634 base pair segments that flank both the 5’ and 3’ ends of the virus, with the 5’ LTR

conventionally being designated as the promoter of the virus and the 3' LTR as most important for polyadenylation of mRNA transcripts. Only the 5' LTR acts as an initiator for transcription as multidirectional transcription would lead to interference in the 3' LTR R/U5 junction between the 3' LTR U3 region newly forming transcripts and the termination of the RNA synthesises from the 5' LTR direction (18, 19). Both are also heavily involved in viral reverse transcription, integration, and replication. The LTR can be subdivided into three sections: the U3, R, and U5 regions (20, 21).

Sections = U3, R and U5

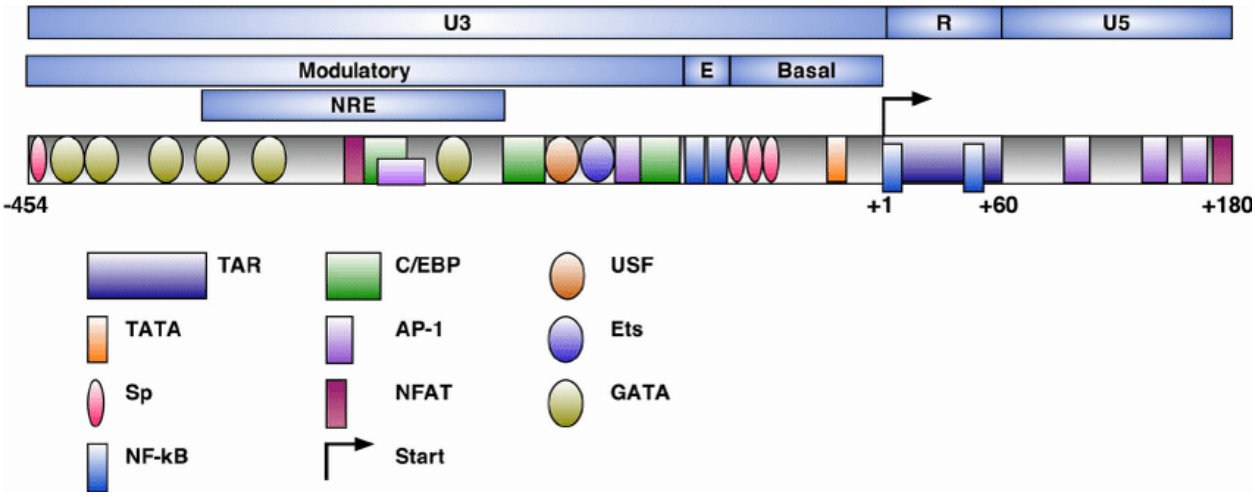

Figure 2 Schematic of the HIV-1 Long Terminal Repeat Region and Major Protein Binding Locations. *The HIV-1 LTR is divided into three regions: U3, R, and U5. All three regions contain multiple transcription factor binding protein sites, with U3 containing the most. The U3 region is further subdivided into the upstream modulatory region, enhancer, and basal promoter. Figure reproduced from (22) with permission from Springer Nature Publishing.*

U3 Region

U3 Roles

The U3 region of the LTR accounts for the first 453 bases and acts as the majority of the viral promoter (20). The U3 is most important for initiating viral transcription because it contains

the viral TATA box, core promoter, enhancer region, modulatory regions, and numerous upstream binding sites for transcription factor binding proteins (20).

U3 Binding Proteins

The most important sites within the upstream modulatory regions of the U3 that regulate transcription of the virus are the cis-acting binding sites for the regulatory transcriptional proteins such as AP-1, NFAT, and STAT5 (23–27). These proteins act as positive regulators of viral transcription (28). This is followed downstream by the enhancer region which contains an NF-κB binding site where inducible NF-κB p65-p50 heterodimers bind in an Sp1+TATA dependent manner to enhance transcription upon cellular activation (29). NFAT and NF-κB are also critical in the recruitment of chromatin remodeling factors such as histone acetyltransferases (HATs) to the viral promoter (28, 30). This is followed by three Sp1 sites and the conserved TATA box which form the bulk of the core promoter. Efficient Sp1 binding is required for both basal and Tat-mediated transcription of HIV-1 while the TATA box is the location of binding for TFIID, the first protein complex to bind the viral DNA in the eventual recruitment of RNA polymerase II (RNA Pol II) (20, 31).

R Region

The transition from the U3 into the R region is delineated by the viral transcriptional start site (TSS) (27). However, arguably the most important location in R is the trans-activation response (TAR) element. The TAR element forms an RNA stem-loop structure that directly binds to the viral protein Tat. Very early on in viral transcription, when Tat is not yet present in the cell, low levels of basal viral transcription are possible. However, RNA Pol II, in the absence of Tat bound to TAR, will often prematurely abort transcription or accumulate in

downstream regions surrounding TAR. This creates a rate limiting step for transcription (28, 32). Upon the synthesis of a few productive mRNA sequences that result in the early production of Tat protein in the cell, synthesized Tat proteins are able to re-enter the nucleus and bind to the TAR element. Once bound, further recruitment of cellular transcriptional elongation factors occurs, forming a much more efficient transcriptional complex (33, 34).

U5 Region

The final 84 bases of the LTRs make up the U5 region. This region contains the fewest transcriptional protein binding sites, with the most important being one more NFAT and two additional AP-1 sites (20). These sites of activation are downstream sequence elements that have been shown to promote induction of the HIV-1 LTR by both Protein Kinase A (PKA) and Protein Kinase C (PKC) activation signals via binding of cAMP response elements (35).

Treatments for HIV-1

History of cART

Initial drug therapies for treating those infected with HIV-1 focused on targeting specific stages in the viral infection cycle. These included drugs that targeted viral attachment to its CD4 receptor and/or CCR5 or CXCR4 coreceptors, envelope fusion inhibitors, nucleoside and non-nucleoside inhibitors of reverse transcription, viral integrase inhibitors, and protease inhibitors that targeted the virus post-release (36). The combination of multiple drugs into a cocktail therapy that targets different stages of the infection cycle was first developed in 1997 and is still referred to as combinatorial anti-retroviral therapy (cART). Current versions of cART are capable of suppressing HIV-1 replication to undetectable levels, reducing the risk of viral transmission and prolonging patients' prognoses. This is demonstrated by the

increase in the proportion of HIV-1 positive individuals who are dying from non-AIDS related causes since the development of cART (37, 38).

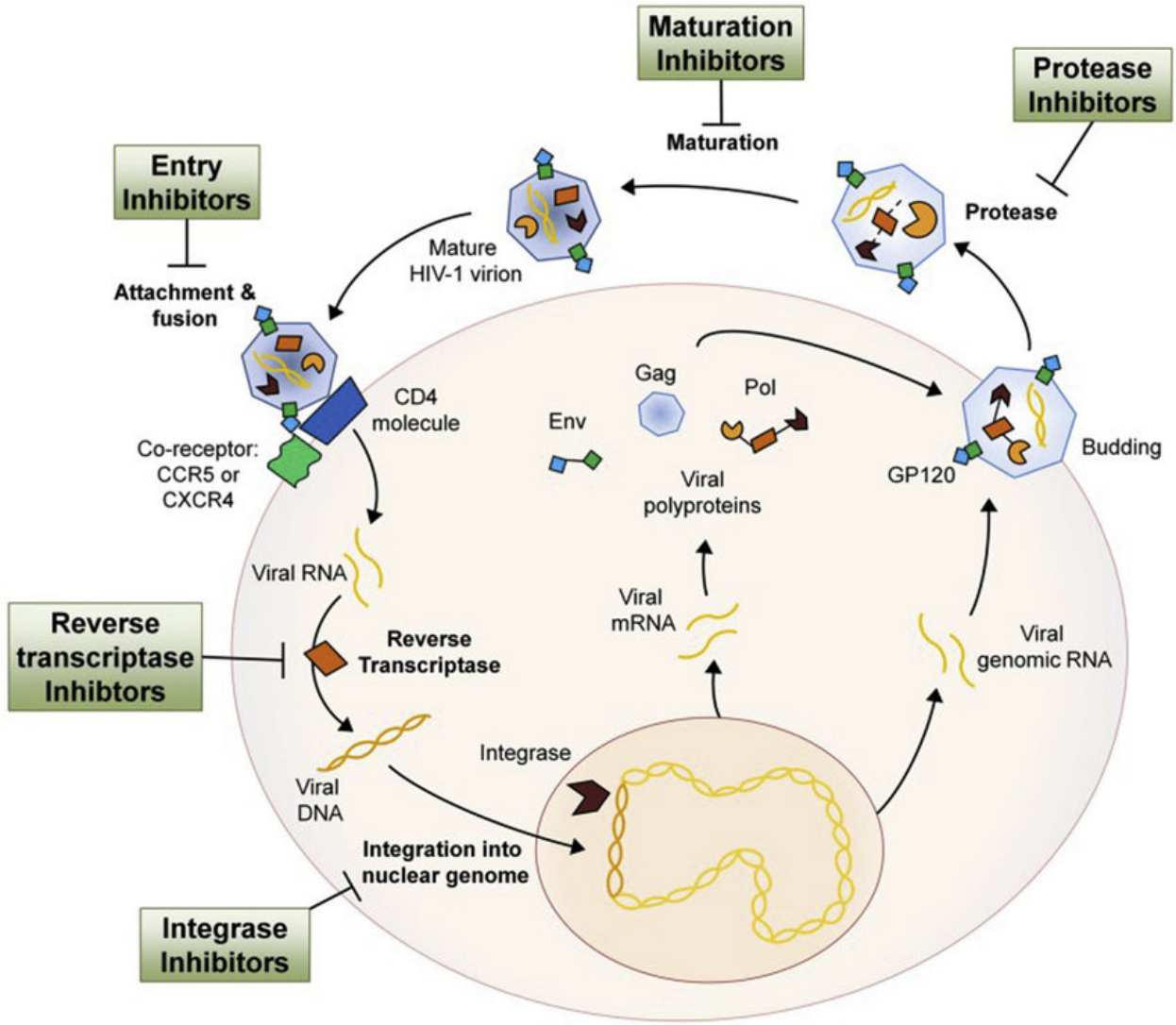

Figure 3 Targets of Anti-Retroviral Therapies *cARTs are capable of targeting multiple stages of the viral infection cycle, both outside and within its target cell. cART reduces viral transcription and spread within a patient. Figure reproduced from* (39) *with permission from Elsevier.*

Drawbacks of Current cART

Although current cARTs are able to effectively suppress HIV-1 replication to undetectable levels, current therapies are unable to completely eradicate all infected cells. Individuals on

cART are required to take these drugs for their entire lives (40–43), with any interruption in cART leading to a rebound in viremia within 2-8 weeks (44, 45). Even for those who receive treatment extremely early on in their infection or have low viral reservoir sizes rebounds may occur (45). This need for lifelong treatment creates issues involving drug costs; adherence; and side effects such as fatigue, nausea, insomnia, and in extreme cases long term organ damage for some patients (46, 47). Nor has the presence of cART for HIV-1 infections managed to reduce the levels of new infections, with approximately 1.7 million new infections globally in 2019 holding as the steady state (5).

HIV-1 Latency

Definition of HIV-1 Latency

Current cART therapies do not completely eradicate HIV-1 within an infected individual due to the presence of the HIV-1 latent reservoir. Latently infected cells are defined as cells containing an integrated HIV-1 DNA genome that is replication-competent but transcriptionally silent (28, 48–51). The total HIV-1 latent reservoir is the accumulation of cells and anatomical sites in which replication-competent HIV-1 can accumulate and persist (52). Because there is little to no expression of viral proteins, latently infected cells are able to avoid immune detection and subsequent clearance (43). Upon cessation of cART, latent reservoirs are the primary drivers behind the dissemination of viral infection and the increase in post-treatment viremia.

Size of Latent Reservoir

Total Size Estimate

As of 2016, the estimated size of the latent cell population within an individual living with HIV-1 was 10^8 cells (53), with approximately 10% of all integrated, latent proviruses being replication competent (54, 55). It is further estimated that $10^5 \rightarrow 10^7$ of this population are established in the first weeks of infection (56). The half-life of the total reservoir under cART is approximately 44 months (57), meaning that it would take at least 60 years of treatment to clear the known reservoir (58).

Reservoir Cell Types

Non-Lymphocytes

While the majority of research on the HIV-1 latent reservoir has thus far been performed on CD4+ T lymphocytes, the presence of latently infected macrophages, monocytes, and dendritic cells have also been shown to exist (59–62). Monocytes make up a small fraction of the overall latent reservoir (<0.1%) likely due to extremely low levels of CCR5 expression, with CD16+ and intermediate monocytes demonstrating the greatest HIV-1 susceptibility among monocytes due to higher levels of CCR5 (59, 63, 64). Reservoirs of resident macrophages within the mucosal surfaces are established within the first few days of an infection and are key contributors to the recruitment of CD4+ T lymphocytes to the sites of infection through the upregulation of cytokine production (65). Not only does this increase the number of target lymphocytes for extracellular HIV-1 virions to infect, macrophages are also capable of directly transmitting virions through cell-to-cell contact with CD4+ T lymphocytes during antigen presentation (66–68). Because of monocyte-derived

macrophages' added ability to migrate into tissues upon differentiation, they have also become candidates for spreading latent viruses into locations that are anatomically difficult for immune system recognition and clearance. This allows for further spreading of the virus into locations such as the lungs, gut-associated-lymphoid tissues, testes, brain, liver, and lymph nodes among others (59, 69–74). Dendritic cells display a much lower infection rate *in vivo* as compared to CD4+ T lymphocytes, and may play a role in spreading HIV-1 infection through the presentation of sequestered, intact virions to T cells (75). Follicular dendritic cells are thought to increase the latent reservoir through capturing/binding intact virions on their surface without being infected themselves (76).

Lymphocytes

CD4+ T lymphocytes represent the most well-characterized cell population within the viral latent reservoir. CD4+ T cells can be categorized by their effector functions upon stimulation as well as by their memory status (77). When analyzing by memory status, the frequency of lymphocytes that contain latent provirus is much higher in memory CD4+ T cells compared to naïve and recent thymic emigrant CD4+ cells (78). CD4+ stem cell memory (T_{SCM}), central memory (T_{CM}), transitional memory (T_{TM}), and effector memory (T_{EM}) cells are the four subtypes of CD4+ memory T cells that harbour the highest levels of replication-competent HIV-1 DNA within patients undergoing cART (77, 79, 80). T_{CM} cells primarily localize in lymph nodes until an activation event which stimulates their conversion into T_{EM} cells that are capable of moving into tissues and exerting cytotoxic responses (81). T_{TM} cells show an intermediate phenotype between central and effector memory cells (82).

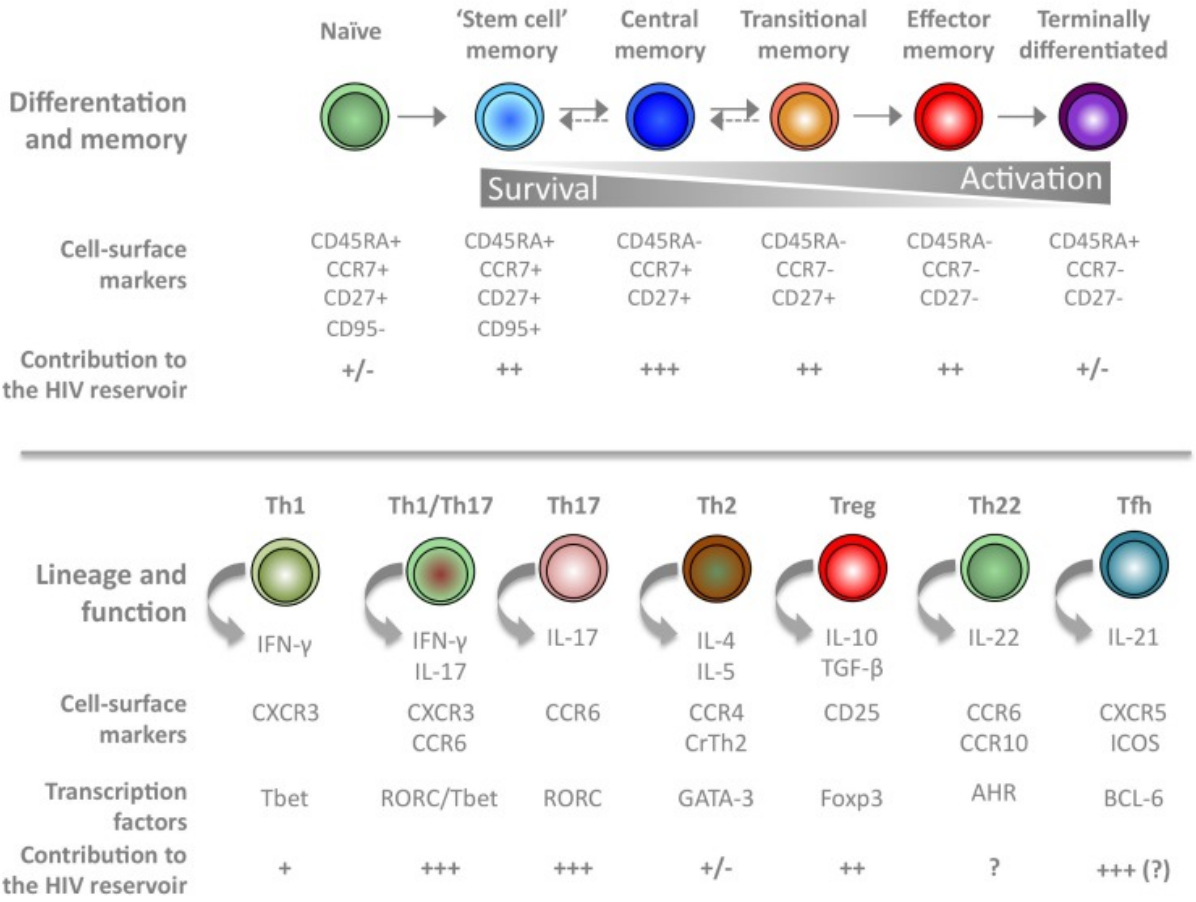

Figure 4 Categorization of Various CD4+ T cell Subtypes and Their Contribution to the HIV-1 Latent Reservoir. *CD4+ T cells can be categorized based upon their level of differentiation as well as by their memory status, with many groups playing a role in the establishment of the latent reservoir. Figure reproduced from* (77) *through Open Access.*

T_{CM} and T_{TM} cells make up the majority of the latent HIV-1 cellular reservoir within memory cells, with T_{CM} cells displaying the highest levels of replication-competent HIV-1 DNA (83). The T_{CM} and T_{TM} reservoirs are also maintained by two different mechanisms of action. In patients undergoing cART who have seen a recovery of CD4+ T cell counts or who have experienced only a slight decrease in CD4+ T cell counts due to early cART initiation, T_{CM} cells are more often seen as the primary HIV-1 latent reservoir likely through maintained T cell survival and low-level HIV-1 antigen-driven proliferation. In patients who have experienced a large decrease in their CD4+ T cell counts prior to cART initiation, T_{TM} cells play a larger role

within the latent reservoir likely through IL-7 mediated homeostatic proliferation and by detecting proviral DNA (79). T_{SCM} cells are the longest lasting and most capable of self-renewing CD4+ memory T cells, and these cells play an increasing role within the latent reservoir as T_{CM}, T_{TM}, and T_{EM} cells are slowly lost by apoptosis throughout an infection (80). When analyzing CD4+ T lymphocytes by effector status, the variable levels of chemokine receptors, cytokine secretion, and concentration of transcription factor binding proteins all influence the ability for each effector T cell subset to act as a cellular reservoir for latent HIV-1 (77, 84). Although activated, effector CD4+ T cells are the preferential target for productive HIV-1 infection, they do not make up the majority of the latent reservoir because of their short life spans due to a contraction phase following the effector response and HIV-induced cytopathic effects (85, 86). When looking specifically at the HIV-1 latent reservoir, Th17 cells, CD4+ regulatory T (T_{reg}) cells, and follicular T helper (T_{fh}) cells all demonstrate high levels of integrated, latent proviruses within patients undergoing cART (87, 88). Th17 cells that demonstrate high levels of CCR6, a marker for gut-directed homing, are highly susceptible to HIV-1 infection and thought to be a major factor in the establishment and maintenance of the latent reservoir within the gut associated lymphoid tissue (89).

Timing of Latency Creation in Infection Cycle

The majority of the latent reservoir within CD4+ T lymphocytes is established very early in the infection process due to the molecular environment within the T cells during early HIV-1 infection (90). HIV-1 first primarily targets effector CD4+ T cells during acute infection because of their high external CCR5 expression and high internal dNTP concentrations (which HIV-1 requires for reverse transcription) (91). The majority of these effector CD4+ T cells that

HIV-1 infects will die off after the initial acute infection period due to HIV-1 induced apoptosis or immunological contraction, leading to a decrease in overall CD4+ T cell levels. However, a subset of the infected cells will remain and transition into the aforementioned memory CD4+ T cells which help to establish immunological memory against HIV-1 protein epitopes, as happens for all foreign pathogens that the human immune system contacts (92, 93). These transitioning cells dramatically shut down their transcriptional machinery and enter a resting memory T cell state (93). The establishment of immunological memory, which in this case so happens to contain cells with integrated latent proviruses within their genomes, is considered outside of the effects of cART, and rather due to the natural mechanisms that the human immune system follows in responding to foreign pathogens and subsequently establishing immunological memory (28, 94).

Requirements for Latency Induction

Cellular conditions

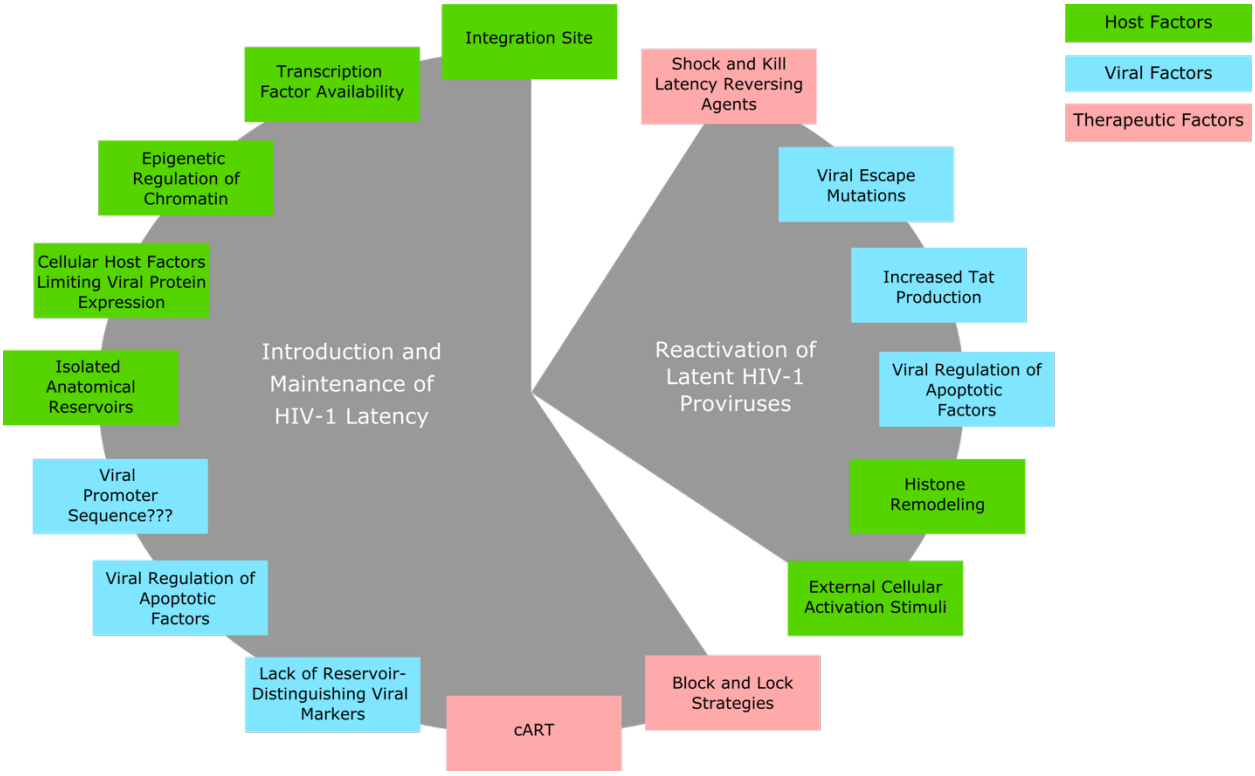

Figure 5 Factors of HIV-1 Latency Establishment, Maintenance and Reversal. *HIV-1 latency is a complex and multi-factorial process that is established early in an infection. The latent cellular reservoir is a diverse cell population which is maintained through factors associated with the host environment, infection timing, viral protein expression as well as therapeutics given to patients.*

Upon completion of the effector-to-memory CD4+ T cell transition, integrated proviruses may maintain a latent phenotype in CD4+ memory cells due to multiple environmental factors within the host memory cell. First, the presence or absence of key HIV-1 transcription factors can affect HIV-1 latency. Transcription of viral genes requires the presence of the two key initiation transcription factors NF-κB and NFAT. However, in memory cells NF-κB and NFAT are sequestered in the cytoplasm of the cell, thereby decreasing their ability to increase viral transcription (23, 24, 28, 95, 96).

Secondly, low levels of CyclinT1 (CycT1) in the nucleus of resting memory cells are critical for establishing and maintaining viral latency. When an effector CD4+ T lymphocyte is activated during the initial HIV-1 infection, CycT1 will bind to CDK9 to form P-TEFb, a cyclin dependent kinase that has three critical roles for transcription initiation: the phosphorylation of the negative elongation factors NELF and DSIF, the recruitment of RNA Pol II, and the recognition and binding of Tat (which leads to a conformational change in Tat and its binding with TAR). However, once the effector CD4+ T cell transitions into a resting memory cell, CycT1 becomes degraded before it may bind with CDK9. This decreases the ability for the virus to transcribe its genes and thus allows for maintaining a latent phenotype (27, 28, 97–102).

Thirdly, viral latency is maintained by the biochemical nature of the histones where the virus integrates. It has been shown that the LTRs of latent proviruses are known to accumulate histone deacetylases (HDACs) and histone methyltransferases (HMTs), leading to deacylated and methylated histones that are less accessible to transcriptional proteins and thus aid in protecting the virus from spontaneous latency reversal (103–105). HIV-1 has also been shown to integrate into areas of heavy heterochromatin where viral reactivation and detection is more difficult due to the compact and inaccessible nature of the chromatin (28, 106). Finally, when HIV-1 does integrate into an area that is actively expressing proteins, *in vivo* studies of CD4+ T cells have shown that 93% of integration events occur in the introns of actively transcribing genes, meaning that no HIV-1 proteins become expressed by the cell and latency may be maintained (107).

So what happens when viral transcripts do start to become transcribed and expressed in latently infected memory cells? Two interesting mechanisms exist that demonstrate the ties

between natural host functions and latency maintenance. The first involves viral RNA retention in the nucleus. It was found in individuals on cART that there was an increase of polypyrimidine tract binding protein (PTB) in the nucleus of resting CD4+ T cells. PTB binds the mRNA for the viral proteins Tat and Rev, thus affecting their splicing and keeping them from leaving the nucleus. This lead to a decrease in multiple viral positive feedback loops that Tat and Rev are responsible for creating, and thereby allowed for the cell to prolong latent proviruses (108).

The second interaction comes through the cellular apoptotic pathway. When the infected cells begin to detect viral proteins, they can enter into apoptosis. However, the virus can counter this during early infection by expressing Nef, Tat, and Vpr which all lead to increases in anti-apoptotic proteins, allowing for the cells to survive longer than they want to. During late infection after latency is reversed and the virions wish to lyse the cells the reverse occurs and Env and Vpu expression lead to increases in apoptotic regulators. By affecting levels of apoptotic regulators, whether by upregulating or downregulating certain checkpoints, HIV-1 can affect the length of time that the cell survives and thus gives itself a better chance at maintaining a latently infected, resting phenotype (43, 109).

What does Latency do to the Creation of HIV-1?

How can Latency be Reversed in a Cell?

Cellular Changes Leading to Viral Activation

A variety of interactions between viral and cellular factors have been shown to promote not only the initiation but also the maintaining of HIV-1 latency. However, the cellular environment is dynamic and there are also specific conditions which can reverse latency,

leading to the upregulation of viral transcription and protein presentation. The foremost change that can occur is the activation of an infected CD4+ T cell which leads to an increase in NFAT and/or NF-κB levels in the cell. In CD4+ T cells, NFAT seems to be the dominant protein in reactivating latent virus compared to NF-κB, with both NFATc1 and NFATc2 activating HIV-1 transcription (23). NF-κB, in the absence of stimulation, is bound to the inhibitory molecule I-κB. In *in vitro* experiments, when stimulation by mitogens, cytokines, oxygen radicals or other T cell stimulatory agents results in I-κB phosphorylation and disassociation from NF-κB. I-κB is then degraded and NF-κB is allowed to travel to the nucleus to upregulate transcription (110, 111). Upregulating the host transcription factors of NF-κB and NFAT leads directly to HIV-1 gene expression upregulation (24, 112).

Latency can also be naturally reversed in a cell through the recruitment of host HDAC inhibitors and HMTs (113). This will lead to histones that are less compact and biochemically more available for transcriptional binding protein access.

These processes can occur naturally as an infected cell receives different stimuli from the body and responds accordingly. However, a reversion from latency to viral expression can also be induced through a targeted stimulation of the aforementioned signalling pathways with exogenous reagents. Molecules that specifically stimulate a reversion in HIV-1 latency for therapeutic and research purposes are classified as Latency Reversing Agents (LRAs).

Improving cART Through Targeting the Latent Reservoir

Shock and Kill

The 'Shock and Kill' strategy for identifying and clearing latently infected cells is based on the premise of using LRAs to upregulate latent proviral transcription, which would then lead to

the cells being recognized and subsequently cleared through an immune response (43). Because HIV-1 transcription is closely linked to cell signaling pathways that also govern T cell receptor (TCR) engagement and T cell activation, a delicate balance between using LRAs to activate viral transcription and not inducing a global T cell activation must be reached to avoid potential toxic 'cytokine storms' (114–116). Preliminary 'Shock and Kill' studies have demonstrated that a significant hurdle to the success of this technique is their inability to completely reactivate the full complement of latent proviruses. The majority of HIV-1 proviruses integrate into transcriptionally active regions of the genome, and thus are heavily influenced by the chromosomal structure and epigenetic status of these regions (117). Studies that have used single molecules to induce host cell transcription through T cell signalling pathways (PMA+I, IL-2, IL-7 etc), through increasing Protein Kinase signalling pathways (PKC agonists), or through chromatin remodeling (HDAC or HMT inhibitors) have all found that only a small subset of proviruses are reactivated to transcribe (115, 118). Because of this, combinations of various LRAs that will target integrated HIV-1 through various pathways are now being combined in an attempt to create an optimal viral 'shock' (119).

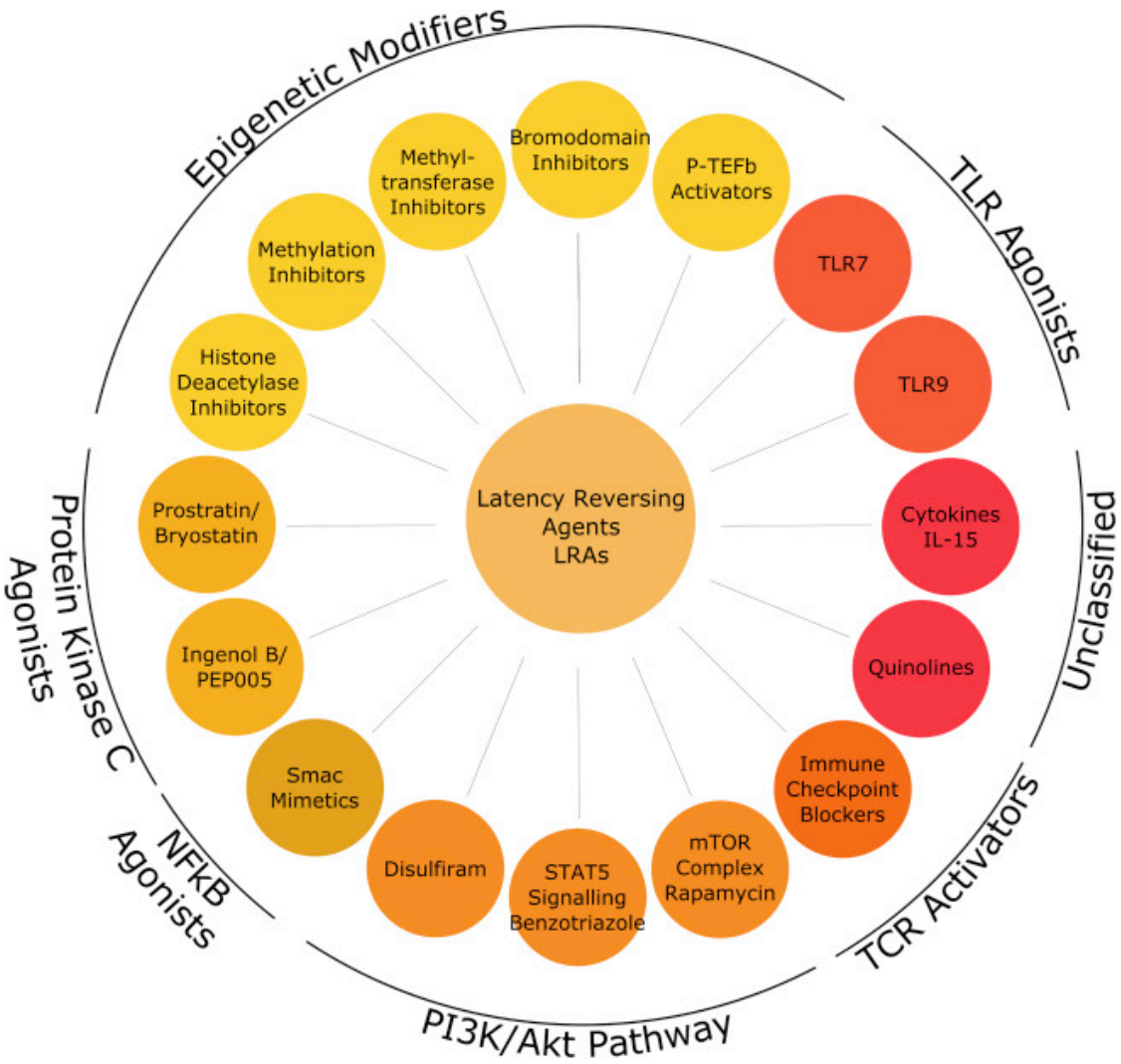

Figure 6 Categories of Latency Reversing Agents. *LRAs are used to reverse viral latency within the 'Shock and Kill' technique, leading to a detectable increase in viral expression within latently infected cells. Figure reproduced from* (43) *with permission from Elsevier.*

Clinical trials to date have demonstrated that although *in vivo* LRA activation of the latent reservoir does lead to a small increase in transcription of HIV-1, and that latently infected CD4+ T cells treated with LRAs do allow for an increase in susceptibility to antigen-specific CD8+ T cells (91, 120), 'Shock and Kill' efforts do not lead to clearance of latently infected cells by CD8+ T cells (121–125). It has been shown that combinations of LRAs used to reactivate latent HIV-1 can affect HIV-1 antigen processing within the CD4+ T cells as well as alter the CD3 and CD4 expression levels within CD8+ T cells (126, 127). HIV-1-specific CD8+ T

cells also need to overcome the accumulation of escape mutations in dominant epitopes of HIV-1, a physical exclusion from the lymph node follicles where infected CD4+ T cells are abundant, and an enduring epigenetic dysregulation carried over from their previous exhausted state during the acute infection stage (128–131). Because CD8+ T cells do not seem to be capable of clearing reactivated latent cells on their own, methods to improve the 'kill' have also been developed. These include inhibiting anti-apoptotic activity of the viral proteins Tat, Nef, and Vpr (109); inhibiting viral budding causing cellular apoptosis in response to a virion build up (132); and inhibiting the p38/JNK pathway leading to increased cell death upon reactivation (133).

To be considered a successful 'Shock and Kill' technique, four tenants must be achieved:

1. All replication-competent proviruses must be reactivated
2. A decrease in the overall number of infected cells must be demonstrated
3. It cannot cause an increase in viremia leading to an increase in newly infected cells
4. It must avoid a global T cell reactivation that can be toxic to the patient when maintained for a prolonged period of time (55, 134, 135)

Latency Reversing Agents

Four classes of LRAs were used in this thesis: HDAC inhibitors, Protein Kinase C (PKC) agonists, aldehyde dehydrogenase inhibitors, and retinoids.

HDAC Inhibitors

Included in this study are the HDAC inhibitors Panobinostat, Romidepsin, Valproic Acid, and Vorinostat. HDAC inhibitors are robust agents that reverse the acetylation of histones, leading to DNA that is less compact and more available to activators, transcription factors,

and RNA pol II (136, 137). HDAC inhibitors have been shown to reactivate latent HIV-1 proviruses to varying degrees *in vitro* and in CD4+ T lymphocytes (121, 124, 144, 145, 125, 137–143).

Alcohol Dehydrogenase Inhibitors

Disulfiram is an alcohol dehydrogenase inhibitor that is included in this study. Disulfiram was originally marketed for treating alcoholism through the inhibition of acetaldehyde dehydrogenase, however it has since been shown to reactivate latent HIV-1 expression in the U1 primary cell line and some primary CD4+ T lymphocyte models (122, 146–148). Disulfiram activates latent HIV-1 proviruses by inhibiting the copper-containing enzyme dopamine B-hydroxylase, as well as by depleting intracellular levels of PTEN, leading to an increase in NF-κB dependent proviral transcription (146, 147).

Protein Kinase C (PKC) Agonists

Bryostatin-1, a macrocyclic lactone, and phorbol 12-myristate 13-acetate (PMA), a phorbol ester and the gold standard in reactivation studies when given in conjunction with Ionomycin, are both included in this study. Increases in PKC levels lead to increases in NF-κB and AP-1 signalling cascades, two critical transcription factors for HIV-1 as shown above (149). Bryostatin-1 and PMA+I have both been shown to reactivate latent proviruses in *in vitro* T cell lines and in *ex vivo* CD4+ T lymphocytes (127, 148–152). The efficacy of either to induce transcription of latent provirus *in vivo* has yet to be proven (123).

Retinoids

Included in this study is the first-generation retinoid All Trans Retinoic Acid (ATRA). ATRA causes an upregulation in cell differentiation and proliferation through a still unknown

mechanism. ATRA has been shown to increase HIV-1 reactivation in CCR6+CD4+ T lymphocytes (153, 154).

Block and Lock

In direct comparison to 'Shock and Kill' strategies are 'Block and Lock' methods which seek to use therapeutic interventions that 'lock' the virus inside the cell by 'blocking' any further viral transcription, thereby aiming to allow for patients to discontinue cART without a subsequent viral rebound. Methods thus far have included using small molecule protein repressors, chromatin remodeling, small interfering RNAs (siRNAs), and genome editing techniques (115). Major current hurdles for 'Block and Lock' therapy development include delivery of the transcriptional repressors, identifying cells containing latent HIV-1, and avoiding non-specific targeting of uninfected cells (115).

Proteins and Signalling Repression

The HIV-1 LTR uses many transcription factor binding proteins to regulate its viral transcription. Because of this variety, small molecules that target for repression only one transcription factor binding protein are typically not highly effective in locking down the full HIV-1 latent reservoir (115). A more effective strategy is through complete histone remodeling, but opposite to which it is used by LRAs in 'Shock and Kill'. In 'Block and Lock', histones containing integrated proviruses are targeted for repression, meaning that HDACs, HMTs, and DNA methyltransferases are all upregulated directly or through repression of their inhibitors (115, 155).

RNA and Signalling Repression

Double stranded siRNAs that target the enhancer region of the HIV-1 5' LTR have been shown to increase repression of the viral LTR in a reversible manner (156). RNAs against highly conserved regions of the viral genome have also been used in combination with recombinant fusion proteins designed to inhibit the transcription of HIV-1 (157). Finally, RNAs have been used to target the Tat-TAR interaction of HIV-1 transcription, specifically by interfering with TAR RNA folding, by binding and sequestering TAT-pTEFb, and by interfering with Tat binding (115, 158–160).

Genome Editing

A final method to target the HIV-1 genomes of latent proviruses for transcriptional repression is through genome editing. Both CRISPR/Cas9 and TALEN-mediated endonucleases have been developed and evaluated against highly conserved sequences within the HIV-1 5' LTR (115, 161, 162). Preliminary efforts to suppress HIV-1 transcription through genome editing have been fairly successful *in vitro* as well as in mouse and rat *in vivo* models (163, 164). Similar to aforementioned 'Block and Lock' strategies, identification of cellular reservoirs and delivery of necessary reagents to those sites remain the primary hurdles for testing genome editing in cART patients (115).

Latency Determined by Viral Sequence

As of yet, 'Shock and Kill' and 'Block and Lock' remain unachievable until the complete mechanisms of HIV-1 latency induction, maintenance, and reversal are fully understood. Only then can we achieve an HIV-1 sterilizing cure, the complete eradication of all replication competent viruses in an individual as demonstrated in "Shock and Kill", or a functional cure,

the control of infection spread without persistent cART use as proposed through “Block and Lock” (36). The sequence of the latent HIV-1 5’ LTRs is very important for identifying the best molecules/proteins to use for latency reversal under ‘Shock and Kill’ and is also critical when designing LTR sequence-specific transcriptional repressors under ‘Block and Lock’. Therefore, we began to question whether the sequence of the infecting virus could play a role in HIV-1 latency creation, maintenance, and reversal along with what is already known about the role of the cellular environment. What if the availability of transcription factor binding proteins that seem so key in establishing, maintaining and reversing viral latency were not only being affected by the cellular signalling pathways, but also by changes in the sequences in the viral genome where they were trying to bind? Specifically, what if sequence mutations in the viral LTR/promoter could affect viral latency induction and reversion in a manner consistent to what is typically accepted as being dependent only on the molecular environment of the cell? To ask these questions we first must look at ways that the viral LTR sequence can become mutated.

APOBEC3 Proteins

An Overview

Definition

Apolipoprotein B mRNA editing enzyme, catalytic protein-like 3 (APOBEC3 or A3) proteins are a set of innate, antiretroviral proteins encoded by 7 clustered APOBEC3 genes that are located on chromosome 22 in humans (165). APOBEC3 proteins are expressed in almost all human cells, however are found at much higher expression levels in immune cells (166).

Certain A3 proteins are also highly inducible, particularly A3G and A3F in CD4+ T cells, macrophages, and dendritic cells (166).

Differences Between Mammals

The human genome encodes for 7 APOBEC3 genes clustered on chromosome 22 (A3A, A3B, A3C, A3DE, A3F, A3G, and A3H) (165). A3 proteins are not solely a protein expressed in humans. A3 proteins are found in all mammals with different isoforms expressed between species. For example, chimpanzees have 7 APOBEC3 genes, while horses have 6, mice 5, cats 4, cows and sheep 3, and pigs 2 (165, 167).

APOBEC3 Targets?

APOBEC3 proteins are polynucleotide cytidine deaminases that are effective at inhibiting the replication of viruses that use reverse transcriptase (RT) during their infection cycle such as HIV-1 and other lentiviruses; other viruses such as Hepatitis B Virus; as well as retroelements in the cell such as LINES, SINES, and long terminal repeat (LTR) regions (168). Certain A3 subsets also are capable of deaminating free floating dsDNA in the cytoplasm (one of the ancestral roles for the proteins) and targeting these dsDNAs for degradation (169).

Which APOBECs Are Effective Against HIV-1?

The two A3 proteins that show the highest restriction capability of HIV-1 are A3G and A3F. A3G is highly effective against HIV-1 and prefers to mutate GG locations in the viral genome (170) while A3F has been shown to have activity similar to that of A3G, but prefers to mutate AG locations (171). In addition, A3DE and A3H haplotype II have been shown to restrict HIV-1 in a Vif-dependent manner, A3B to a lesser extent in a Vif-independent manner, while A3A and A3C have not been shown to restrict HIV-1 in T cells (172–174). There have been some

suggestions that A3A may have anti-HIV-1 activity in monocytes where protein translation begins at residue 13 instead of the methionine at residue 1, but this has not been conclusively proven (175).

Anti-HIV-1 Mechanism of Action

During viral nucleocapsid formation in HIV-1 producer cells, A3 proteins are expressed by the host cell and become co-packaged within the virus inside the nucleocapsid, allowing for transportation of A3 proteins inside the virus to cells that the virions will infect downstream (176). Upon the initiation of reverse transcription by the virus once inside a downstream cell, A3 proteins are able to restrict RT activity through two mechanisms: a deamination dependent mechanism and a deamination independent mechanism.

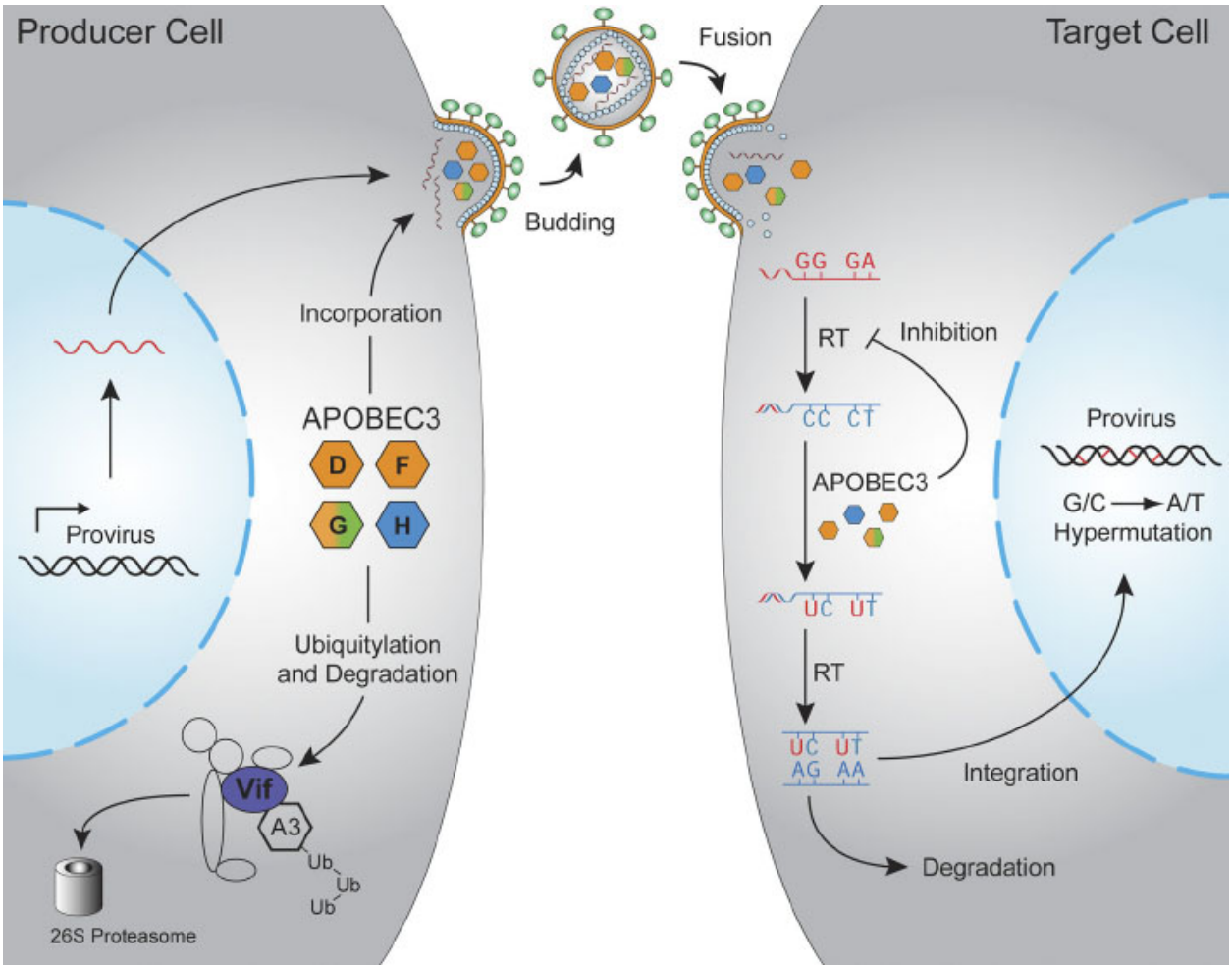

Figure 7 Packaging of HIV-1 and APOBEC3 Proteins *APOBEC3 proteins become copackaged within budding HIV-1 virions in primary cells and are capable of restricting viral reverse transcriptase within secondary infected cells. A3 proteins can also be sequestered in the primary cell by Vif and targeted for degradation. Figure reproduced from* (173) *with permission from Elsevier.*

Deamination independent

A3 proteins have been shown to be effective against reverse transcription in a deaminase-independent manner. This means that during reverse transcription of the virus, the mere presence of the bulky A3 proteins within the nucleocapsid physically blocks multiple aspects of the viral reverse transcription process. This leads to increased RT mutations, lack of efficient full strand reverse transcriptase synthesis and abortions of synthesis. Specifically this can include physically blocking the binding of $tRNA_{lys3}$ to its primer binding site during the initiation of reverse transcription, the transfer of DNA strands, and altering the

integration of the virus (177–179). It is estimated that for A3G, 0.7% of anti-viral activity is deaminase-independent, while 30.2% of A3F is deaminase-independent (180).

Deamination Dependent

Mechanism

The majority of APOBEC3 restriction of HIV-1 comes through its deamination dependent pathway. A3 enzymes are cytidine deaminases, meaning that they convert cytidine bases to uracil bases (C→U) in the newly synthesized -ssDNA strand of reverse transcribing retroviruses (168). These C→U mutations in the minus strand of the virus are then copied from guanine into adenine mutations (G→A) in the subsequently synthesized positive DNA strand of the incorporating virus (170). Due to both the overall number of A3-induced mutations as well as the potential placement of the mutations in locations of high importance to viral fitness, a decrease in the number of integrated, replication-competent, proviral sequences occurs (166).

GG and GA Locations

A3G preferentially deaminates the 3'C of 5'CC in the -ssDNA sequence of reverse transcribing HIV-1, resulting in GG→GA mutation profiles (181, 182) while A3DE, A3F and A3H all prefer to deaminate the 3'C of 5'TC motifs, which results in GA→AA mutation profiles (171, 183, 184). High levels of A3-induced hypermutation profiles, foremost among them being A3G-induced patterns, have been shown in integrated proviruses (54).

Vif

Protein Creation and Genomic Location

Although APOBEC3 proteins are highly efficient at mutating and limiting the replication efficiency of HIV-1 in early infection, they are not capable of sustaining this activity throughout the infection process due to the presence of Viral Infectivity Factor (Vif). Vif is a non-structural HIV-1 viral protein that binds A3 proteins in HIV-1 producer cells and recruits the E3 ubiquitin ligase complex Cullin5-ElonginB/C to target A3 proteins for polyubiquitination (185–188). Polyubiquitination of A3s results in their degradation by the 26S ribosome prior to co-packaging in viral nucleocapsids in the producer cell, negating any potential effects of A3s on downstream HIV-1 infected cells. In the early stages of an infection within a host cell, levels of Vif produced by the virus are extremely low, allowing for the successful packaging of A3 in early budding virions and high levels of mutagenesis within reverse transcribing downstream virions (189). However, as the levels of viral Tat increase in the primary cell, an increase in viral protein expression occurs leading to an abundance of synthesized Vif proteins which are capable of fully inhibiting A3 copackaging, leading to the degradation of A3 and the rapid spread of virus uninhibited by A3 (185, 186).

Commonality of A3 vs RT Errors

APOBEC3 proteins are not the only proteins that can introduce mutations within the viral genome during the replication process. Viral RT is also capable of HIV-1 mutagenesis because of its lack of intrinsic 3'-5' proofreading activity (190–192). HIV-1 RT has an error rate of approximately 2-3 x 10^{-5} mutations per nucleotide per cycle, resulting in 2-3 mutations introduced into the viral genome every replication cycle (190–192). HIV-1 overall has an

estimated $1.2 \times 10^{-5} \rightarrow 3.4 \times 10^{-5}$ mutations per nucleotide per cycle (192, 193). It is estimated that 98% of mutations within integrated HIV-1 DNA (replicative and non-replicative) in an individual are associated to A3 cytidine deamination while 2% to RT. However in circulating plasma where replication competent and transcriptionally active viruses are present, levels of A3-induced and RT-induced mutations are almost equal (190).

It was subsequently found that mutations accumulated from RT and A3 induction can contribute to viral subpopulations that contain weakly mutated viral-genomes, which can influence infectivity and disease pathogenesis (190). Taken together, it can be seen that although Vif is capable of eliminating the mutagenesis of A3 proteins on HIV-1 during late infection in one particular cell, there remains a window during the 'middle infection' of a cell where Vif proteins are beginning to accumulate and only a few A3 proteins are being incorporated into budding virions. The HIV-1 genomes of these 'middle' viruses accumulate low levels of mutations from both the few copackaged A3 proteins and also RT. Because only low levels of mutations accumulate, these sub-lethally mutated HIV-1 viruses remain replication and transcriptionally competent as seen through their presence in plasma samples. If this was not the case, then there would be no evidence of A3 or RT mutation patterns in the replicating pool of virus.

Rationale

It has become quite apparent that there are multiple factors affecting viral latency, and that the traditional model of latency being solely influenced by the transcriptional environment within the cell is an incomplete picture of HIV-1 latency. For example, all attempts by 'Shock and Kill' techniques at reversing the full complement of replication-competent, latent proviruses have thus far failed. We therefore asked the question whether the specific sequence of HIV-1 prior to integration may play a role in the virus' ability to both create and maintain a state of viral latency. Specifically, we asked whether low to moderate levels of G→A transition mutations accumulating in the viral LTR (promoter) region acquired through exposure to APOBEC3 and RT could cause a change in sequence great enough to create a latency-like phenotype.

Hypothesis

We hypothesize that G→A transition mutations in the HIV-1 5' LTR region introduced through RT and low levels of A3 protein activity can create HIV-1 sequences that display a reversible, latency-like phenotype.

Implications

The ability for sequence changes in the DNA of HIV-1 to create sequences that portray a latency-like phenotype would give rise to a completely new mechanism of HIV-1 latency. Previously, we have primarily looked at latency as being dependent on the environment in which the HIV-1 proviral genomes are within, however this research will show that HIV-1 latency may also be dependent on the molecular sequence of the virus itself. Secondly, this work may help to shed light on why certain LRAs are less effective than others at activating the full spectrum of replication competent, latent proviruses. If viruses have mutations that lend themselves less susceptible to activation by specific transcriptional proteins, then LRAs that target these proteins for reactivating HIV-1 during 'Shock and Kill' should not be considered for whole reservoir reactivation. Finally, this work will continue to develop the understanding of the relationship between the A3 family of proteins and HIV-1. A3 proteins are traditionally seen as proteins that act effectively in limiting HIV-1 spread early on during infection and are not effective in later infection once Vif levels rise. This picture is very much a binary On-Off switch. This work will continue to show that the effect of A3 proteins on HIV-1 is very much a sliding scale of effect, with a middle window where A3 proteins can still package into HIV-1 virions at low levels, allowing for sub-lethal mutagenesis of the virus.

Outline of Approach

In order to answer the question as to whether G→A transition mutations in the HIV-1 5' LTR affect viral latency, our lab first created a library of HIV-1 viruses that contained transition G→A mutations in their 5' LTR region through exposure from co-packaged A3F or A3G proteins. These viruses were identical to the wild-type HIV-1 virus except in their LTR, in which they contained mutations in various numbers and locations. We termed these viruses latency prone viruses (LPVs). It is with a subset of this LPV library on which my role in the project began.

Objectives

My thesis revolves around three central objectives:

1. Objective #1 is to take a subset of LPVs and to compare the transfection, infection, and activation levels of the viruses when exposed to various LRAs. This will determine if differences in mutation patterns may lead to viruses that are more likely to reactivate to specific LRAs. This objective is first to be completed in an *in vitro* setting, followed by repeating the infections and activations within *ex vivo* CD4+ T lymphocytes.
2. Objective #2 is to determine if the LPVs integrate to similar levels. This is important because the LTR regions are critical in reverse transcription and integration. This will tell us if differences in infection and activation among LPVs are due to differences in integration/infection or due to transcription.
3. Objective #3 is to determine if our LPVs are capable of evolving from a state of latency back to a near-wild type phenotype. This is vital for establishing that transition mutations found in the LTR do not simply create reduced, dead end-infections, rather proviral genomes that are capable of reseeding viremia post rebound.

Materials and Methods

Tissue Culture Cell Propagation

Human Embryonic Kidney Epithelium 293T cells (HEK 293T) (ATCC # CRL-3216) were cultured in Dulbecco's Modification Eagle's Medium (DMEM) containing 584 mg/L L-glutamine, 110mg/L sodium pyruvate and 4.5g/L glucose (Wisent, #319-005-CL, St Bruno, QC, Canada) supplemented with 10% v/v Fetal Bovine Serum (FBS) (Corning 35-015-CV), 100U/mL penicillin and 100ug/mL streptomycin (P/S) (both GE Healthcare, Chicago, IL, USA), herein referred to as complete DMEM. HEK 293T cells were passaged to a density of 2.0 x 10^5 cells/mL every 48 hours.

U87 CD4+ CXCR4+ cells (NIH AIDS #4036) (herein referred to as U87 cells) were cultured in complete DMEM supplemented with 1ug/mL puromycin, and 300ug/mL G418. U87 cells were passaged to a density of 2.0 x 10^5 cells/mL every 72-96 hours.

Ghost CD4+ CXCR4+ CCR5+ cells (NIH AIDS #3942) (herein referred to as Ghost cells) were cultured in complete DMEM, supplemented with 1ug/mL puromycin, 500ug/mL G418, and 100ug/mL hygromycin. Ghost cells were passaged to a density of 2.0 x 10^5 cells/mL every 48 hours.

Jurkat cells (ATCC #TIB-152) were cultured in RPMI 1640 (Wisent, St. Bruno, QC, Canada) supplemented with 10% v/v Fetal Bovine Serum (FBS) (Corning 35-015-CV), 100U/mL penicillin and 100ug/mL streptomycin (P/S) (both GE Healthcare, Chicago, IL, USA), herein referred to as complete RPMI. Cells were passaged to a density of 2.0 x 10^5 cells/mL every 48 hours.

All cell lines were propagated in a 37°C + 5% CO_2 incubator (Forma Series II Water Jacket CO_2 Incubator) (Thermo Scientific Inc., Burlington, Ontario, Canada).

Latency Prone Virus Plasmid Creation

Non-replicative pNL4.3-Δenv-Δvif plasmids carrying distinct LTR transition mutation patterns were previously created in lab by Cindy Lam. For complete details on LPV synthesis see Appendix 3. For the mutation profiles of each LPV, see Table 1 located in Results section.

Plasmid Stock Propagation

For the propagation of LPV plasmid stocks to be used, along with a vesicular stomatitis virus glycoprotein (VSVG) plasmid (Addgene, Cambridge, Massachusetts, USA), 50ng of plasmid was introduced into 50uL of Stbl-2 E. coli cells and incubated on ice for 30 minutes. Tubes were mixing by gentle tapping and heat shocked in a 42°C water bath for 90 seconds, followed by 2 minutes on ice. 1mL of 2XTY broth (16g bacto tryptone, 10g bacto yeast extract, 10g NaCl, 1L ddH_2O, pH 7.2) was added to each transformation, followed by a 90 minute incubation at 30°C with shaking at 600rpm. 200uL of bacterial broth was spread onto a 30°C prewarmed LB + Amp plate (20g LB powder, 17g bacto agar, 1L ddH_2O, 100mg ampicillin). Plates were kept in a 30°C incubator overnight for 20-24h. One colony per transformation was then picked with a 200uL pipette tip and placed in a 250uL Erlenmeyer flask containing 100uL of LB medium (10g NaCl, 10g bactotryptone, 5g yeast extract, 1L ddH_2O) and ampicillin at a concentration of 1:500. Flasks were placed in a 30°C shaker at 225rpm for 20-24h. Midipreps of each plasmid were then prepared using an E.Z.N.A Plasmid DNA Midi Kit (Omega Biotek Inc. #D6904-04, Norcross, GA, USA) with a final resuspension in 1mL of sterile

RNAse-free water. Plasmid stocks were kept at -20^{o}C with working solutions of each plasmid at 100ng/uL in sterile RNAse-free water at 4^{o}C.

Viral Transfections

24 hours prior to transfection, HEK 293T cells were passaged, centrifuged at 500g for 5 minutes at 24^{o}C, and resuspended in complete DMEM. Cells were counted using a hemocytometer and plated in 6 well tissue culture plates (VWR International #10062-892, Mississauga, ON, Canada) at 625,000 cells per well with a final volume of 2mL complete DMEM.

At the time of transfection, 1.7mL eppendorf tubes were used to set up each transfection. 375ng of VSVG plasmid, 1125ng of LPV plasmid, and 200uL non-serum DMEM (Wisent #319-005-CL, St Bruno, QC, Canada) were added to each appropriate tube and mixed together by vortexing. 4.5uL of 1ug/uL polyethylenimine (PEI) (Wisent, St Bruno, QC, Canada) was added to each tube for a final concentration of 3ug PEI/1ug DNA, mixed through lightly tapping tubes 8 times on a constantly running vortex, and incubated at room temperature for 30 minutes. During the 30 minute incubation, 24hr-old DMEM media was aspirated carefully out of each well and replaced with 1.8mL of fresh, complete DMEM. After 30 minutes, the tubes were inverted 3 times to mix, and each transfection solution was added to the appropriate well through dropwise addition. Plates were mixed in the hood through light biaxial mixing and placed in a 37^{o}C + 5% CO_2 viral incubator for 72hr.

After 72 hours, supernatant containing virus was collected from each well, centrifuged at 500g for 5 minutes and 0.45um filtered (VWR #CA28143-312, Canada) to remove cellular debris. Supernatants were then stored at 4^{o}C. Cells were picked up using 500uL of 1X PBS+

5mM EDTA. Cells were centrifuged at 500g for 5 minutes and resuspended in 1mL of 1X PBS to wash. Cells were centrifuged again at 500g x 5 min and then resuspended in 600uL basic sort buffer (1X PBS, 5mM EDTA, 25mM Hepes, 1% globulin free bovine serum albumin, pH 7.2-7.4, 0.2um filtered) and fixed with the addition of 600uL 4% paraformaldehyde (PFA). Fixed cell solutions were then 40um filtered (Bio Basic Inc #SP104151, Markham, ON, Canada) into 5mL Falcon polystyrene round bottom FACS tubes (Corning #352054, Tewksbury, Massachusetts, USA) for flow cytometry analysis. Cells were analyzed on a BD FACSCelesta or BD LSRFortessa using BD FACSDiva v8.0.1 (BD Biosciences, Mississauga, ON, Canada). FITC channel (488nm laser, 530/30) was used to measure eGFP fluorescence. Post-acquisition analysis was performed on a separate computer using FlowJo (software v10.4.2).

ELISA p24 (gag) Quantification

Anti-p24 antibodies 183-H12-5C and (biotinylated) 31-90-25 were both previously prepared in the lab by senior lab members. See Appendix 4 for full methods on antibody production and conjugation.

A p24 sandwich ELISA was necessary to quantify the amount of virus from each viral transfection. High binding 96 well ELISA plates (Santa Cruz Biotechnology #204463, Dallas, TX, USA) were coated with 100uL anti-p24 183-H12-5C at a final concentration of 2.5ug/mL diluted in 0.1M sodium bicarbonate buffer (8.4g $NaHCO_3$ in 1L sterile Mili-Q water, pH 9.5). Plates were placed on a slow rotator at 4^{o}C for at least 24h (often approximately 48 hours). Plates were washed 3 times with 200uL ELISA wash buffer (1X PBS + 0.05% Tween-20) per well and blocked with 200uL of ELISA blocking buffer (1X PBS + 0.05% Tween-20, 5% milk, 2.5% globulin free bovine serum albumin) for 2 hours at room temperature on a slow rotator.

A recombinant HIV-1 p24 standard (Abcam #ab43037, Cambridge, MA, USA) was diluted using DMSO into aliquots of 200ug/mL, then 100ug/mL, and finally 10ug/mL. 10ug/mL aliquots were used for each round of ELISAs. Standard p24 was diluted from 10ug/mL to 100ng/mL using ELISA blocking buffer (10uL of 10ug/mL p24 + 990uL ELISA blocking buffer), followed by 7 1:2 serial dilutions down to 0.78125ng/mL. Virus supernatants were warmed in 37 ^{o}C incubator for 10 min, then diluted initially 1:100 in ELISA blocking buffer (10uL supernatant + 990uL ELISA blocking buffer), followed by 1:2 serial dilutions down to 1:200, 1:400 and 1:800. Samples were mixed by vortexing at each step in the dilution process. After each sample was adjusted to a final volume of 500uL, 125uL of ELISA lysis solution (1X PBS + 0.05% Tween-20, 2.5% Triton X-100, 0.02% Thimerosal) was added to each sample, mixed by 8 inversions, and incubated at 37^{o}C for 30 minutes. After 30 minutes tubes were inverted 3 times, and 125uL of each dilution was added in triplicate to the ELISA plates which were washed 3 times with 200uL ELISA wash buffer just prior to the addition of sample. Plates were placed on a rotator overnight (approximately 16 hours) at 4^{o}C.

Plates were washed 3 times with 200uL ELISA wash buffer and then placed on a room temperature rotator with 100uL of biotinylated p24 antibody 31-90-25 diluted to 840ng/mL in ELISA blocking buffer for 2 hours. Plates were washed 3 times with 200uL ELISA wash buffer followed by a 1 hour incubation on a room temperature rotator with 100uL of Streptavidin-HRP (ThermoFisher Scientific #S911, Waltham, MA, USA) diluted 1:10000 in ELISA blocking buffer. Plates were washed 3 times with ELISA wash buffer followed by the final addition of 100uL per well of 37^{o}C pre-warmed Super Aqua Blue ELISA substrate **(**ThermoFisher Scientific Invitrogen #00-4203-58, Waltham, MA, USA). Plates were wrapped in foil to shield from light,

and after approximately 45 minutes were optical densities were quantified at 405nm and 600nm wavelength filters using a BioTek ELISA plate reader. Using Microsoft Excel 2016, the concentration (ng/mL) of each LPV supernatant was calculated by placing a regression line comparing quantified optical density to known concentration of the standard curve. The equation of each regression line was then used in the quantification of all samples on the plate, with normalized infection volumes being calculated from the estimated concentrations. Regression lines that provided an R^2 values above 0.9 were accepted.

293T Activation Assays

24 hours prior to infection, HEK 293T cells were passaged, counted, and plated at 125,000 cells per well in 12 well tissue culture plates (VWR International #10062-894, Mississauga, ON, Canada) in a final volume of 1mL complete DMEM. At the time of infection, viral supernatants were centrifuged at 900g for 10 min at 25°C. Each infection well had the volume of virus to be added removed and polybrene (Sigma-Aldrich, Oakville, Ontario, Canada) added to a final concentration of 8ug/mL. Plates were gently mixed through biaxial shaking in the hood before 10 minutes in a 37°C + 5% incubator. 345ng of each LPV supernatant was added to each appropriate well and gentle biaxial shaking again briefly mixed plates. A 1-hour spinoculation at 900g and 25°C occurred before plates were placed in a 37°C + 5% CO_2 incubator.

24 hours post-infection, medium was removed from each well by careful aspiration and replaced with 1mL of complete DMEM containing the appropriate latency reversing agent diluted to the correct concentration or a DMSO control that matched in volume to PMA+I. Plates were then placed back in the 37°C + 5% CO_2 incubator.

24 hours post-activation, medium was removed by aspiration, and cells were detached from the plates using 500uL 1X PBS + 5mM EDTA. Cells were centrifuged at 1000g for 10 minutes, washed with 1ml 1X PBS before being resuspended in 300uL of basic sort buffer with a pipette, and finally fixed with the addition of 300uL 4% PFA and gentle vortexing (for a final concentration of 2% PFA).

200uL of each fixed cell suspension was 40um filtered into a 96 well U-bottom plate (VWR International #10062-902, Mississauga, ON, Canada) and analyzed on a BD FACSCelesta using BD FACSDiva (Software v8.0.1). FITC channel (488nm laser, 530/30) was used to measure eGFP fluorescence. Post-acquisition analysis was performed on a separate computer using FlowJo (software v10.4.2).

Jurkat Activation Assays

24 hours prior to infection, Jurkat cells were passaged, counted, and plated at a concentration of 250,000 cells per well in 12 well plates (VWR International #10062-894, Mississauga, ON, Canada) in 500uL of complete RPMI.

Just prior to infection, complete RPMI was added to each appropriate well according to the following equation:

Volume to be added = 1mL final volume - 500uL previous media – volume of virus to be added for 345ng (as determined by ELISA results)

1uL of polybrene was added to each well for a final concentration of 8ug/mL before plates were mixed through gentle biaxial shaking and placed in the 37^{o}C + 5% CO_2 incubator for 10 minutes. During this incubation, viral supernatants were centrifuged at 900g and 25 ^{o}C for 10 minutes. 345ng of each LPV was added to each appropriate well, plates were again lightly

mixed, followed by a 1-hour spinoculation at 900g and 25^{o}C. Plates were then placed in a 37^{o}C + 5% CO_2 incubator.

24 hours post-infection, LRAs were diluted in complete RPMI to a concentration of 2X. 500uL of old media from each well was carefully removed by pipette without disturbing the suspension of Jurkat cells followed by the addition of 500uL of the complete RPMI + 2X LRA solution. Plates were then returned to the 37^{o}C + 5% CO_2 incubator.

24 hours post-activation, cells in suspension were collected by pipette from wells and centrifuged at 1000g for 10 minutes. Cells were washed with 1mL of 1X PBS before being resuspended in 300uL basic sort buffer by pipette and fixed with the addition of 300uL 4% PFA and gentle vortexing. 200uL of each fixed cell suspension was transferred into a 96 well U-bottom plate (VWR International #10062-902, Mississauga, ON, Canada) and analyzed on a BD FACSCelesta using BD FACSDiva (software v8.0.1). FITC channel (488nm laser, 530/30) was used to measure eGFP fluorescence. Post-acquisition analysis was performed on a separate computer using FlowJo (software v10.4.2).

293T Infections at 1X, 5X and 10X

The infectivity and activation of some low-infecting LPVs was tested in HEK 293T cells at greater p24 concentrations. This included the LPVs D9, E8, E9, G9, H7, H9, along with the wild type pNL4.3-Δenv-Δvif as a control. 24 hours prior to transfection, HEK 293T cells were plated in 10cm^2 dishes at a concentration of 3 million cells/dish in 10mL complete DMEM. At the time of transfection, 7500ug of LPV plasmid, 2500ug of VSVG plasmid, and 500uL of non-serum DMEM was combined in a 1.7mL Eppendorf tube and mixed through vortexing. 30uL of 1ug/uL PEI was added to each tube for a final concentration of 3ug PEI/1ug DNA, mixed

through lightly tapping 8 times on a constantly running vortex, and incubated at room temperature for 30 minutes. Old media in dishes was removed and replaced with 9.6mL of complete DMEM. After 30 minutes tubes were inverted 3 times and added dropwise to each appropriate dish. Dishes were mixed gently and placed in a 37^{o}C + 5% CO_2 incubator.

48 hours post-transfection, supernatant containing virus was collected, while cells were collected and fixed for flow analysis as described previously.

To achieve useful infection volumes, supernatants were then concentrated. One 24mL ultracentrifuge tube was prepared for each LPV transfection supernatant. Supernatant was centrifuged at 900g for 8 minutes and then 0.45um filtered into each appropriate ultra-centrifuge tube. 10mL of 20% sucrose in 1X PBS was added to the bottom of each tube, followed by the remaining approximate 4mL being filled with non-serum DMEM. Tubes were then ultra-centrifuged at 100,000G, 4^{o}C, acceleration 5 and deceleration 5 for 3 hours using a 70-Ti rotor (Beckman Coulter #337922, Mississauga, ON, Canada) in an L-100XP ultracentrifuge (Beckman Coulter #969347, Mississauga, ON, Canada). Supernatant was removed by aspiration and viral pellet resuspended in 500uL of complete DMEM. The above protocol for p24 ELISA to determine p24 concentration was followed with dilutions of supernatant changed to 1:500, 1:1000 and 1:2000. The above protocol for HEK 293T infection, activation and fixations was then followed, with infections being performed with 345ng, 1715ng, and 3435ng of p24.

Integration

To determine the levels of integration among each of the LPVs in the pNL4.3-Δenv-Δvif backbone, the above Jurkat Activation assays were repeated with the following three

activation conditions: No LRA activation (DMSO mock activation), 10ng/mL PMA + 1uM Ionomycin, or 50nM Panobinostat. 24 hours post-activation, cells were collected with 1X PBS + 5mM EDTA and centrifuged at 500g x 5min. Cells were then resuspended in 1mL 1X PBS and split by volume with 1/3 going towards flow cytometry fixation as previously described and the remaining 2/3 going towards gDNA extraction. The 2/3 for gDNA extraction were centrifuged at 17,000g for 1min and 1X PBS aspirated off. gDNA of cells was extracted using Wizard gDNA Purification Kit (Promega #A1120). gDNA was resuspended in 100uL of gDNA rehydration buffer and rehydrated overnight at room temperature.

gDNA samples were primarily diluted in RNAse/DNAse sterile water to 10ng/mL aliquots. A two stage Alu-qPCR reaction was performed to assess levels of integrated HIV-1. The first stage was an Alu PCR between the Alu regions of the cellular genome and the U5 region of the HIV-1 LTR. The following were the conditions for this first stage PCR reaction: 50ng gDNA, 2uL Primestar GXL, 10uL 5X Primestar GXL Buffer, 4uL dNTPs, 26uL sterile water, 0.2uM Alu1 primer, 0.2uM Alu2 primer and 0.2uM Lambda R U5 Rev 1 primer (see Table 2 in Appendix 1 for primer sequences). Reactions were placed in a semi-skirted qPCR 96 well plate and centrifuged at 900g x 2min to bring liquid down to bottom of well. PCRs were run in an Eppendorf Vapo.Protect Pro S Mastercycler. Alu PCR settings were as followed: 94 ^{o}C for 1min; followed by 30 cycles of 98 ^{o}C for 10sec, 55 ^{o}C for 15 sec and 68 ^{o}C for 10min; followed by a final 68 ^{o}C for 10min and 10 ^{o}C hold.

Alu PCR amplified results were diluted 1/10 in DNAse/RNAse free sterile water. The second round was an LTR or Actin qPCR. LTR qPCRs were performed by taking 5uL of 1/10 diluted first round product, 10uL of 2X PowerUp SYBR Green Master Mix (Thermo Fischer Sci. Ref#

A25742), 0.2uM lambda R Rev 2 primer, 0.2uM late U3 Fwd primer, 50nM LTR Probe and 3.75uL sterile water. Actin qPCRs were performed by taking 5uL of 1/10 diluted first round product, 10uL of 2X PowerUp SYBR Green Master Mix, 0.2uM Actin 1 primer, 0.2uM Actin 2 primer, 50nM Actin Probe and 3.75uL sterile water Reactions were added to a 96 well plate and centrifuged at 900g for 2min. LTR qPCR reactions were performed at the following protocol: 95 ^{o}C for 3min; 60 cycles of 95 ^{o}C for 15sec, 60 ^{o}C for 30sec and 72 ^{o}C for 30sec; followed by a melt curve of 95 ^{o}C for 15sec, 60 ^{o}C for 1min and 95 ^{o}C for 15 sec. Results were first normalized by actin results which controlled for loading volumes. Secondly, the integration levels of all LPVs were compared to the wild-type, unactivated control that was present on every plate run. Finally, the mean integration of the unactivated LPVs was set to 1.0, with all other samples normalized by this value.

CXCR4 and CCR5 LPV Cloning

In order to move into a system that allows for multiple rounds of infections, our mutated LTRs needed to be cloned out of a non-replicative pNL4.3-Δenv-Δvif plasmid and into a fully replicative pNL4 CXCR4-tropic or pNL4 CCR5-tropic plasmid. A CXCR4 plasmid backbone was chosen as the first option for cloning because the majority of the viral infection cycle takes place in a CXCR4-tropic configuration where infectivity levels and disease progression markers are very high (194–196). We also saw higher preliminary levels of infection by the CXCR4-tropic pNL4 compared to our CCR5-tropic virus.

To accomplish this transition, we used a simple cut and paste cloning strategy using a NcoI cut site downstream of the 3’ end of the 3’ LTR and an XhoI cut site upstream of the 5’ end of the 3’ LTR (within Nef). Mutated 3’ LTRs were cut out of pNL4.3-Δenv-Δvif plasmids with

20U of NcoI-HF and 20U of XhoI. Products were electrophoresed on a 0.6% agarose gel and gel purified using the E.Z.N.A. Gel Extraction Kit (Omega BioTek D2500-02). Purified inserts were cloned into a pNL4.3 CXCR4-tropic digested backbone at a 5:1 ratio using T4 DNA Ligase (NEB #M0202S) at 16 °C overnight. Transformations of products were performed in Stbl-2 E-coli cells using LB-Ampicillin plates. Colonies were picked and viral miniprep stocks generated as stated above under "latency prone virus plasmid creation".

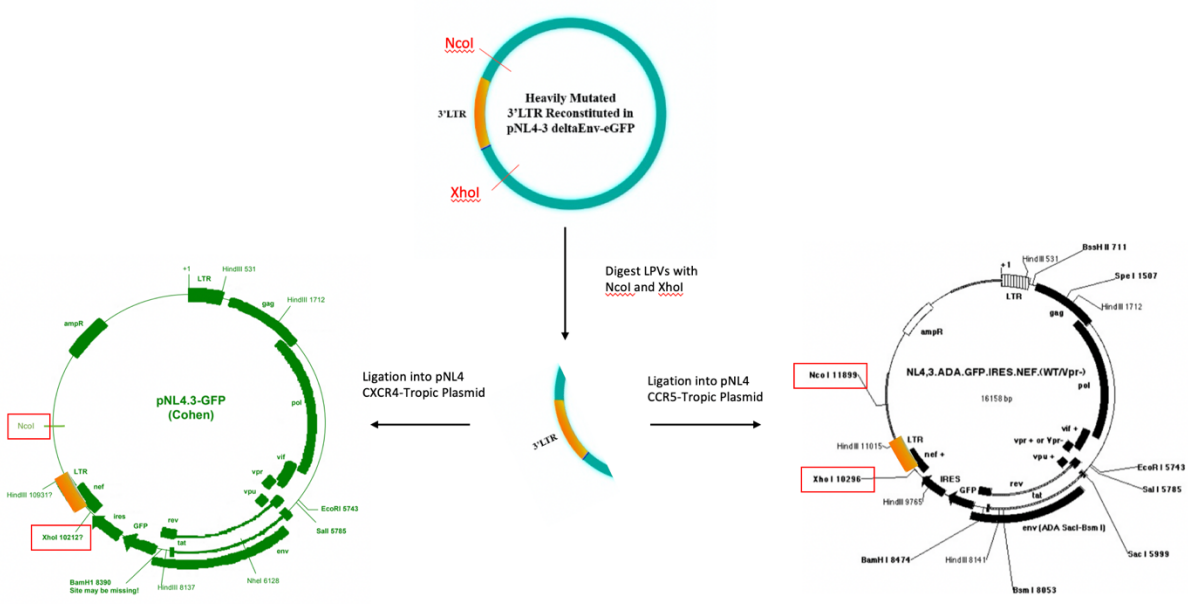

Figure 8 Cloning of LTRs into Replicative HIV-1 Backbone. *LTRs of LPVs were cloned from a non-replicate pNL4-Δenv-Δvif plasmid into a fully replicative, CXCR4-tropic or CCR5-tropic NL4 plasmid. XhoI in the Nef and NcoI in the plasmid were used in the excision and ligation. See 'CXCR4 and CCR5 LPV Cloning' in Materials and Methods for full details.*

Evolution Experiment-Constant Conditions

The previously stated viral transfection protocol was used to generate replicative, latency prone viral supernatants. The above ELISA p24 quantification protocol was used to determine the concentration of virus in the transfection supernatant.

6 hours prior to infection, 100,000 U87 cells were plated in 500uL of complete DMEM (without antibiotics) in a 12 well. At the time of infection, wells were topped up with complete DMEM by the following equation:

Media to be added = 1mL final volume - 500uL plated - volume of virus equal to 25ng p24

1uL of 1000X Polybrene was added to each well. Cells were biaxially mixed for 30 seconds and placed at 37 ^{o}C for 10min. During this 10 min incubation viral transfection supernatants were also warmed at 37 ^{o}C. 25ng of p24 of each LPV supernatant was then added dropwise to each appropriate well (in duplicates), followed by gentle biaxial shaking. Plates were spinoculated at 900g for 1hr at 24 ^{o}C. Plates were then placed in 37 ^{o}C +5% CO_2 incubator.

24 hours post-infection, all media was removed from each well. 1mL of 1X PBS was gently placed in each well to help remove residual media/virus, then also removed by pipette. One duplicate well for each LPV was then given 1.5mL complete DMEM + 5ng/mL PMA + 0.5uM Ionomycin. The second duplicate well of each LPV was given 1.5mL complete DMEM containing DMSO controlled to the volume of PMAI added.

18 hours post-activation with PMA+I, media containing PMAI was removed followed by a 1mL 1X PBS wash. 1X PBS was removed and 1.5mL complete DMEM added to each well and placed back into incubator.

7 days post-infection, 6 days post-activation, media from wells was collected and centrifuged at 500g x 5min. Media was then filtered through 0.45um filter into a new tube to remove cellular debris and kept at 4 ^{o}C overnight. 1.5mL of complete DMEM without any LRAs added to each well and plates returned to 37 ^{o}C incubator for another 7 days. On the same day

12,500 Ghost cells were plated in 500uL complete DMEM without antibiotics in a 24 well plate.

24 hours post-Ghost plating, 0.75uL 1000X polybrene was added to each well, gently biaxially shaken, and placed in 37 ^{o}C incubator for 10 min. During this 10 min period, filtered day 7 supernatants were warmed in 37 ^{o}C incubator also. After 10 min, 250uL of LPV supernatant added to each Ghost well, plates were biaxially shaken and spinoculated at 900g for 1 hr at 24 ^{o}C. Infection plates were then placed in 37 ^{o}C incubator for 72 hours. The remainder of filtered supernatants were then placed at -20 ^{o}C until RNA isolation was ready to be performed.

72 hours post Ghost infection, infected Ghost cells were picked up using 500uL 1X PBS +5mM EDTA and centrifuged at 500g for 5 min. Cells were washed with 1mL of 1X PBS and centrifuged again. Cells were then fixed with 200uL of basic sort buffer and 200uL 4% PFA. Cells were analyzed on a BD FACSCelesta using BD FACSDiva (software v8.0.1). FITC channel (488nm laser, 530/30) was used to measure eGFP fluorescence from the Ghost cells. Post-acquisition analysis was then performed on a separate computer using FlowJo (spftware v10.4.2). The number of Ghost cells that had become infected with virus released from U87 cells was calculated as a percentage out of 100.

Supernatant was removed and replaced from the U87 primary infected cells on a weekly basis according to the above protocol. The process was continued for 4-5 weeks. Ghost cells were continually used as above for measuring viral output.

Evolution- Biweekly Transferring

The previously stated viral transfection protocol was used to generate supernatant containing replicative LPVs. The above ELISA p24 quantification protocol was used to determine the concentration of virus in the supernatant for tittering purposes.

100,000 U87 cells were plated in 500uL of complete DMEM (without antibiotics) in a 12 well, 6 hours prior to infection. At the time of infection, wells were topped up with complete DMEM by the following equation:

Media to be added = 1mL final volume - 500uL plated - volume of virus equal to 25ng p24

1uL of 1000X Polybrene was added to each well. Cells were biaxially mixed for 30 seconds and placed at 37 ^{o}C for 10min. During this 10 min incubation viral transfection supernatants were also warmed at 37 ^{o}C. 25ng of p24 of each LPV supernatant was then added dropwise to each appropriate well (in duplicates), followed by gentle biaxial shaking. Plates were spinoculated at 900g for 1hr at 24 ^{o}C. Plates were then placed in 37 ^{o}C +5% CO_2 incubator.

24 hours post-infection, all media was removed from each well. 1mL of 1X PBS was gently placed in each well to help remove residual media/virus, then also removed by pipette. One duplicate well for each LPV was then given 1.5mL complete DMEM + 5ng/mL PMA + 0.5uM Ionomycin. The second duplicate well of each LPV was given 1.5mL complete DMEM containing DMSO controlled to the volume of PMAI added.

18 hours post-activation with PMA+I, media containing PMAI or DMSO was removed followed by a 1mL 1X PBS wash. 1X PBS was removed and 1.5mL complete DMEM added to each well and placed back into incubator.

7 days post-infection, 6 days post-activation, media from wells was removed from cells and centrifuged at 500g x 5min. Media was then filtered through 0.45um filter into a new tube and kept at 4 ^{o}C overnight. 1.5mL of complete DMEM without any LRAs added to each well and plates returned to 37 ^{o}C incubator for another 7 days. On the same day 12,500 Ghost cells were plated in 500uL complete DMEM without antibiotics in a 24 well plate.

24 hours post Ghost plating, 0.75uL 1000X polybrene added to each well, gently biaxially shaken, and placed in 37 ^{o}C incubator for 10min. During this 10 min period, filtered day 7 supernatants were warmed in 37 ^{o}C incubator also. After 10 min 250uL of LPV supernatant was added to each Ghost well, plates were biaxially shaken and spinoculated at 900g for 1 hr at 24 ^{o}C. Infection plates were then placed in 37 ^{o}C incubator for 72 hours. The remainder of filtered supernatants were then placed at -20 ^{o}C until RNA isolation was ready to be performed.

72 hours post Ghost infection, infected Ghost cells were picked up using 500uL 1X PBS +5mM EDTA and centrifuged at 500g for 5 min. Cells were washed with 1mL of 1X PBS and centrifuged again. Cells were then fixed with 200uL of basic sort buffer and 200uL 4% PFA. Cells were analyzed on a BD FACSCelesta using BD FACSDiva (software v8.0.1). FITC channel (488nm laser, 530/30) was used to measure eGFP fluorescence from the Ghost cells. Post-acquisition analysis was then performed on a separate computer using FlowJo (software v10.4.2). The number of Ghosts cells that had become infected by virus produced from the U87-primary infected cells was calculated as a percentage out of 100.

14 days post initial U87 infection, 100,000 U87 cells were plated in 500uL complete DMEM in a 12 well plate. 6 hours after U87 plating, viral supernatants were removed and filtered as

previously described for day 7, with 14 day old U87 cells safely discarded. 1uL of 1000X Polybrene was added to each newly plated U87 well and incubated for 10 min at 37 ^{o}C. 500uL of day 14 supernatant containing released LPVs was then added dropwise to new U87 cells and biaxially mixed. Plates were centrifuged at 900g for 1hr at 24 ^{o}C, then placed in 37 ^{o}C incubator. 12,500 Ghost cells plated in 500uL complete DMEM in a 24 well as before.

24 hours post U87 supernatant transfer (day 15), media containing mix of new and old media containing virus was removed, followed by a 1mL 1X PBS wash. 1.5mL of complete DMEM without any LRA or antibiotics was replaced into each well and cells not touched for another 6 days until day 21. 250uL of day 14 supernatant was used to infect Ghost cells as previously described for 72 hours, with remaining viral supernatant placed at -20 ^{o}C.

This protocol was repeated on a 2 week rotation for 4-5 weeks (2+ transfers) with supernatants being collected from infected U87 cells every 7 days and collected supernatant being transferred to new U87 cells every 14 days. Ghost cells were continued to be used as above for measuring viral output.

Viral RNA Isolation

U87 supernatants containing released virus from evolution experiments was kept at -20^{o}C between the time point of the experiment and the time for RNA extraction. Samples were thawed and centrifuged at 1000g for 5 min. 134uL of U87 supernatant sample was then added to 15uL of 10X DNAse (RNAse free) buffer and 1uL of DNAse for a final volume of 150uL in 1.5mL Eppendorf tubes. Tubes were mixed by tapping 10 times and then placed in a 37 ^{o}C incubator for 1 hr.

After 1 hr, DNAse-treated samples were cooled to room temperature and 140uL of sample processed through the QIAamp viral RNA mini kit (Qiagen #52909) to isolate RNA. RNA was resuspended in 60uL AVE elution buffer and stored at -20 ^{o}C. RNA will be sent for RNA sequencing to determine if there are any sequential changes to the genetic sequence of each LPV at specific time points throughout the experiments.

Results

LTR Mutations

A subset of 12 LPVs were selected which contained a broad range and localization of G→A mutations within their 5'LTRs. To confirm the locations of the LTR mutations within the subset of LPVs that I would be testing, LTRs were sequenced with primers NL4 Pre/Post XhoI For and NL4 3LTR Rev (see Table 2 in Appendix 1). Plasmids underwent Sanger sequencing at Genome Quebec and resulting sequences were aligned and analyzed using Sequencer 4.10.1 software (Gene Codes Corp., Ann Arbor, Michigan, USA).

Mutations in the viral LTR were defined as G→A transition mutations that had been introduced through A3G or A3F exposure as described in Appendix #3 protocols. Table 1 and Figure 9 highlight the overall number, dispersion and specific location of the introduced G→A mutations within the LPV subset. LPVs displayed varying levels of overall mutation counts, as well as different mutation locations and patterns. All LPVs, with the exception of B7 and C6B, had at least one mutation in each of the three sub-regions of the LTR, with the U3 subregion containing the most mutations for all LPVs.

Table 1 Location of LTR Mutations Within Each Latency Prone Virus.

Purple refers to mutations located in the U3 of the 3' LTR, green for mutations in the R region of the 3' LTR and yellow for mutations in the U5 region of the 3' LTR. Numbering begins at the 5'end of LTR.

LPV	Total # of LTR Mutations	Mutation Locations
B7	5	6, 246, 255, 394, 620
B10	9	3, 7, 99, 350, 375, 393, 454, 485, 620
C6B	7	2, 3, 242, 244, 402, 620, 621
C9	17	3, 6, 7, 350, 351, 363, 364, 399, 400, 454, 485, 505, 542, 583, 591, 620, 621
D3	7	2, 156, 226, 246, 485, 620, 621
D9	21	2, 3, 7, 99, 106, 129, 240, 365, 384, 393, 399, 400, 464, 479, 485, 496, 505, 542, 583, 620, 621
E8	38	99, 106, 225, 230, 255, 259, 267, 298, 300, 311, 312, 350, 351, 364, 365, 375, 376, 389, 393, 394, 399, 400, 401, 402, 409, 454, 455, 464, 479, 485, 486, 496, 505, 506, 542, 583, 620, 621
E9	19	49, 105, 106, 129, 133, 156, 167, 350, 363, 364, 389, 393, 399, 400, 454, 455, 485, 583, 620
F8	10	2, 106, 240, 259, 350, 393, 454, 485, 620, 621
G9	9	6, 7, 364, 389, 399, 400, 454, 620, 621
H7	18	2, 7, 106, 240, 262, 350, 364, 389, 393, 399, 454, 455, 479, 485, 542, 583, 620, 621
H9	18	6, 66, 99, 106, 107, 129, 133, 255, 259, 364, 389, 393, 400, 401, 402, 464, 620, 621

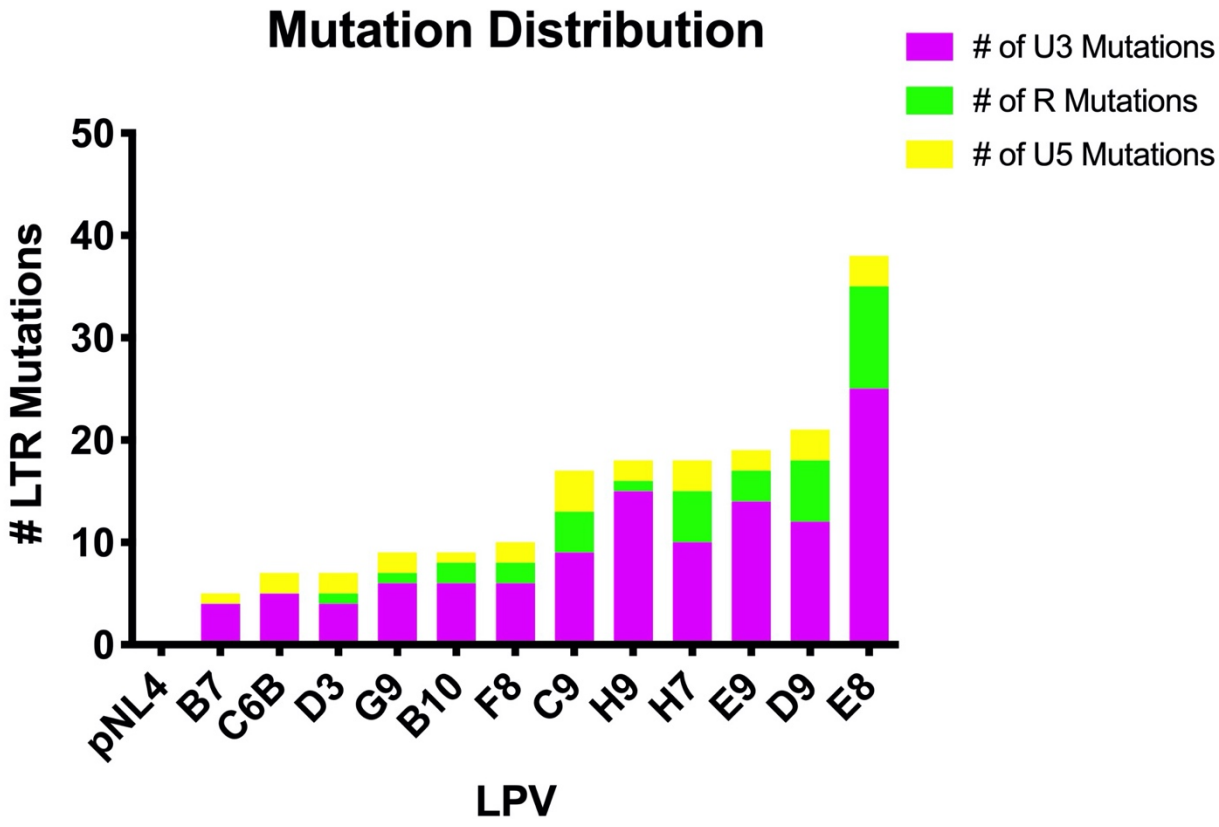

Figure 9 Distribution of G →A Mutations Within the LTR Subregions. *5'LTRs of each LPV were sequenced in both the forward and reverse direction through Sanger Sequencing by Genome Quebec. Mutations were classified by the conversion of a guanine base into an adenine base within the 5' Long Terminal Repeat region of each virus. U3 region represents bases 1-453, R represents bases 454-549 and U5 represents bases 550-634.*

Flow Cytometry vs ELISA p24 Quantification of Transfections

Propagation of virions was achieved by the co-transfection of pNL4.3-Δenv-Δvif plasmids, containing unique LTR mutation patterns, with VSVG plasmid at a 3:1 ratio in HEK 293T cells. An eGFP reporter gene inserted inside the truncated envelope glycoprotein expressed within transfected cells allowed for the number of cells expressing viral proteins to be calculated by flow cytometry, quantifying the number of eGFP+ cells. Transcription levels were then normalized to the wild type pNL4.3-Δenv-Δvif (herein referred to as pNL4) as 100 (Figure 10). Due to the different levels of virus being produced from each LPV transfection, subsequent infections performed using LPV transfection supernatants necessitated normalization by viral quantity.

Viral titres were estimated using a p24 sandwich ELISA with two different in-house antibodies for p24: clone 183-H12-5C for plate coating/viral capture and biotinylated clone 31-90-25. Detection of btn-31-90-25 was enabled with a streptavidin-HRP followed by Super Aqua Blue ELISA detection substrate. The functionality of both antibodies and successful biotinylation of 31-90-25 had previously been confirmed in the lab via western blotting (not shown). p24 concentrations were calculated for each LPV supernatant using a known p24 standard and used to normalize infections to 345ng of p24. The ELISA was successful in determining the concentration of virus released form each LPV transfection, and ELISA concentrations matched very similarly to eGFP expression levels post transfection when both were normalized. No significant difference was observed between ELISA quantification of p24 in viral supernatants and cellular transfection levels post normalization to 100 (Figure 10). No correlation was found between the number of LTR mutations within each LPV and their

relative transfection outputs measured through either the ELISA or flow cytometry (Figure 24).

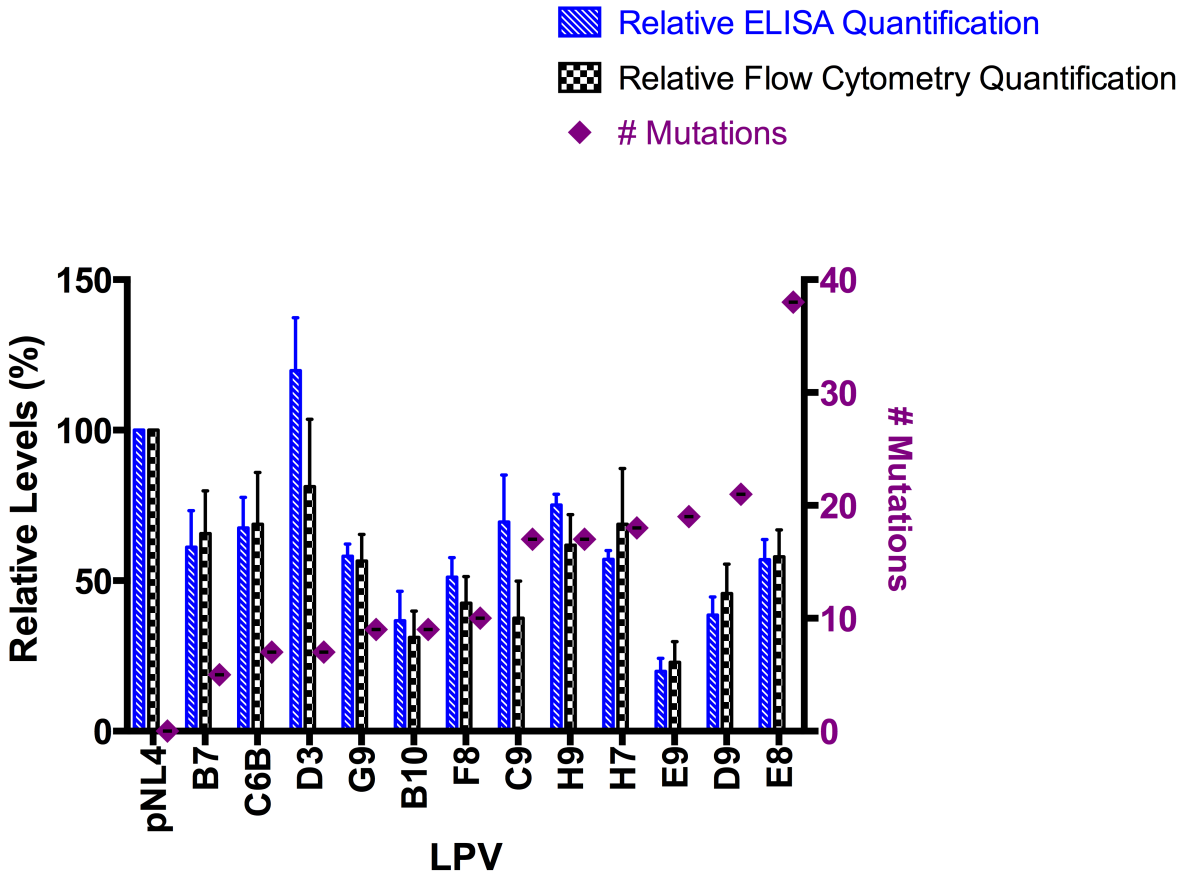

Figure 10 Normalized Viral Supernatant Concentrations & Internal Viral Transcription vs LTR Mutation Counts. *HEK 293T cells were co-transfected by 1125ng LPV plasmid and 375ng VSVG for 72 hours at 37°C +5% CO_2. Cells were collected, fixed and analyzed by flow cytometry to determine the % of eGFP+ cells. Viral supernatant was collected and LPV concentrations (ng/mL) were measured by a p24 sandwich ELISA using a p24 standard curve. All values were normalized to pNL4 values = 100. Mutation numbers were previously determined intra-lab by sequencing of plasmids. N=6 for transfection and ELISA. Student's T test performed comparing the normalized ELISA and transfection means within each individual LPV. No significant difference found for any LPV ($p > 0.05$ for all LPVs).*

In Vitro Infections

Infections were performed using 345ng of p24 of each LPV and pNL4 in both the HEK 293T and Jurkat cell lines. Infections proceeded for 24 hours before infected cell populations were activated for a subsequent 24 hour period with various LRAs or DMSO as an unactivated control. Activation levels were determined via flow cytometry by measuring eGFP expression levels. Mean fluorescence intensity was also collected on eGFP+ cells to measure the intensity of the protein expression post-activation. Percent activations for both Mean FI and eGFP+ levels were calculated for every condition by the following equation:

% Activation = (Activated – Unactivated) / Unactivated x 100% (Figures 13 and 15).

Activations using each LRA were performed in triplicates for both cell lines.

All LPVs demonstrated significantly lower baseline levels of eGFP expression compared to the wild-type control pNL4 (Figure 11) in both HEK 293T and Jurkat cells. In both HEK 293T and Jurkat cells, LPV unactivated infection levels were moderately inversely correlated to the number of LTR mutations in an exponential manner. This inverse correlation provided an R2 value of 0.7614 in HEK 293T cells and 0.7609 in Jurkat cells (Figures 11 and 25).

After an activation of 24 hours with PMA+I, the subset of LPVs demonstrated various levels of expression, as well as percent increases, of eGFP expression (Figure 12). This result was seen in both HEK 293T and Jurkat cells, with Jurkat cells seeing a greater percent increase in viral protein expression likely due to their lower starting infection levels (Figure 13). Most importantly, the response of each individual LPV to PMA+I did not follow on any trend as it related to the overall number of promoter mutations. Although LPVs with more promoter mutations could not match the LPVs with fewer mutations when it came to the overall

number of cells expressing eGFP, LPVs with higher number of mutations often providing greater percent activation responses. This suggests that the different mutation profiles in the viral LTR were having an effect on the ability for each individual promoter to respond to the PMA+I that was dependent on the location and number of mutations.

Figure 14 demonstrates the response of each LPV within Jurkat cells to the eight tested LRAs as it pertains to both the overall number of cells expressing eGFP post-activation, as well as the levels of viral protein expression on a per cell basis as measured by the eGFP mean fluorescence intensity (MFI). The greater the intensity of the eGFP MFI, the greater the amount of viral protein transcripts that are being transcribed and translated as both are under the control of the LPV promoter. See Table #3 in Appendix 3 for all LRA concentrations used.

For all LPVs, PMA+I induced the greatest levels of viral activation among all LRAs tested for percentage of cells expressing eGFP as well as for MFI. The HDAC inhibitors Panobinostat, Vorinostat and Romidepsin were the only LRAs capable of matching PMA+I, with B10 being the only LPV that responded better to the HDAC inhibitors than to PMA+I (Figure 14). ATRA and Valproic Acid failed to demonstrate noticeable levels of activation while Bryostatin-1 and Disulfiram demonstrating moderate activation levels. There were no major patterns of activation that linked a mutation pattern to only responding to one class of LRA.

When comparing the activation of the wild type pNL4 within the HEK 293T and Jurkat cells, HEK 293T cells demonstrated greater percent activation than Jurkat cells in responses to all LRAs except for Bryostatin-1 (Figure 15). Statistical comparisons were not performed between HEK 293T and Jurkat cells as it related to the baseline levels of infection nor percent

activation of wild-type pNL4 as the two cell lines underwent differing infection protocols and p24:cells ratios (Figure 15).

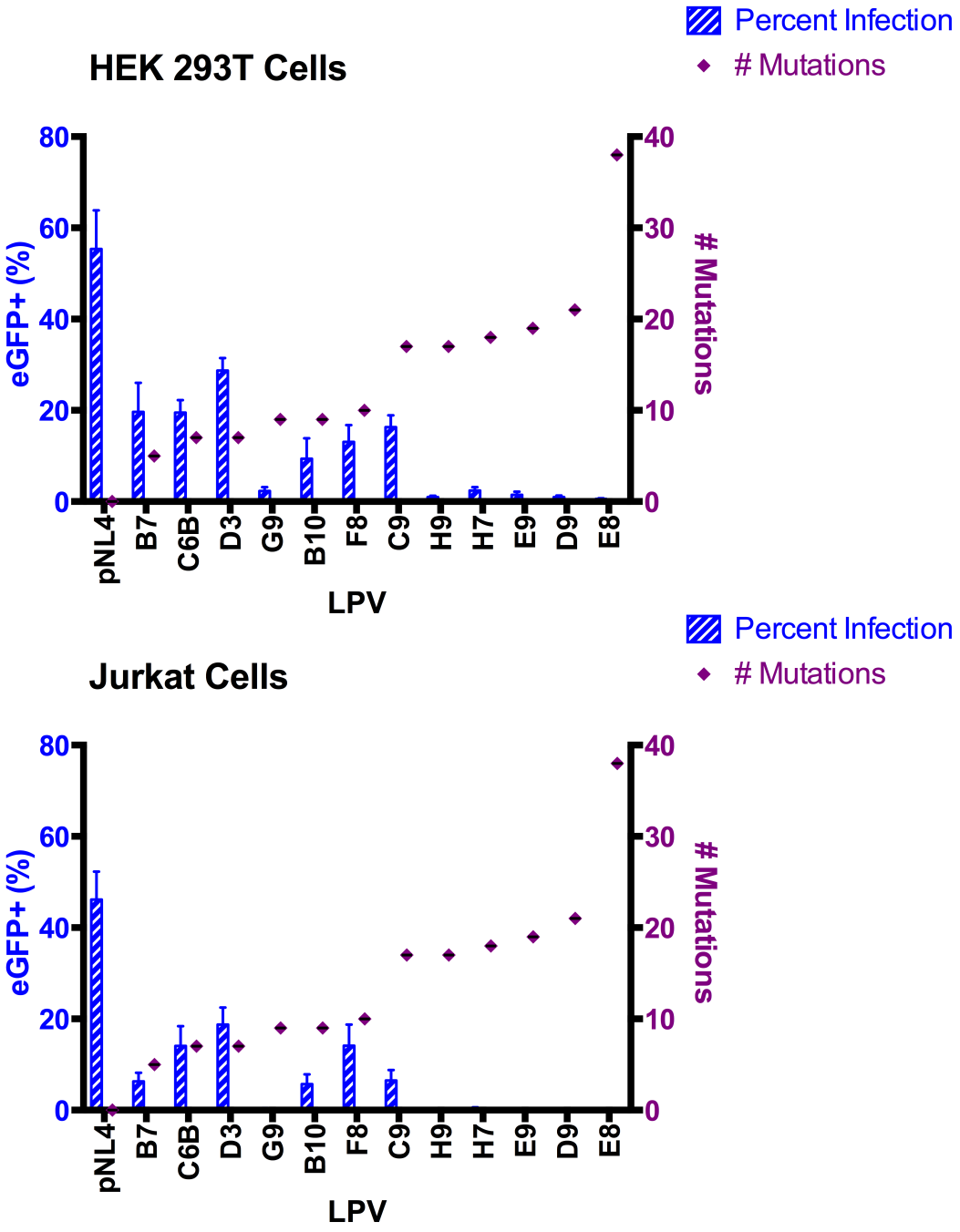

Figure 11 Comparison of Latency Prone Viral Mutation Counts to Baseline Infection Levels within HEK 293T and Jurkat Cells ***HEK 293T*** *or* ***Jurkat cells*** *were infected with 345ng of p24 from all LPVs. Spinoculation was performed at 900g and 25°C for 1hr. 48hr post infection cells were fixed with 2% PFA and number of eGFP+ cells determined by flow cytometry. The number of LPV mutations was previously determined by LPV sequencing. N=3. Student's T test performed between the levels of eGFP post pNL4 wild type infection and that of each individual LPV. All LPVs demonstrated a significantly different infection level when compared directly to pNL4.* $p \leq 0.05$.

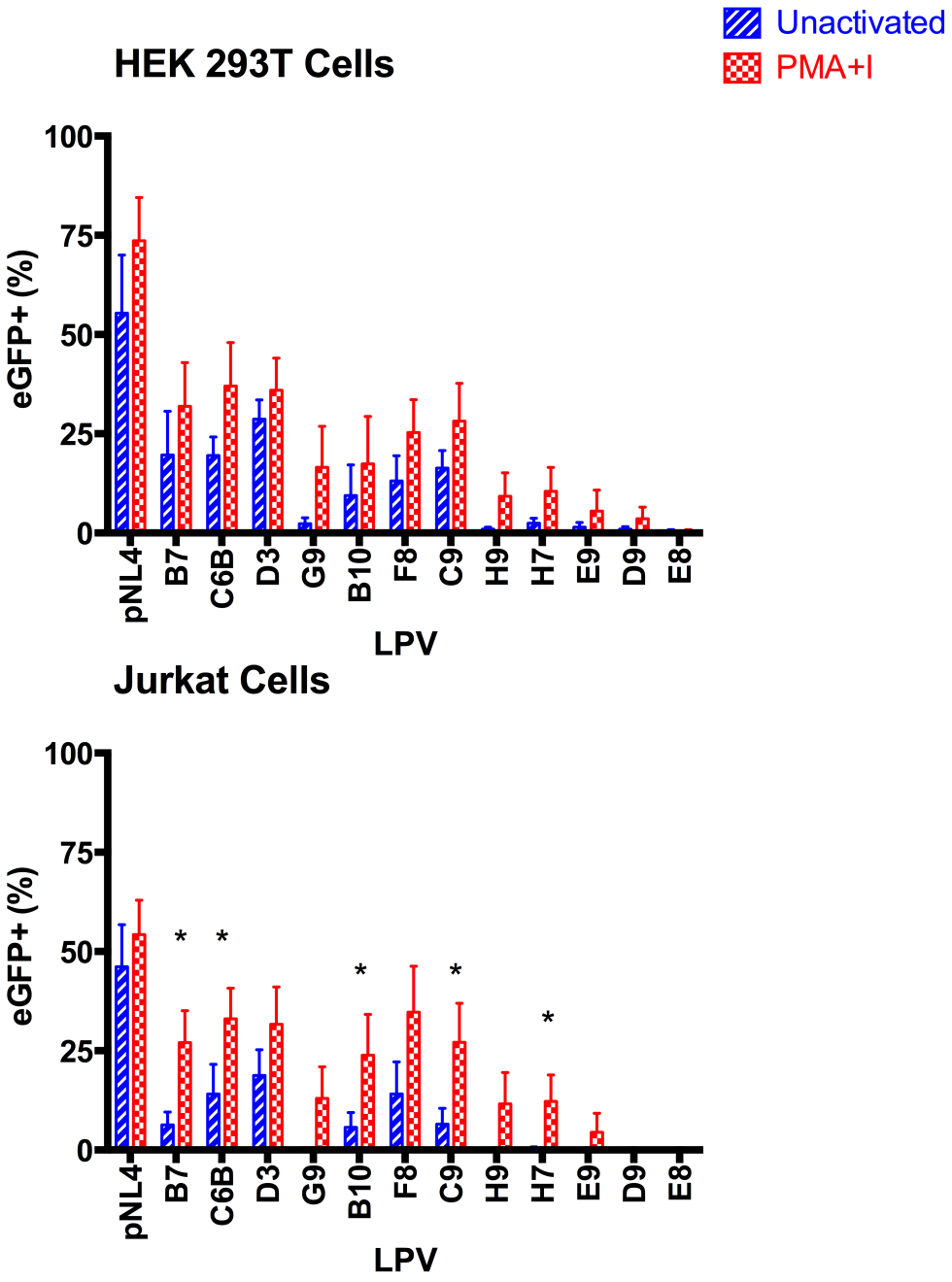

Figure 12 Activation of Latency Prone Viruses within HEK 293T and Jurkat Cells by PMA+I. ***HEK293T*** *or* ***Jurkat cells*** *were infected with 345ng of p24 from all LPVs. Spinoculation was performed at 900g and 25°C for 1hr. 24 hours post infection, 10ng/mL PMA + 1uM Ionomycin was diluted and added for a 24 hour activation. Cells were fixed with 2% PFA and number of eGFP+ cells determined by flow cytometry. N=3. Student's T tests performed for every LPV individually between the unactivated and PMA+I-activated conditions. No significant difference found in the HEK 293T activations when p > 0.05. However in the Jurkat cells five LPVs showed statistical significant differences. * = p ≤ 0.05.*

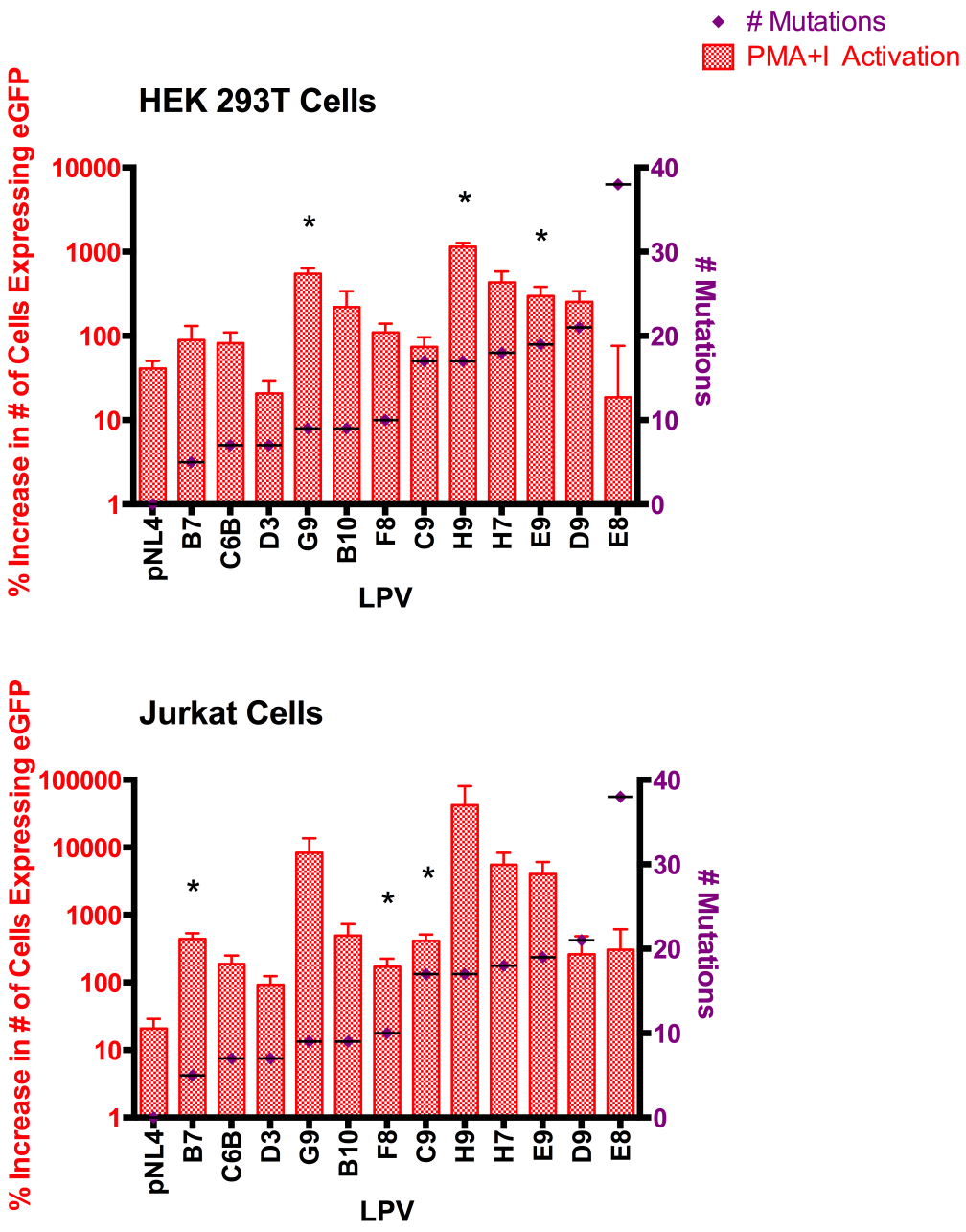

Figure 13 Percent Increase in Number of Cells Expressing eGFP Post Activation by PMA+I. HEK 293T *and* ***Jurkat Cells*** *were infected with 345ng of p24 from all LPVs. Spinoculation was performed at 900g and 25°C for 1hr. 24 hours post infection, PMA+I was diluted to 10ng/mL PMA + 1uM Ionomycin for a 24hr activation. Cells were fixed with 2% PFA and number of eGFP+ cells determined by flow cytometry. % Increase was determined by comparison of the percentage of cells expressing eGFP after PMA+I activation of infected cells vs percentage of cells expressing eGFP post DMSO mock activation. Number of LPV mutations was previously determined intra-lab. N=3. Student's T test performed between pNL4% increase and each LPV's % increase individually. * = p ≤ 0.05.*

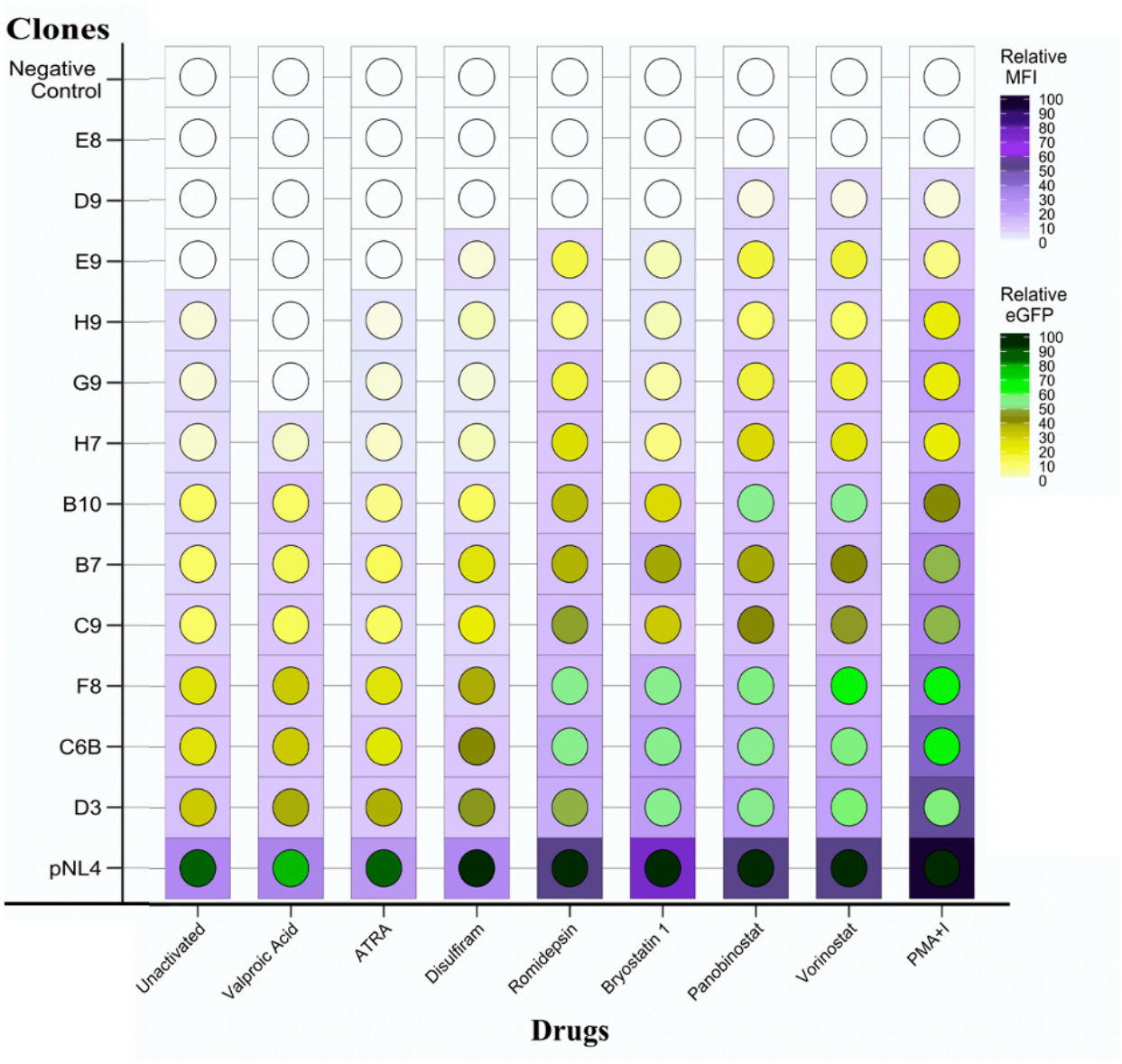

Figure 14. Comparison of Latency Prone Virus Activation by 8 Latency Reversing Agents in Jurkat Cells. *Jurkat cells were infected with 345ng of p24 from all LPVs. Spinoculation was performed at 900g and 25°C for 1hr. 24 hours post infection, cells were exposed to LRAs for 24hr activation. Cells were fixed with 2% PFA and number of eGFP-expressing cells and the eGFP mean fluorescence intensity was determined by flow cytometry. N=3. Circle shading represents the number of cells expressing eGFP post-activation by an LRA, while square shading represents the intensity of viral protein expression post-activation.*

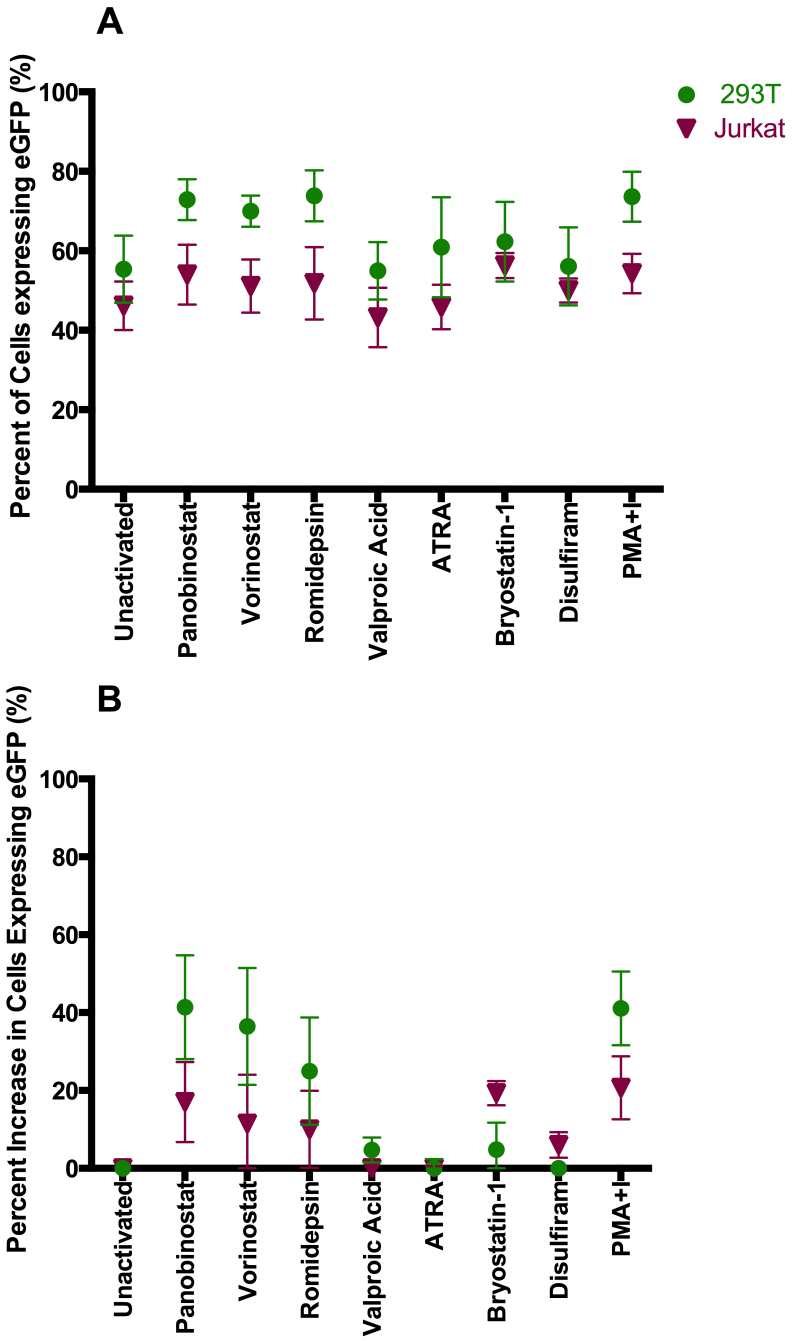

Figure 15 Comparing the Response of Wild Type HIV-1 to 8 Latency Reversing Agents In HEK 293T and Jurkat Cells. *HEK 293T and Jurkat cells were infected with 345ng of p24 from all LPVs. Spinoculation was performed at 900g and 25°C for 1hr. 24 hours post infection, cells were exposed to LRAs for 24hr activation. Cells were fixed with 2% PFA and* ***A)*** *% of cells expressing eGFP was determined by flow cytometry.* ***B)*** *% Increase in cells expressing eGFP was determined by the comparison of the percentage of cells expressing eGFP after LRA activation vs the percentage of cells expressing eGFP post DMSO mock activation (unactivated). N=3.*

Increasing Infection and Activation

Some of the LPVs demonstrated extremely low levels of infection and activation when infections were performed at 345ng of p24. To determine if these LPVs would show larger/detectable infection and activation at higher concentrations of virus, infection and PMA+I activation assays were repeated in HEK 293T cells with increasing amounts of virus. This included the LPVs D9, E8, E9, G9, H7, and H9. Bulk transfections were performed for each LPV followed by concentration of viral supernatants using an ultra-centrifuge. Infections were performed for each LPV with 345ng of p24 (1X), 1725ng (5X), and 3450ng (10X) (10X E9 sample was excluded due to lack of virus). Activation with PMA+I was performed as usual for 24 hours (Figure 16). Each LPV successfully activated viral transcription as observed by the increase in the number of eGFP+ cells post activation. Secondly, as the amount of virus used to infect with increased, no infection plateau was reached in any case. Therefore, all six of the low-expressing LPVs were still transcriptionally competent and able to respond to PMA+I, however more virus was needed within this smaller LPV subset to obtain readily-detectable levels of eGFP+ cells post infection and activation.

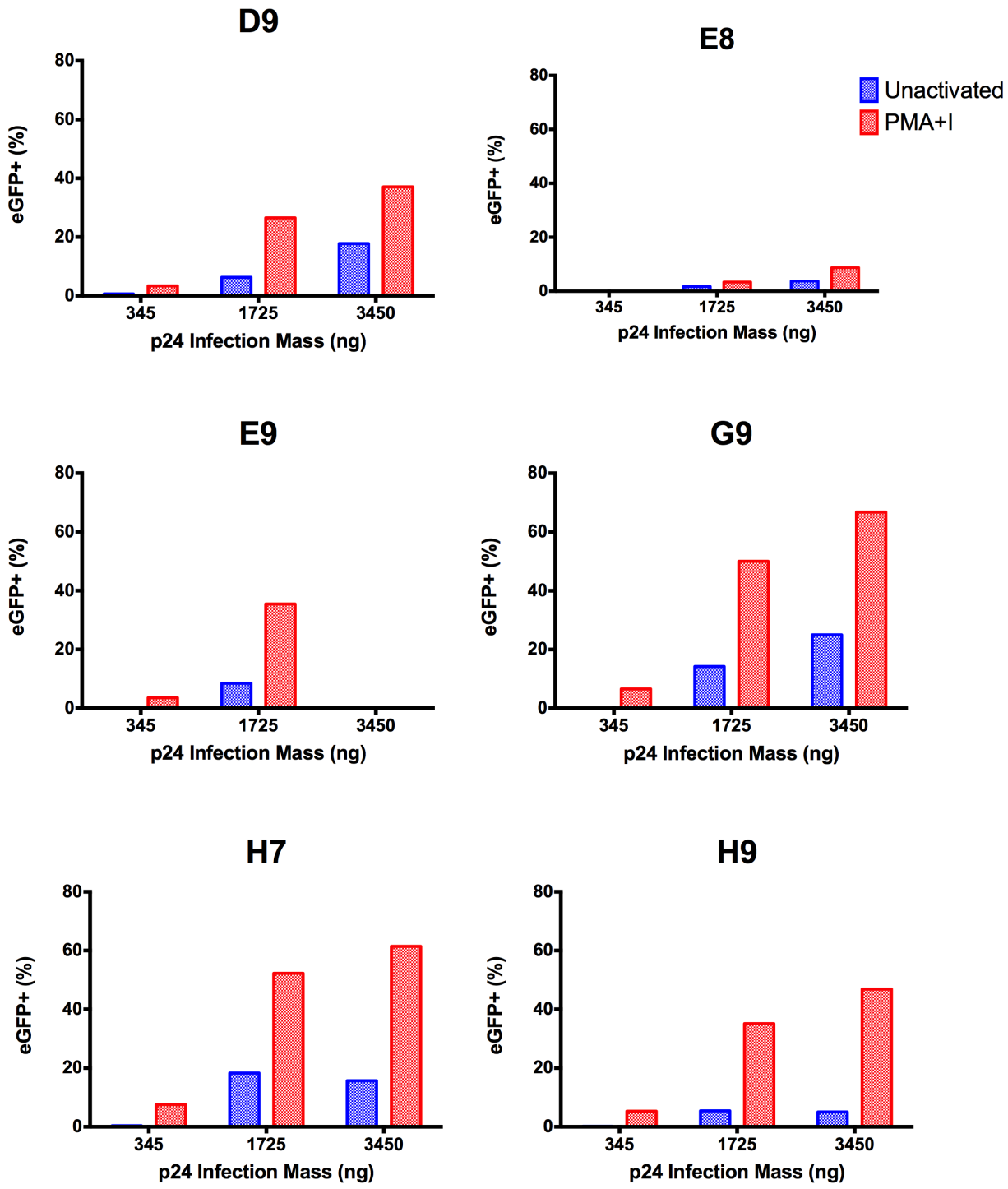

Figure 16 Activation of Low-Transcribing Latency Prone Viruses by PMA+I at Increasing p24 Quantities. *HEK 293T cells were infected with concentrated 345ng, 1725ng, or 3450ng of p24 from 6 LPVs that had shown previous low levels of infectivity. Spinoculation was performed at 900g and 25°C for 1 hr. 24 hours post infection, PMA+I was diluted and added for a 24 hour activation. Cells were fixed with 2% PFA and number of eGFP+ cells determined by flow cytometry. N=1*

Viral Integration

To determine if the variances in viral activation were due to a difference in response to the LRAs or due to a difference in preliminary viral integration, a two-step Alu-qPCR was performed. Jurkat cells were infected with each LPV or pNL4 as previously described, and activated by 50nM Panobinostat, 10ng/mL PMA + 1uM Ionomycin, or DMSO as a negative control. 24 hours post activation, 1/3 of each cell population was analyzed by flow cytometry to confirm activation profiles, while the remaining 2/3 of cells had their gDNA isolated. A preliminary Alu-LTR PCR was performed on normalized samples, followed by an internal qPCR on amplified stage 1 product. Therefore, integrated virus would make up the vast majority of amplified final viral product. Relative levels of integrated virus were calculated by first considering Actin amplification to normalize for initial DNA loading volumes. Secondly, samples were collected and compared between multiple trials by using an unactivated wild-type pNL4 sample that was on each plate. Finally, the mean of the LPVs under the DMSO 'mock' activation condition was set to 1.0, and all samples were normalized to this value (Figure 17).

In summary, firstly there was no significant difference between the mean integration of all LPVs when comparing between activation conditions (Figure 17). Secondly, there was no significant difference between LPVs within each activation condition (Figure 17). Therefore, it was determined that neither the LPV mutations nor the presence of LRAs post infection had a significant impact on the integration of the viruses, and therefore differences seen between LPV infection and activation percentages must be due to differences in viral transcription and not integration.

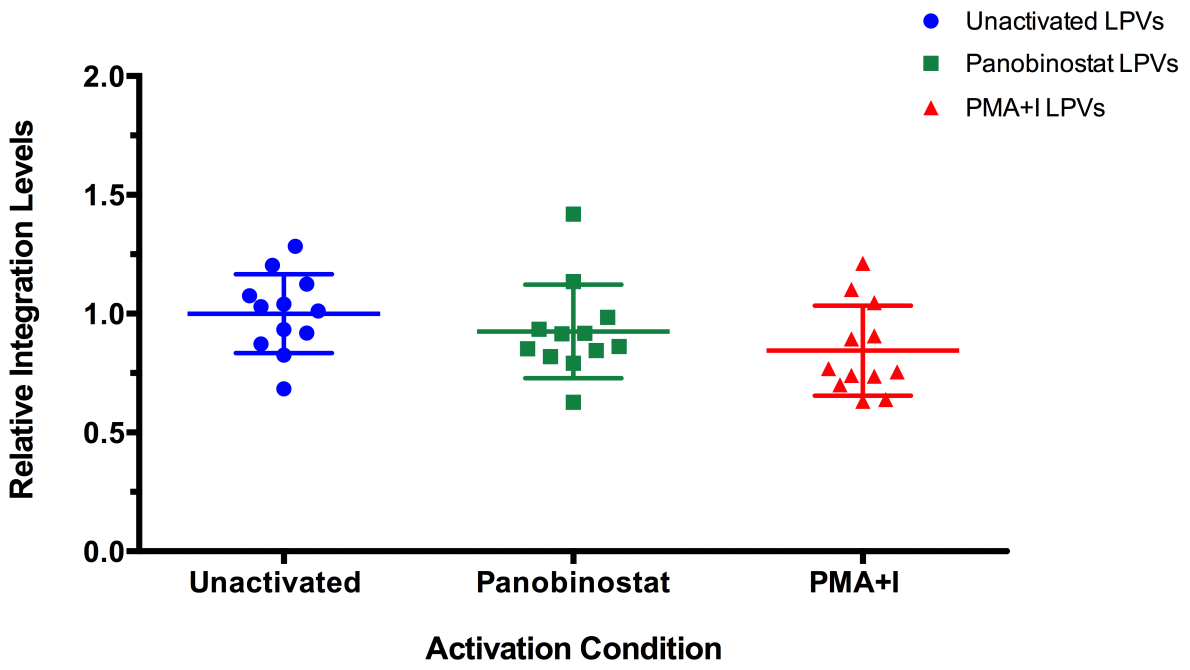

Figure 17 Comparison of Latency Prone Viral Integration Under Latency Reversing Agent Exposure. *Levels of viral integration were determined for each LPV. Jurkat cells were infected with 345ng of p24, and activations performed with 10ng/mL PMA + 1uM I, 50nM Panobinostat or DMSO. Cellular gDNA was isolated 24 hours post activation. Integrated viral LTRs were amplified using a two stage Alu-qPCR. Levels of integration were normalized to actin amplification, followed by a normalization between plates by a constant DMSO pNL4 sample, and finally by setting the mean LPV DMSO integration value to 1.0. Each symbol represents the mean of 3 repeats for one LPV activated by one LRA. N=3. One way ANOVA performed between the three activation groups. No significant difference between the LPV mean integrations when comparing by activation condition. $p \leq 0.05$ for analysis.*

Evolution of Latency Prone Viruses

Now that we had established that the mutations in the LTR of the LPVs were affecting the viruses' baseline infection levels and activation potentials, we next asked whether these LPVs were capable of viral rebound. That is to say, whether viruses that initially appeared as latent due to lower levels of viral expression could rebound over time and show higher levels of viral expression and spread within a cell population.

Mutated LTRs were first cloned out of the non-replicative pNL4.3-Δenv-Δvif plasmid and into a fully replicative pNL4.3 CXCR4-tropic plasmid. These viruses were now capable of multiple rounds of infection.

Next, populations of U87 CD4+ CXCR4+ cells were infected with a low p24 mass (25ng) of each replicative latency prone viral supernatant. These viruses were pseudotyped with VSV-G to allow for efficient preliminary entry into the U87 cells that would act as a viral reservoir. Initial transfected virus was removed, and cells were activated with either PMA+I or DMSO for 24 hours. Weekly, the supernatants of these cell cultures were collected and the quantity of released replication-competent virus within those supernatants was measured through an infection assay on Ghost cells. In the first 14 days of all trials, no LPV population was capable of producing a detectable secondary infection as measured through the expression of eGFP by the Ghost reporter cells. However, in the first trial performed, both the B7 and D3 LPVs rebounded to show detectable, infectious virus output between day 14 and day 21 as measured through the detection of infected Ghost cells that were now expressing eGFP. In subsequent experiments only the LPV C6B showed detectable, infectious viral rebound anywhere between day 14 and day 27. C6B rebounded both in the presence and absence of

PMA+I. In some cases the levels of LPV rebound matched that of the wild type output (D3 in Figure 18), in others the virus rebounded but could not match wild type levels within the experimental window of time (C6B in Figure 20), and in some cases the LPV disappeared again after a brief rebound (B7 in Figure 18). B7, D3, and C6B are the LPVs that contain the lowest number of total LTR mutations, and all demonstrated that at least some of the LPVs are in fact replication competent and able to reseed an infection when given enough time.

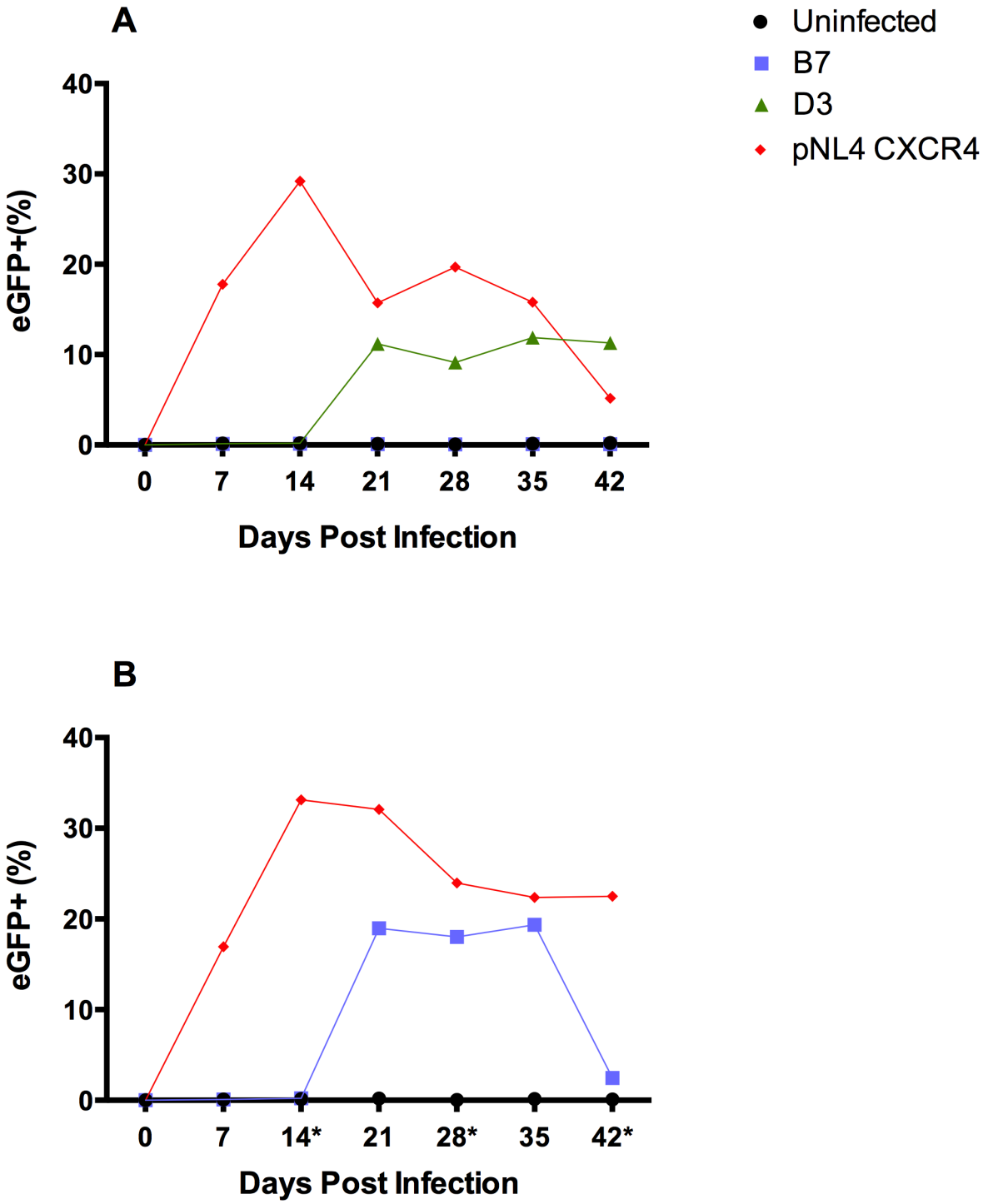

Figure 18 Infectivity of Latency Prone Viral Supernatant from U87 Cells on Ghost Cells - Trial 1. *100,000 U87 cells were infected with 25ng of p24 or B7, D3 or CXCR4-tropic pNL4 in 2mL total volume. Every week 250uL of supernatant was placed on a Ghost cell reporter population.* ***A) Constant:*** *Virus was grown in the same U87 cells from the beginning of the experiment to the end.* ***B) Biweekly Transfer:*** *U87 supernatants containing virus were transferred onto new 100,000 U87 cell every two weeks (* represents the date of supernatant transfer). N=1.*

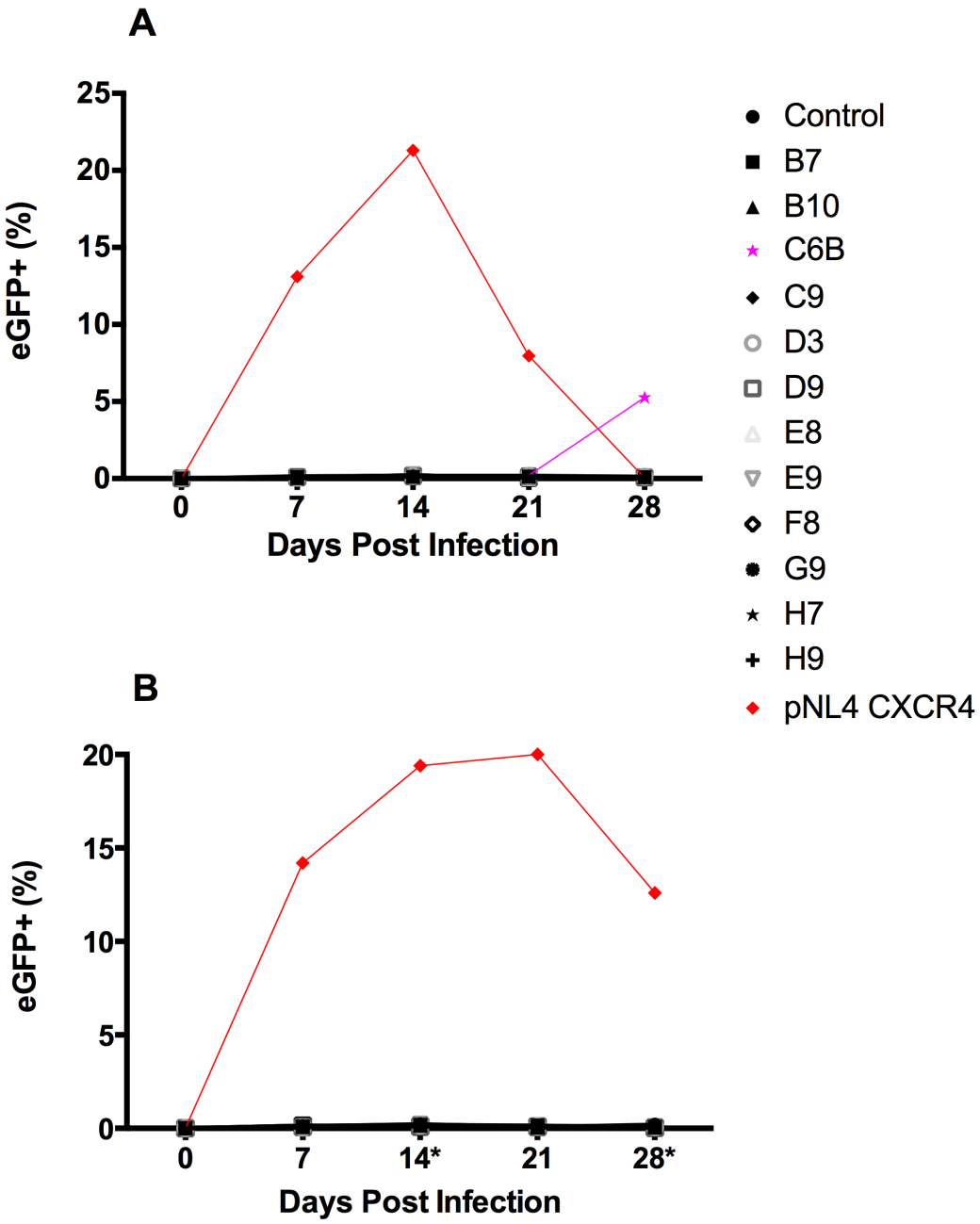

Figure 19 Infectivity of Latency Prone Viral Supernatant from U87 Cells on Ghost Cells - Trial 2 - No PMA+I Exposure. *100,000 U87 cells were infected with 25ng of p24 of an LPV or CXCR4-tropic pNL4 in 2mL total volume. Every week 250uL of supernatant was placed on a Ghost cell reporter population.* ***A) Constant:*** *Virus was grown in the same U87 cells from the beginning of the experiment to the end.* ***B) Biweekly Transfer:*** *U87 supernatants containing virus were transferred every two weeks onto new 100,000 U87 cells every two weeks (* represents the day of supernatant transfer). N=1.*

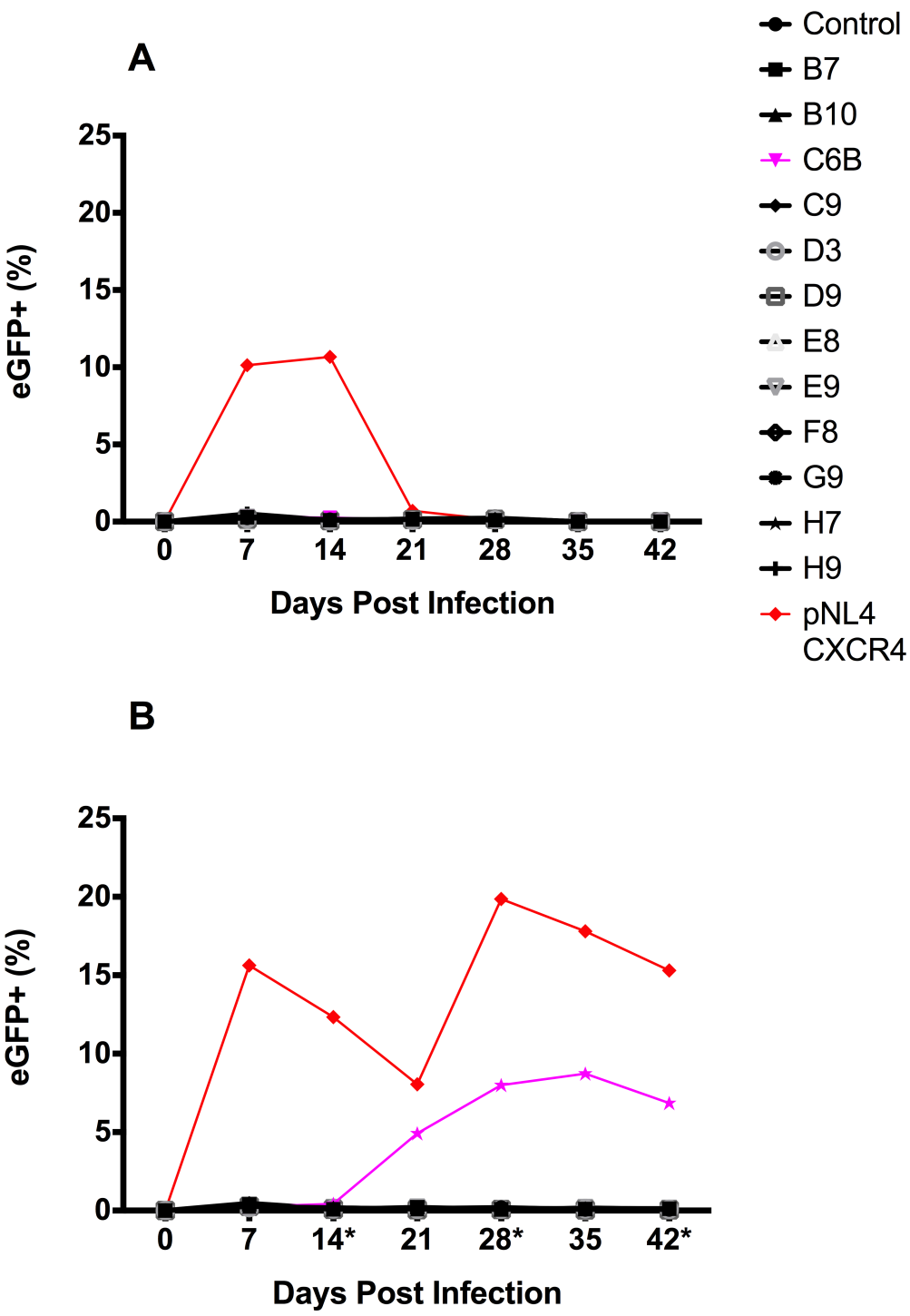

Figure 20 Infectivity of Latency Prone Viral Supernatant from U87 Cells on Ghost Cells - Trial 3 - PMA+I. *100,000 U87 cells were infected with 25ng of p24 of an LPV or CXCR4-tropic pNL4 in 2mL total volume. 24 hours post infection, U87 cells were exposed to 24 hours of 5ng/mL PMA +0.5uM Ionomycin. Every week 250uL of supernatant was placed on a Ghost cell reporter population.* ***A) Constant:*** *Virus was grown in the same U87 cells from the beginning of the experiment to the end.* ***B) Biweekly Transfer:*** *U87 supernatants containing virus were transferred onto new 100,000 U87 cell every two weeks (* represents the day of supernatant transfer). N=1.*

Discussion

The presence of latent reservoirs in those living with HIV-1 remains the foremost hurdle in developing a curative treatment for HIV-1 (56, 197, 198). Latent reservoirs are established early in the infection process, primarily through the infection of effector CD4+ T cells that are in the process of transitioning to memory T cells, with the presence of latently infected macrophages, monocytes, and dendritic cells now also being recognized as important for the establishment of latent reservoirs throughout various tissues and anatomical locations (60, 92, 93). Combinatorial anti-retroviral therapy regimes are capable of limiting the spread of HIV-1 *in vivo*, however the presence of the latent reservoir necessitates life-long cART treatment (40–43). 'Shock and Kill' and 'Block and Lock' are attempts at improving cART by targeting latent virus for reactivation and subsequent clearance (43). Thus far all attempts *in vivo* have proven ineffective at targeting the full complement of latent viruses (43, 199).

Latent infections are characterized by integrated viruses that are replication-competent but currently transcriptionally inactive (28, 48–51). Traditionally the establishment and persistence of viral latency is thought to be primarily mediated by the transcriptional environment within the host cell. However, thus far this reasoning has failed to explain why 'Shock and Kill' and 'Block and Lock' are not capable of targeting all latent viruses.

We propose that not only can the transcriptional environment within the cell affect the ability for HIV-1 to establish and persist within a latency-like phenotype, but also that the sequence of the integrated viral promoter can affect the transcription, or lack thereof, of certain HIV-1 proviruses. Specifically, we hypothesize that G→A transition mutations within the LTR region of HIV-1, whether induced through APOBEC3 sublethal mutagenesis or by RT

error, affect the reactivation of proviruses in a location and quantitative-dependent manner. Our lab has developed a library of sublethally mutated HIV-1 LTRs that contain different frequencies and locations of G→A transition mutations. A subset of these LTRs were preliminarily cloned into a non-replicative HIV-1 backbone to begin to test our hypothesis, viruses that we referred to as latency prone viruses.

Measurement of Viral Output by Flow Cytometry and ELISA

All of the LPVs tested in this study, with the exception of D3, demonstrated lower levels of viral protein expression post-transfection than that of the wild-type, positive control pNL4 (Figure 10). The number of cells internally expressing viral proteins post-transfection was calculated by flow cytometry based on the expression of an eGFP reporter gene inserted into the Env of the virus. The concentration of extracellular viral protein in culture (whether that be associated with intact virions or free capsid) was estimated by a p24 ELISA. A potential explanation as to why the majority of LPVs displayed lower viral expression is that the G→A transition mutations are originally placed within the 3' LTR of the LPV plasmids, with the majority being found in the U3 region of the 3' LTR (Figure 9). During the first round of viral reverse transcription, the virus uses the 3' LTR as a template in synthesizing its 5' LTR. Therefore, to achieve G→A transition mutations that are within the 5' LTR preliminary integrating virus, they must be first placed in the 3' LTR of the plasmid.

The 3' LTR U3 region is also the location within the viral genome of the viral-polyadenylation site for the first round of plasmid-based viral transcription, as well as the location of other sites which influence the termination of transcription by RNA polymerase II. The poly-A tail sequence and surrounding area is important for the virus in terminating transcription, mRNA

stability, allowing nuclear export of the +ssRNA/mRNA, and alternative splicing (200). By affecting the 3' end during the first round of viral transcription, this can potentially affect the expression of viral proteins, the early expression of non-structural proteins, and transcription of complete viral genomes. Because a similar decrease compared to the wild type pNL4 control was seen among the LPVs in both their internal viral protein expression as well as in their release into the supernatant (Figure 10), this would indicate that the problem for the LPVs is occurring in the transcription and translation of viral proteins, and likely not in the release of virus from the cell. If it was a problem with packaging and release of the LPVs, we would expect to see similar transfection levels of eGFP inside the cell among the LPVs but dissimilar levels of virus being released into the extracellular supernatant. This aligns with the aforementioned theory that the stability of +ssRNA/mRNA transcripts is affecting the overall levels of viral proteins being produced.

To normalize the number of viral particles in supernatant for all downstream infections, viral concentrations were estimated using a p24 sandwich ELISA. p24 is the main component of the viral capsid and is the common target of diagnostic immunoassays for detecting HIV-1 in serum (201–203). The quantification of p24 was calculated by extrapolating optical density values of LPV supernatants in the ELISA to a curve of known p24 concentration. Only the linear region of the curve was used in the analysis, with a line of best fit being drawn through the linear region comparing optical density values to known p24 concentration. The equation of this line was then used to estimate the unknown p24 concentrations in the p24 transfection supernatants. When comparing normalized ELISA and flow cytometry results by a Student's T test, there was not a statistical difference between the number of cells

expressing eGFP+ and the calculated supernatant p24 concentrations for the LPVs when each were normalized to the pNL4 wild type control (Figure 10). Therefore, the concentration of p24, as determined by our in-house p24 ELISA, was deemed a suitable method for normalizing downstream infection volumes between each of our LPVs.

We decided to sort all the LPVs by their overall number of mutations to see if there was a noticeable trend between the number of LTR mutations and viral output post-transfection (Figure 10). There was no statistical correlation between a decreasing viral output as the number of LTR mutations increased (Figure 24), therefore the effect of the G→A mutations within the 3' LTR of our plasmids seems to be dependent on the specific locations and combination of mutations, and not singularly dependent on the overall quantity of mutations.

PMA+I Activation Assays

Normalized volumes of LPV supernatants were used to infect the HEK 293T and Jurkat cell lines. Jurkat cells were chosen as the first non-293T cell line to infect because they are a T-lymphocyte cell line that is highly susceptible to HIV-1 infection due to high levels of IL-2 production (204). Preliminary infections were performed without any exposure to LRAs to determine the baseline infection levels of each LPV. All infection assays were performed within a non-replicative HIV-1 plasmid that was missing its Env and Vif genes. This meant that to allow for an initial entry into a cell, we needed to pseudotype all infections with Vesicular Stomatitis Virus G protein (VSV-G), the protein of VSV responsible for entry of the virus via endocytosis into the cells (205). Because the VSV-G was co-transfected with the non-

replicative viruses it would only allow for one round of infection, with all secondary virions lacking the VSV-G envelope glycoprotein.

Using flow cytometry, the ability of each virus to produce viral proteins post integration was measured through the presence or absence of eGFP, a protein that was only found in the viral genome. Levels of eGFP mean fluorescence intensity (MFI) were also measured to determine the relative levels of viral protein expression of each LPV within a given cell. The first finding was that all LPVs demonstrated significantly lower levels of eGFP expression when compared to the wild type, pNL4 positive control (Figure 11). Secondly, there also was a moderate correlation between the number of overall mutations that each virus contained in its promoter and the baseline levels of infection that each LPV displayed as measured through number of cells expressing eGFP (Figure 25). This moderate correlation was deemed to follow an exponential pattern rather than a linear pattern, with an exponential line of best fit R^2 value of 0.7614 in HEK 293T cells and 0.7609 in Jurkat cells. The LPVs with the highest number of mutations generally showed the lowest levels of eGFP expression in infected cells. This is likely due to the fact that the more mutations an LPV promoter has the greater the number of transcription factor protein binding sites that are affected. A decrease in transcription factor binding then leads to a reduction in efficient viral transcription post-integration (206, 207).

We then wanted to know how each of our mutated viruses would respond to a simulated latency reversal event. To accomplish this, we added a 24-hour activation step of the cells with PMA+I, which is the gold standard in activating cells to increase their transcription levels. PMA+I exposure would simulate a situation where a cell has been infected with an

HIV-1 virus that is not currently transcribing high levels of virus, but an environmental change has “shocked” the cell into an increase in transcription that could potentially lead to an a reversion from viral latency to viral expression. The combination of PMA+I broadly stimulates transcription of the cell, particularly through activation of the PKC pathway. PKC then can lead to the recruitment of multiple downstream viral transcription factors to the nucleus and viral promoter that may have previously either been present at low concentrations in the nuclei or bound inefficiently to their mutated binding sites, thus helping to boost viral transcription (127, 148–152).

When exposed to PMA+I, we saw that all LPVs, except for E8, were not only able to increase viral protein expression as measured through the MFI of each cell’s eGFP expression, but also that cells that had previously not been expressing any virus began to express viral proteins, as seen by the increase in the overall number of cells expressing eGFP (Figure 12). E9, H7, and H9 all showed <2% infection percentages prior to PMA+I activation in both 293T and Jurkat cells, however increased to 10-20% infection levels after activation. E8 demonstrated no viral expression before or after PMA+I exposure as measured through the absence of eGFP expression in infected cells and was thus classified as our “dead clone”, later being used as a negative control for activation. This indicated that all the LPVs, with the exception of E8, were capable of infecting the cells as well as contained promoters that were still capable of increasing their viral transcription levels when stimulated. Most importantly we also observed a difference between the percentages of activation post PMA+I for each LPV (Figure 13). Subsequently, there was also no pattern between the number of LTR G→A mutations and the percentage of LPV promoter activation (Figure 13). This means that how our LPVs

responded to PMA+I activation was more so dependent on the pattern and location of their promoter mutations and not in the overall number that each contained. However, there does seem to be a threshold where the overall number of mutations becomes too much for a virus to handle and no transcription is possible under a normal level of infectious virus, whether they be un-activated or activated. In our case, we observed this between 21 mutations (D9) where minimal levels of activation were observed and 38 mutations (E8), where no activation was observed.

We were able to overcome this lack of activation of E8 when we repeated the infection and activation assays with supernatants containing 5X and 10X total virus (Figure 16). All 6 of our lowest expressing LPVs were able to reactivate at 5X and 10X the original p24 amount, with no infection plateaus being reached. Even E8, which we had previously designated as our dead control, demonstrated for the first time a slight ability to reactivate. This is likely explained by the overwhelming number of proviral integrations per cell that would have occurred at such high concentrations of virus. When infecting with a large surplus of virus, it is possible that a few proviruses integrate into areas of high host-associated transcriptional activity. When this happens RNA polymerases that are reading upstream of integrated virus within the host gene that the virus integrated into may also continue transcribing through the integrated provirus, thus creating the potential for viral transcripts that originate from integrated proviruses that would have otherwise had difficulty recruiting RNA polymerase II to their promoter due to their high levels of LTR mutations (208).

Seeing our LPVs with the highest levels of mutations struggle to transcribe post-integration follows what is known about the relationship of HIV-1, APOBEC3, and Vif. Early in the

infection process, A3 proteins are able to completely inactivate an HIV-1 genome through high levels of mutagenesis, however as Vif levels increase A3 becomes further sequestered and degraded, leading to lower levels of mutations and eventually no mutagenesis (185–188). The LPVs which contain high levels of mutations which limit their transcriptional capability represent viruses that would have high exposure to A3 proteins early in a cellular infection. We are adding to this picture with this work by saying there is also a time period where viruses can accumulate low levels of mutations, as demonstrated by our LPVs with fewer mutations. These mutations, when found in the promoter region of the virus, lead to an overall decrease in viral transcription levels as compared to a wild type, non-mutated virus (Figure 10). However, these viruses are still capable of activating upon LRA exposure and the activation of viral transcription seems to be dependent on the locations of G→A mutations within the promoter (Figures 12 and 13).

So why would the locations matter so much on the activation of our viruses? As discussed in the introduction, the LTR of HIV-1 is divided into the U3, R and U5 regions, with the U3 being important for the initiation of transcription through a plethora of transcription factor binding sites and the R region being important for elongation of transcription (Figure 2) (206). The U3 region, where the majority of our mutations are found, can be further subdivided into the upstream modulatory region, the core enhancer, and the core promoter. All three of the U3, R, and U5 contain transcription factor binding sites that are critical for promoting transcription of the virus, or in some cases through the removal of a transcriptional antagonist (like NELF) (23–28, 30).

Within our subset of tested LPVs, we have mutations that reside in the binding sites of NF-κB, NFAT, all three critical Sp-1 sites, COUP, AP-1, and more. Therefore, we believe that the G→A transition mutations within the binding site sequences of these transcriptional regulatory proteins affects the ability for each of our LPVs to efficiently recruit the proteins required for optimal initiation of transcription similar to the wild-type control HIV-1. Not all transcription factors are required for viral basal transcription (20, 28, 206), therefore we also believe that certain mutations that alter the binding of complementary and enhancer transcription factor binding proteins are likely somewhat less important to the virus' transcriptional capacity when compared to proteins that are necessary for transcriptional initiation such as NF-κB and NFAT (28, 30). The LPVs that contain a greater overall number of mutations tend to have mutations that hit more transcription factor binding sites and thus demonstrate lower baseline transcription levels as more transcription factors have difficulty adhering to the proviral promoter. The specific sites of mutation seem to become more important than just the overall number of mutations when analyzing the virus' percent activation to PMA+I as seen through the variation in activations not being solely dependent on overall number of mutations (Figure 12).

Because we had LPVs that reacted differently to PMA+I activation, we next decided to test the activation potentials of each of our viruses against a variety of LRAs. We chose eight LRAs that spanned four drug categories, each category affecting transcription factor binding proteins differently. The HDAC inhibitors Panobinostat, Vorinostat, Romidepsin, and Valproic Acid increase acetylation levels of lysine residues on histones, allowing for histones that are more available for transcriptional binding protein access (137–145). The PKC agonists PMA+I

and Bryostatin-1 increase levels of NF-κB and AP-1 signalling in the cell which leads to increases in genomic transcription levels (149). The aldehyde dehydrogenase inhibitor Disulfiram works by increasing PKB levels while increasing pTEFb binding of the promoter (146, 209). Finally, the retinoid All Trans Retinoic Acid (ATRA) causes an upregulation in multiple cell proliferation pathways. All have previously been used in HIV-1 activation studies (153, 154).

We found that PMA+I was the most potent latency reversing agent among the LPVs and wild type control (Figures 12 and 13). PMA+I was closely followed by the three HDAC Inhibitors Panobinostat, Vorinostat, and Romidepsin as it relates to the levels of eGFP activation of each virus. Bryostatin-1 provided moderate activation while Valproic Acid, Disulfiram and ATRA demonstrated the lowest abilities to activate viral transcription. Figure 14 summarizes the relative increases in the percentage of cells expressing eGFP as well as their mean fluorescence intensity after activation by the eight LRAs. The fact that HDAC inhibitors are excellent LRAs is likely due to the fact that they function by opening up the histones as a whole for all transcription factor binding proteins (210). This allows for greater access to the integrated viral promoter for every viral transcription factor. Opening up the entire histone also leads to a greater chance of viral transcription via readthrough from other genes now being transcribed at greater frequencies. In comparison, Bryostatin-1 for example works more so only on increasing the availability of the NF-κB and AP-1 transcription factors, and thus would be more limited in the scale that it could act on increasing viral transcription, no matter how important these two proteins are for transcriptional initiation. The difference between the two PKC activators PMA+I and Bryostain-1 was quite large, and this can be

partially explained by the presence of Ionomycin. Ionomycin leads to an increase in cellular proliferation, cytokine release, and most importantly PKC activation by phosphorylation (211). Ionomycin works in conjunction with PMA to increase PKC levels within the cell, which in turn leads to high levels of NF-κB within the nucleus of the cell (149). NF-κB is one of the most important factors in initiating viral transcription, which is why PMA is often the most potent activator within our system.

We were hoping to find that certain LPVs would react much better to some LRAs while not responding well to others. The rationale behind this thinking was that if we had an LPV that had a mutation in transcription factor binding site X, and if we exposed the virus separately to multiple LRAs, that it might reactivate better to an LRA that specifically increased the availability of transcription factor X. There were a few small examples of LPVs acting differently to an LRA such as H7 seeming to be most activated by Romidepsin, B10 responded quite well to Panobinostat and Vorinostat, and the most heavily mutated LPVs only responding to PMA+I and a selection of the HDAC Inhibitors (Figure 14). Overall we were unable to identify among the LPVs specific connections between a category of LRA and an activation pattern. Because we were dealing with viruses that contained mutations in multiple binding domains, drugs such as the HDAC Inhibitors worked the best as they were able to upregulate transcription of the virus in a protein factor-independent manner. In order to reach the levels of activation of PMA+I, Panobinostat, or Vorinostat, the lesser effective LRAs which only target specific proteins would likely need to be used in a combinatorial manner to upregulate the availability and binding of as many transcription factors as possible. This coincides with current 'Shock and Kill' field theories that a combinatorial

approach that targets multiple transcription factors is necessary to activate the full complement of integrated, latent proviruses (43). The ability to link viral reactivation to specific mutation sites in the viral promoter region would be a major step forward in the design of future LRAs, along with the novel design of combinatorial approached that would target all mutation preferences.

Latency Prone Viral Integration

We next wanted to ask the question if the differences that we saw in the infection and activation profiles among each LPV were not due to differences in transcriptional response, but rather due to a difference in the integration levels of each virus. Specifically, we asked whether there were differences among the LPVs in their ability to integrate into the cells, as well as if the presence of LRAs given post infection might be affecting integration. The LTRs of HIV-1 are important in the integration process of the virus, meaning adding mutations within them may have an effect on integration (212).

To answer these two questions, we first repeated *in vitro* infections in Jurkat cells followed by a 24-hour activation with PMA+I, Panobinostat, or DMSO as a negative control. We then split the cellular populations, with 33% of the cells being analyzed by flow cytometry to determine the percentage of activation and MFI increase. The remaining 66% was used to extract cellular genomic DNA which would contain the integrated proviruses. A two stage Alu-qPCR was performed on all conditions. Alu elements are 300 base pair long, transposable elements that integrate throughout the genome (213). By placing one end of the first round PCR on the Alu element, this allowed for the amplification of only viruses that had integrated into the cellular DNA genome. Actin was used as a control across all conditions for

normalizing loading volumes. Samples between qPCR plates were next compared to each other by using a wild-type pNL4 DMSO control sample that was present on every plate run. Finally, the mean integration of all DMSO activated LPVs was determined and set to 1.0, with all samples being normalized around this.

We found that when comparing the mean normalized integration levels of all LPVs across the three activation conditions, there was not a significant difference among activation groups (Figure 17). There was also not a significant difference between the integration levels of each LPV when looking at one activation group at a time. Therefore, the variable increases in eGFP expression among LPVs when exposed to the LRAs were likely due to differences in the individual promoter responses to the drugs, and not due to any differences in LPV integration efficiency caused through internal sequence mutations or drug presence.

Evolution of Latency Prone Viruses

Throughout the normalized infection assays all LPVs displayed reduced viral protein expression levels as compared to the non-mutated wild type virus caused by G→A transition promoter mutations accumulated through exposure to RT and low levels of APOBEC3. This difference spurred on the question if further changes in the viral sequence through continued A3 and RT exposure might allow for a reversion back in infection levels.

To perform infection assays which would last for multiple rounds of infection allowing for multiple rounds of exposure to APOBEC3 and RT, we first had to clone our latency prone viral LTRs out of the non-replicative plasmid and into a fully replicative HIV-1 plasmid. This was performed by cutting out the 3' mutated LTRs from the non-replicative pNL4 plasmid with the surrounding restriction cut sites XhoI and NcoI (Figure 8). Gel purified LTRs were then

inserted into either CXCR4-tropic or CCR5-tropic, replicative NL4 plasmids that had been likewise digested.

To test the infectivity of the LPVs over multiple rounds of infectivity, cultures of U87 cells were infected with very low levels of an LPV and allowed to grow out. Every week U87 supernatants containing released viruses were tested on Ghost reporter cells to determine if viruses that originally showed limited infection levels were increasing their infectivity over time. These ghost cells were highly susceptible to viral infection due to the addition of the CD4, CCR5, and CXCR4 receptors on their surface. They were also good candidates for probing for the presence of HIV-1 as they also contain a tat-dependent HIV-2 LTR-eGFP construct (214). That meant that the Ghost cells could express eGFP in two different ways, either by the detection of Tat or through the expression of eGFP coming from integrated and transcribing LPVs. Over the first 14 days of all infection conditions no LPV reached a viral supernatant concentration capable of infecting more than 1% of secondary Ghost cells. However, between days 14 and 21 we observed viral rebounds from the LPVs B7, D3, and C6B, as evidenced by their ability to produce a detectable, secondary infection in Ghost cells. B7 and D3 both rebounded once without any exposure to LRAs (Figure 18) while C6B rebounded twice, once after 14 days under PMA+I activation (Figure 20) and once after 21 days without PMA+I activation (Figure 19). B7, D3, and C6B contain the fewest LTR mutations out of the subset of LPVs tested so it is not surprising that these are the three LPVs that were capable of rebounding in infectivity the earliest. B7 and C6B are also the only two LPVs of the library tested that do not contain a mutation in their TAR region, a region that forms a stem-loop structure that Tat critically recognizes and binds to Tat to initiate enhanced levels of

transcription. Without Tat binding to TAR, efficient, high levels of HIV-1 transcription are almost impossible (215, 216). Previous viral evolution work has also shown that HIV-1 can evolve with a combination of mutations in its viral enhancer, core promoter, and NF-κB /Sp1 binding sites, similar to our LPVs, with no mutations being found in the TAR region (217). Mutations in TAR have also been shown previously to be highly detrimental to viral trans-activation and translation (215). The fact that B7 and C6B rebounded the most frequently among all LPVs seems to indicate G→A transition mutations throughout the entirety of the viral LTR are all capable of affecting viral transfection, infection, and activation with mutations found specifically in TAR being the most difficult to overcome for viral transcription.

Experiments were generally stopped after 4-5 weeks because of the high rate of cell death within the constant wells due to over-confluence. By four weeks the biweekly transfer conditions had also undergone two supernatant transfers and the likelihood of having infection-competent virus passed on to a new, third culture of cells was very low. Genomic sequencing of viral RNA sequences isolated from supernatants at each time point should allow for the indication as to what viral sequence mutations/changes resulted in the viruses overcoming the effects of their latency-prone promoters.

It is highly unlikely that the LPVs evolved into a viremia-inducing version due to a straight reversion back in the specific G→A transition mutations that were originally introduced. This would not be possible through further APOBEC3 exposure as A3 proteins solely create G→A transition mutations in the +ssDNA strand, and not A→G. For a perfect reversion to occur through RT error, one would have to consider the very low odds of having the 2-3 new RT

mutations per round hitting exactly the previously mutated bases, the odds that the subsequent new mutations are in fact adenine substitutions, and the odds that no further deleterious mutations were introduced outside of these specific promoter locations.

It is more likely that an evolution occurred through the accumulation of subsequent mutations outside of the mutated LTRs. It is well characterized that HIV-1 evades immune recognition through the accumulation of mutations within its target epitopes which help to disrupt viral protein processing, HLA presentation, and TCR recognition (218, 219). Mutations in the viral capsid are commonly introduced for immune evasion, however these mutations often lower viral replication rates and thus are accompanied by compensatory, pro-replication mutations elsewhere in the viral Gag, Pol, and Nef proteins (218, 220). Low levels of APOBEC3-mediated mutations within the viral Env protein have also been shown to lead to a positive reversion in HIV-1 replication fitness. These Env mutations allowed the virus to decrease its fusogenicity while packaging higher levels of Gag-Pol within virions, which in turn allowed for faster viral replication and protection from A3G-mediated hypermutation (189). This information, when combined with the fact that the addition of PMA+I on the U87 cells did not boost the number of viruses that rebounded in fitness, leads me to believe that the LPVs that showed a reversion in viral infectivity did so thanks to secondary mutations, introduced outside of their primary promoter region, that helped to overcome the replication hurdle that the LTR-based mutations induced.

A second possibility is that cellular and molecular signalling changes occurred due to the stress of the confluent environment which may have allowed for greater binding of Tat and transcription factor binding proteins. Multiple rounds of infection within the same cellular

subculture would have allowed the virus to experience continued exposure to environmental changes within the cell, A3 mutagenesis, RT-induced errors, and possibly even crossing over/copackaging events between multiple viral genomes in the potential cases of co-infection.

The ability for our LPVs to show a reversion in viral infectivity is very important because it demonstrates that the LPVs we have used are not all viruses one step away from a dead-end infection. To be given the term latent, they must prove that they are both activatable and able to reseed an infection. During the preliminary activation assays we demonstrated that the LPVs increased viral transcription upon LRA exposure (Figures 12-14). In the evolution experiments we showed that the LPVs are capable of reseeding an infection when given enough time and allowance to continue to experience environmental and sequential changes (Figures 18-20). In two cases the viral rebound demonstrated a concentration of viral output that did not match the wild type control, once when it almost matched before disappearing again, and once when it was able to exceed wild type output (Figures 12-14).

Conclusions

Until now the reasons for which HIV-1 may become latent have primarily encompassed the timing of infection as well as the state of the reservoir cell as it relates to histone availability, dNTP levels, and integration location (28, 221). The path to latency and back rarely has been thought to involve the sequence of the viral promoter itself. We demonstrate in this work however, that G→A sequence mutations are capable of being introduced into the HIV-1 promoter region through exposure to APOBEC3-mediated sublethal mutagenesis, and that these mutations can accumulate within transcription factor binding sites (Figure X). We next showed that different mutation patterns created viruses that showed variable levels of transcription post-transfection, as well as variable levels of viral protein expression post-infection (Figures 10-11). Most importantly, although the sub-lethally mutated viruses experienced an early reduction in infection and variation in subsequent activation to LRAs (Figures 12-16), they did not always stay dormant and a few were capable of reseeding an infection (Figures 18-20). This work demonstrates a new pathway for establishing latent HIV-1 proviruses, and future attempts at activating or blocking the full latent reservoir should consider the potential sublethal mutagenesis of the HIV-1 promoter sequence in therapy design.

Contribution of Collaborators

Genome Quebec provided Sanger Sequencing services. Cindy Lam constructed the library of LPVs. Dr. Joanne McBane was responsible for preliminary testing of the LPVs and the production of the two antibodies used in the in-house p24 ELISAs. Anna Fritszhe, Dr. Tyler Renner and Dr. Vera Tang provided tissue culture and flow cytometry training. Tasneem Abbas provided support in molecular cloning preparations.

References

1. 1981. Kaposi's sarcoma and Pneumocystis pneumonia among homosexual men--New York City and California. MMWR Morb Mortal Wkly Rep.

2. Barre-Sinoussi, F., J. C. Chermann E Al. 1983. Isolation of a T-lymphotropic retrovirus from a patient at risk for acquired immune deficiency syndrome (AIDS). Science (80-) 220(4599):868–71.

3. Hladik F, McElrath MJ. 2008. Setting the stage: Host invasion by HIV. Nat Rev Immunol.

4. Sharp PM, Hahn BH. 2011. Origins of HIV and the AIDS pandemic. Cold Spring Harb Perspect Med 1.

5. Global HIV & AIDS statistics — 2019 fact sheet | UNAIDS.

6. Seitz R. 2016. Human Immunodeficiency Virus (HIV). Transfus Med Hemotherapy.

7. Lindenbach BD, Rice CM. 2007. Flaviviridae: The Viruses and Their Replication. Fields Virol.

8. Watts JM, Dang KK, Gorelick RJ, Leonard CW, Bess JW, Swanstrom R, Burch CL, Weeks KM. 2009. Architecture and secondary structure of an entire HIV-1 RNA genome. Nature 460:711–716.

9. Gelderblom HR, Özel M, Pauli G. 1989. Morphogenesis and morphology of HIV structure-function relations. Arch Virol.

10. Nkeze J, Li L, Benko Z, Li G, Zhao RY. 2015. Molecular characterization of HIV-1 genome in fission yeast Schizosaccharomyces pombe. Cell Biosci 5:47.

11. Martin Stoltzfus C. 2009. Chapter 1 Regulation of HIV-1 Alternative RNA Splicing and Its Role in Virus Replication. Adv Virus Res.

12. Frankel AD, Young JAT. 1998. HIV-1: Fifteen Proteins and an RNA. Annu Rev Biochem.

13. Fiorentini S, Marini E, Caracciolo S, Caruso A. 2006. Functions of the HIV-1 matrix protein p17. New Microbiol.

14. Campbell EM, Hope TJ. 2015. HIV-1 capsid: The multifaceted key player in HIV-1 infection. Nat Rev Microbiol.

15. Muller B, Patschinsky T, Krausslich H-G. 2002. The Late-Domain-Containing Protein p6 Is the Predominant Phosphoprotein of Human Immunodeficiency Virus Type 1

Particles. J Virol.

16. Basmaciogullari S, Pizzato M. 2014. The activity of Nef on HIV-1 infectivity. Front Microbiol.

17. Dubé M, Bego MG, Paquay C, Cohen ÉA. 2010. Modulation of HIV-1-host interaction: Role of the Vpu accessory protein. Retrovirology.

18. Gallastegui E, Millan-Zambrano G, Terme J-M, Chavez S, Jordan A. 2011. Chromatin Reassembly Factors Are Involved in Transcriptional Interference Promoting HIV Latency. J Virol.

19. Cullen BR, Lomedico PT, Ju G. 1984. Transcriptional interference in avian retroviruses - implications for the promoter insertion model of leukaemogenesis. Nature.

20. Roebuck KA, Saifuddin M. 1999. Regulation of HIV-1 transcription. Gene Expr.

21. Liu R, Wu J, Shao R, Xue Y. 2014. Mechanism and factors that control HIV-1 transcription and latency activation. J Zhejiang Univ Sci B 15:455–65.

22. Churchill MJ, Cowley DJ, Wesselingh SL, Gorry PR, Gray LR. 2015. HIV-1 transcriptional regulation in the central nervous system and implications for HIV cure research. J Neurovirol.

23. Kinoshita S, Su L, Amano M, Timmerman LA, Kaneshima H, Nolan GP. 1997. The T cell activation factor NF-ATc positively regulates HIV-1 replication and gene expression in T cells. Immunity.

24. Nabel G, Baltimore D. 1987. An inducible transcription factor activates expression of human immunodeficiency virus in T cells. Nature.

25. Selliah N, Zhang M, DeSimone D, Kim H, Brunner M, Ittenbach RF, Rui H, Cron RQ, Finkel TH. 2006. The γc-cytokine regulated transcription factor, STAT5, increases HIV-1 production in primary CD4 T cells. Virology.

26. Yang X, Chen Y, Gabuzda D. 1999. ERK MAP kinase links cytokine signals to activation of latent HIV-1 infection by stimulating a cooperative interaction of AP-1 and NF-κB. J Biol Chem.

27. Mbonye U, Karn J. 2014. Transcriptional control of HIV latency: Cellular signaling pathways, epigenetics, happenstance and the hope for a cure. Virology.

28. Mbonye U, Karn J. 2017. The Molecular Basis for Human Immunodeficiency Virus Latency. Annu Rev Virol 4:annurev-virology-101416-041646.

29. Liu J, Perkins ND, Schmid RM, Nabel GJ. 1992. Specific NF-kappa B subunits act in

concert with Tat to stimulate human immunodeficiency virus type 1 transcription. J Virol.

30. Sheppard K-A, Rose DW, Haque ZK, Kurokawa R, McInerney E, Westin S, Thanos D, Rosenfeld MG, Glass CK, Collins T. 1999. Transcriptional Activation by NF-κB Requires Multiple Coactivators. Mol Cell Biol.

31. Kamine J, Chinnadurai G. 1992. Synergistic activation of the human immunodeficiency virus type 1 promoter by the viral Tat protein and cellular transcription factor Sp1. J Virol.

32. Laspia MF, Rice AP, Mathews MB. 1989. HIV-1 Tat protein increases transcriptional initiation and stabilizes elongation. Cell.

33. Dingwall C, Ernberg I, Gait MJ, Green SM, Heaphy S, Karn J, Lowe AD, Singh M, Skinner MA. 1990. HIV-1 tat protein stimulates transcription by binding to a U-rich bulge in the stem of the TAR RNA structure. EMBO J.

34. Kao SY, Calman AF, Luciw PA, Peterlin BM. 1987. Anti-termination of transcription within the long terminal repeat of HIV-1 by tat gene product. Nature.

35. Rabbi MF, Saifuddin M, Gu DS, Kagnoff MF, Roebuck KA. 1997. U5 region of the human immunodeficiency virus type 1 long terminal repeat contains TRE-like cAMP-responsive elements that bind both AP-1 and CREB/ATF proteins. Virology 233:235–245.

36. Sengupta S, Siliciano RF. 2018. Targeting the Latent Reservoir for HIV-1. Immunity.

37. Croxford S, Kitching A, Desai S, Kall M, Edelstein M, Skingsley A, Burns F, Copas A, Brown AE, Sullivan AK, Delpech V. 2017. Mortality and causes of death in people diagnosed with HIV in the era of highly active antiretroviral therapy compared with the general population: an analysis of a national observational cohort. Lancet Public Heal.

38. Mor Z, Sheffer R, Chemtob D. 2018. Causes of death and mortality trends of all individuals reported with HIV/AIDS in Israel, 1985-2010. J Public Heal (United Kingdom).

39. Waters DD, Hsue PY. 2019. Lipid Abnormalities in Persons Living With HIV Infection. Can J Cardiol.

40. Panel on Antiretroviral Therapy and Medical Management of HIV-Infected Children. 2012. Guidelines for the Use of Antiretroviral Agents in HIV-1-Infected Adults and Adolescents Developed by the HHS Panel on Antiretroviral Guidelines for. October.

41. Finzi D, Hermankova M, Pierson T, Carruth LM, Buck C, Chaisson RE, Quinn TC,

Chadwick K, Margolick J, Brookmeyer R, Gallant J, Markowitz M, Ho DD, Richman DD, Siliciano RF. 1997. Identification of a reservoir for HIV-1 in patients on highly active antiretroviral therapy. Science (80-).

42. Finzi D, Blankson J, Siliciano JD, Margolick JB, Chadwick K, Pierson T, Smith K, Lisziewicz J, Lori F, Flexner C, Quinn TC, Chaisson RE, Rosenberg E, Walker B, Gange S, Gallant J, Siliciano RF. 1999. Latent infection of CD4+ T cells provides a mechanism for lifelong persistence of HIV-1, even in patients on effective combination therapy. Nat Med.

43. Kim Y, Anderson JL, Lewin SR. 2018. Getting the “Kill” into “Shock and Kill”: Strategies to Eliminate Latent HIV. Cell Host Microbe 23:14–26.

44. Stöhr W, Fidler S, McClure M, Weber J, Cooper D, Ramjee G, Kaleebu P, Tambussi G, Schechter M, Babiker A, Phillips RE, Porter K, Frater J. 2013. Duration of HIV-1 Viral Suppression on Cessation of Antiretroviral Therapy in Primary Infection Correlates with Time on Therapy. PLoS One.

45. Chun TW, Davey RT, Engel D, Lane HC, Fauci AS. 1999. AIDS: Re-emergence of HIV after stopping therapy. Nature.

46. HIV Medications: NRTIs, Protease Inhibitors, and Much More.

47. HIV antiretroviral drugs: Types and side effects.

48. Pedersen C, Orskov Lindhardt B, Lokke Jensen B, Lauritzen E, Gerstoft J, Dickmeiss E, Gaub J, Scheibel E, Karlsmark T. 1989. Clinical course of primary HIV infection: Consequences for subsequent course of infection. Br Med J.

49. Chun TW, Finzi D, Margolick J, Chadwick K, Schwartz D, Siliciano RF. 1995. In vivo fate of HIV-1-infected T cells: Quantitative analysis of the transition to stable latency. Nat Med.

50. Chun TW, Stuyver L, Mizell SB, Ehler LA, Mican JAM, Baseler M, Lloyd AL, Nowak MA, Fauci AS. 1997. Presence of an inducible HIV-1 latent reservoir during highly active antiretroviral therapy. Proc Natl Acad Sci U S A.

51. Koup RA, Safrit JT, Cao Y, Andrews CA, McLeod G, Borkowsky W, Farthing C, Ho DD. 1994. Temporal association of cellular immune responses with the initial control of viremia in primary human immunodeficiency virus type 1 syndrome. J Virol.

52. Blankson JN, Persaud D, Siliciano RF. 2002. The Challenge of Viral Reservoirs in HIV-1 Infection. Annu Rev Med.

53. Boritz EA, Darko S, Swaszek L, Wolf G, Wells D, Wu X, Henry AR, Laboune F, Hu J, Ambrozak D, Hughes MS, Hoh R, Casazza JP, Vostal A, Bunis D, Nganou-Makamdop K,

Lee JS, Migueles SA, Koup RA, Connors M, Moir S, Schacker T, Maldarelli F, Hughes SH, Deeks SG, Douek DC. 2016. Multiple Origins of Virus Persistence during Natural Control of HIV Infection. Cell.

54. Bruner KM, Murray AJ, Pollack RA, Soliman MG, Laskey SB, Capoferri AA, Lai J, Strain MC, Lada SM, Hoh R, Ho YC, Richman DD, Deeks SG, Siliciano JD, Siliciano RF. 2016. Defective proviruses rapidly accumulate during acute HIV-1 infection. Nat Med.

55. Ho YC, Shan L, Hosmane NN, Wang J, Laskey SB, Rosenbloom DIS, Lai J, Blankson JN, Siliciano JD, Siliciano RF. 2013. XReplication-competent noninduced proviruses in the latent reservoir increase barrier to HIV-1 cure. Cell 155.

56. Chun TW, Carruth L, Finzi D, Shen X, DiGiuseppe JA, Taylor H, Hermankova M, Chadwick K, Margolick J, Quinn TC, Kuo YH, Brookmeyer R, Zeiger MA, Barditch-Crovo P, Siliciano RF. 1997. Quantification of latent tissue reservoirs and total body viral load in HIV-1 infection. Nature 387:183–188.

57. Siliciano JD, Kajdas J, Finzi D, Quinn TC, Chadwick K, Margolick JB, Kovacs C, Gange SJ, Siliciano RF. 2003. Long-term follow-up studies confirm the stability of the latent reservoir for HIV-1 in resting CD4+T cells. Nat Med 9:727–728.

58. Pierson T, McArthur J, Siliciano RF. 2000. Reservoirs for HIV-1: Mechanisms for Viral Persistence in the Presence of Antiviral Immune Responses and Antiretroviral Therapy. Annu Rev Immunol.

59. Kruize Z, Kootstra NA. 2019. The Role of Macrophages in HIV-1 Persistence and Pathogenesis . Front Microbiol .

60. Clayton KL, Garcia V, Clements JE, Walker BD. 2017. HIV Infection of Macrophages: Implications for Pathogenesis and Cure. Pathog Immunity; Vol 2, No 2 Vol 2, Number 2.

61. Delobel P, Sandres-Sauné K, Cazabat M, L'Faqihi FE, Aquilina C, Obadia M, Pasquier C, Marchou B, Massip P, Izopet J. 2005. Persistence of distinct HIV-1 populations in blood monocytes and naive and memory CD4 T cells during prolonged suppressive HAART. AIDS.

62. Kandathil AJ, Sugawara S, Balagopal A. 2016. Are T cells the only HIV-1 reservoir. Retrovirology.

63. Ellery PJ, Tippett E, Chiu Y-L, Paukovics G, Cameron PU, Solomon A, Lewin SR, Gorry PR, Jaworowski A, Greene WC, Sonza S, Crowe SM. 2007. The CD16 + Monocyte Subset Is More Permissive to Infection and Preferentially Harbors HIV-1 In Vivo . J Immunol.

64. Furtado MR, Callaway DS, Phair JP, Kunstman KJ, Stanton JL, Macken CA, Perelson

AS, Wolinsky SM. 1999. Persistence of HIV-1 transcription in peripheral-blood mononuclear cells in patients receiving potent antiretroviral therapy. N Engl J Med.

65. Koppensteiner H, Brack-Werner R, Schindler M. 2012. Macrophages and their relevance in Human Immunodeficiency Virus Type I infection. Retrovirology.

66. Waki K, Freed EO. 2010. Macrophages and cell-cell spread of HIV-1. Viruses.

67. Groot F, Welsch S, Sattentau QJ. 2008. Efficient HIV-1 transmission from macrophages to T cells across transient virological synapses. Blood.

68. Herbein G, Gras G, Khan KA, Abbas W. 2010. Macrophage signaling in HIV-1 infection. Retrovirology.

69. Zhang H, Dornadula G, Beumont M, Livornese L, Van Uitert B, Henning K, Pomerantz RJ. 1998. Human immunodeficiency virus type 1 in the semen of men receiving highly active antiretroviral therapy. N Engl J Med.

70. Lambotte O, Chaix ML, Gasnault J, Goujard C, Lebras P, Delfraissy JF, Taoufik Y. 2005. Persistence of replication-competent HIV in the central nervous system despite long-term effective highly active antiretroviral therapy [1]. AIDS.

71. Guadalupe M, Sankaran S, George MD, Reay E, Verhoeven D, Shacklett BL, Flamm J, Wegelin J, Prindiville T, Dandekar S. 2006. Viral Suppression and Immune Restoration in the Gastrointestinal Mucosa of Human Immunodeficiency Virus Type 1-Infected Patients Initiating Therapy during Primary or Chronic Infection. J Virol.

72. Poles MA, Boscardin WJ, Elliott J, Taing P, Fuerst MMP, McGowan I, Brown S, Anton PA. 2006. Lack of decay of HIV-1 in gut-associated lymphoid tissue reservoirs in maximally suppressed individuals. J Acquir Immune Defic Syndr.

73. Ko A, Kang G, Hattler JB, Galadima HI, Zhang J, Li Q, Kim WK. 2019. Macrophages but not Astrocytes Harbor HIV DNA in the Brains of HIV-1-Infected Aviremic Individuals on Suppressive Antiretroviral Therapy. J Neuroimmune Pharmacol.

74. Penton PK, Blackard JT. 2014. Analysis of HIV quasispecies suggests compartmentalization in the liver. AIDS Res Hum Retroviruses.

75. McDonald D, Wu L, Bohks SM, KewalRamani VN, Unutmaz D, Hope TJ. 2003. Recruitment of HIV and its receptors to dendritic cell-T cell junctions. Science (80-).

76. Van Nierop K, De Groot C. 2002. Human follicular dendritic cells: Function, origin and development. Semin Immunol.

77. Kulpa DA, Chomont N. 2015. HIV persistence in the setting of antiretroviral therapy: when, where and how does HIV hide? J virus Erad.

78. Wightman F, Solomon A, Khoury G, Green JA, Gray L, Gorry PR, Ho YS, Saksena NK, Hoy J, Crowe SM, Cameron PU, Lewin SR. 2010. Both CD31 + and CD31 − Naive CD4 + T Cells Are Persistent HIV Type 1–Infected Reservoirs in Individuals Receiving Antiretroviral Therapy . J Infect Dis.

79. Chomont N, El-Far M, Ancuta P, Trautmann L, Procopio FA, Yassine-Diab B, Boucher G, Boulassel MR, Ghattas G, Brenchley JM, Schacker TW, Hill BJ, Douek DC, Routy JP, Haddad EK, Sékaly RP. 2009. HIV reservoir size and persistence are driven by T cell survival and homeostatic proliferation. Nat Med 15:893–900.

80. Buzon MJ, Sun H, Li C, Shaw A, Seiss K, Ouyang Z, Martin-Gayo E, Leng J, Henrich TJ, Li JZ, Pereyra F, Zurakowski R, Walker BD, Rosenberg ES, Yu XG, Lichterfeld M. 2014. HIV-1 persistence in CD4+ T cells with stem cell-like properties. Nat Med.

81. Sallusto F, Lenig D, Förster R, Lipp M, Lanzavecchia A. 1999. Two subsets of memory T lymphocytes with distinct homing potentials and effector functions. Nature.

82. Riou C, Yassine-Diab B, Van Grevenynghe J, Somogyi R, Greller LD, Gagnon D, Gimmig S, Wilkinson P, Shi Y, Cameron MJ, Campos-Gonzalez R, Balderas RS, Kelvin D, Sekaly RP, Haddad EK. 2007. Convergence of TCR and cytokine signaling leads to FOXO3a phosphorylation and drives the survival of CD4+ central memory T cells. J Exp Med.

83. Soriano-Sarabia N, Bateson RE, Dahl NP, Crooks AM, Kuruc JD, Margolis DM, Archin NM. 2014. Quantitation of Replication-Competent HIV-1 in Populations of Resting CD4+ T Cells. J Virol.

84. Bernier A, Cleret-Buhot A, Zhang Y, Goulet JP, Monteiro P, Gosselin A, DaFonseca S, Wacleche VS, Jenabian MA, Routy JP, Tremblay C, Ancuta P. 2013. Transcriptional profiling reveals molecular signatures associated with HIV permissiveness in th1th17 cells and identifies peroxisome proliferator-activated receptor gamma as an intrinsic negative regulator of viral replication. Retrovirology.

85. Vanhamel J, Bruggemans A, Debyser Z. 2019. Establishment of latent HIV-1 reservoirs: what do we really know? J virus Erad.

86. Coffin J, Swanstrom R. 2013. HIV pathogenesis: Dynamics and genetics of viral populations and infected cells. Cold Spring Harb Perspect Med.

87. Perreau M, Savoye AL, De Crignis E, Jean-Marc Corpataux, Cubas R, Haddad EK, De Leval L, Graziosi C, Pantaleo G. 2013. Follicular helper T cells serve as the major CD4 T cell compartment for HIV-1 infection, replication, and production. J Exp Med.

88. Tran TA, de Goër de Herve MG, Hendel-Chavez H, Dembele B, Le Névot E, Abbed K, Pallier C, Goujard C, Gasnault J, Delfraissy JF, Balazuc AM, Taoufik Y. 2008. Resting regulatory CD4 T cells: A site of HIV persistence in patients on long-term effective antiretroviral therapy. PLoS One.

89. Alvarez Y, Tuen M, Shen G, Nawaz F, Arthos J, Wolff MJ, Poles MA, Hioe CE. 2013. Preferential HIV Infection of CCR6+ Th17 Cells Is Associated with Higher Levels of Virus Receptor Expression and Lack of CCR5 Ligands. J Virol.

90. Chun TW, Engel D, Berrey MM, Shea T, Corey L, Fauci AS. 1998. Early establishment of a pool of latently infected, resting CD4+ T cells during primary HIV-1 infection. Proc Natl Acad Sci U S A.

91. Shan L, Deng K, Shroff NS, Durand CM, Rabi SA, Yang HC, Zhang H, Margolick JB, Blankson JN, Siliciano RF. 2012. Stimulation of HIV-1-Specific Cytolytic T Lymphocytes Facilitates Elimination of Latent Viral Reservoir after Virus Reactivation. Immunity.

92. Gasper DJ, Tejera MM, Suresh M. 2014. CD4 T-cell memory generation and maintenance. Crit Rev Immunol.

93. Zerbato JM, Serrao E, Lenzi G, Kim B, Ambrose Z, Watkins SC, Engelman AN, Sluis-Cremer N. 2016. Establishment and Reversal of HIV-1 Latency in Naive and Central Memory CD4 + T Cells In Vitro . J Virol.

94. Lassen K, Han Y, Zhou Y, Siliciano J, Siliciano RF. 2004. The multifactorial nature of HIV-1 latency. Trends Mol Med.

95. Shan L, Deng K, Gao H, Xing S, Capoferri AA, Durand CM, Rabi SA, Laird GM, Kim M, Hosmane NN, Yang HC, Zhang H, Margolick JB, Li L, Cai W, Ke R, Flavell RA, Siliciano JD, Siliciano RF. 2017. Transcriptional Reprogramming during Effector-to-Memory Transition Renders CD4+ T Cells Permissive for Latent HIV-1 Infection. Immunity.

96. Bosque A, Planelles V. 2009. Induction of HIV-1 latency and reactivation in primary memory CD4+ T cells. Blood.

97. Tahirov TH, Babayeva ND, Varzavand K, Cooper JJ, Sedore SC, Price DH. 2010. Crystal structure of HIV-1 Tat complexed with human P-TEFb. Nature.

98. Wei P, Garber ME, Fang SM, Fischer WH, Jones KA. 1998. A novel CDK9-associated C-type cyclin interacts directly with HIV-1 Tat and mediates its high-affinity, loop-specific binding to TAR RNA. Cell.

99. Yamada T, Yamaguchi Y, Inukai N, Okamoto S, Mura T, Handa H. 2006. P-TEFb-mediated phosphorylation of hSpt5 C-terminal repeats is critical for processive transcription elongation. Mol Cell.

100. Fujinaga K, Irwin D, Huang Y, Taube R, Kurosu T, Peterlin BM. 2004. Dynamics of Human Immunodeficiency Virus Transcription: P-TEFb Phosphorylates RD and Dissociates Negative Effectors from the Transactivation Response Element. Mol Cell Biol.

101. Liou L-Y, Herrmann CH, Rice AP. 2002. Transient Induction of Cyclin T1 during Human Macrophage Differentiation Regulates Human Immunodeficiency Virus Type 1 Tat Transactivation Function. J Virol.

102. Ghose R, Liou L-Y, Herrmann CH, Rice AP. 2001. Induction of TAK (Cyclin T1/P-TEFb) in Purified Resting CD4+ T Lymphocytes by Combination of Cytokines. J Virol.

103. Ylisastigui L, Archin NM, Lehrman G, Bosch RJ, Margolis DM. 2004. Coaxing HIV-1 from resting CD4 T cells: Histone deacetylase inhibition allows latent viral expression. AIDS.

104. Pearson R, Kim YK, Hokello J, Lassen K, Friedman J, Tyagi M, Karn J. 2008. Epigenetic Silencing of Human Immunodeficiency Virus (HIV) Transcription by Formation of Restrictive Chromatin Structures at the Viral Long Terminal Repeat Drives the Progressive Entry of HIV into Latency. J Virol.

105. Chéné I Du, Basyuk E, Lin YL, Triboulet R, Knezevich A, Chable-Bessia C, Mettling C, Baillat V, Reynes J, Corbeau P, Bertrand E, Marcello A, Emiliani S, Kiernan R, Benkirane M. 2007. Suv39H1 and HP1γ are responsible for chromatin-mediated HIV-1 transcriptional silencing and post-integration latency. EMBO J.

106. Verdin E. 1997. Transcriptional activation and chromatin remodeling of the HIV-I promoter in response to histone acetylation. Chemtracts.

107. Han Y, Lin YB, An W, Xu J, Yang HC, O'Connell K, Dordai D, Boeke JD, Siliciano JD, Siliciano RF. 2008. Orientation-Dependent Regulation of Integrated HIV-1 Expression by Host Gene Transcriptional Readthrough. Cell Host Microbe.

108. Lassen KG, Ramyar KX, Bailey JR, Zhou Y, Siliciano RF. 2006. Nuclear retention of multiply spliced HIV-1 RNA in resting CD4+ T cells. PLoS Pathog.

109. Timilsina U, Gaur R. 2016. Modulation of apoptosis and viral latency – An axis to be well understood for successful cure of human immunodeficiency virus. J Gen Virol.

110. Daelemans D, De Clercq E, Vandamme AM. 2000. Control of RNA initiation and elongation at the HIV promoter. AIDS Rev.

111. Kim YK, Mbonye U, Hokello J, Karn J. 2011. T-Cell receptor signaling enhances transcriptional elongation from latent HIV proviruses by activating P-TEFb through an ERK-dependent pathway. J Mol Biol.

112. Kinoshita S, Chen BK, Kaneshima H, Nolan GP. 1998. Host control of HIV-1 parasitism in T cells by the nuclear factor of activated T cells. Cell.

113. Nguyen K, Das B, Dobrowolski C, Karn J. 2017. Multiple histone lysine methyltransferases are required for the establishment and maintenance of HIV-1

latency. MBio.

114. Shimabukuro-Vornhagen A, Gödel P, Subklewe M, Stemmler HJ, Schlößer HA, Schlaak M, Kochanek M, Böll B, von Bergwelt-Baildon MS. 2018. Cytokine release syndrome. J Immunother Cancer.

115. Sadowski I, Hashemi FB. 2019. Strategies to eradicate HIV from infected patients: elimination of latent provirus reservoirs. Cell Mol Life Sci.

116. Sadowski I, Mitchell DA. 2005. TFII-I and USF (RBF-2) regulate Ras/MAPK-responsive HIV-1 transcription in T cells. Eur J Cancer.

117. Schröder ARW, Shinn P, Chen H, Berry C, Ecker JR, Bushman F. 2002. HIV-1 integration in the human genome favors active genes and local hotspots. Cell.

118. Hashemi P, Barreto K, Bernhard W, Lomness A, Honson N, Pfeifer TA, Harrigan PR, Sadowski I. 2018. Compounds producing an effective combinatorial regimen for disruption of HIV -1 latency . EMBO Mol Med.

119. Bashiri K, Rezaei N, Nasi M, Cossarizza A. 2018. The role of latency reversal agents in the cure of HIV: A review of current data. Immunol Lett.

120. Jones RB, Mueller S, O'Connor R, Rimpel K, Sloan DD, Karel D, Wong HC, Jeng EK, Thomas AS, Whitney JB, Lim SY, Kovacs C, Benko E, Karandish S, Huang SH, Buzon MJ, Lichterfeld M, Irrinki A, Murry JP, Tsai A, Yu H, Geleziunas R, Trocha A, Ostrowski MA, Irvine DJ, Walker BD. 2016. A Subset of Latency-Reversing Agents Expose HIV-Infected Resting CD4+T-Cells to Recognition by Cytotoxic T-Lymphocytes. PLoS Pathog.

121. Archin NM, Kirchherr JL, Sung JAM, Clutton G, Sholtis K, Xu Y, Allard B, Stuelke E, Kashuba AD, Kuruc JD, Eron J, Gay CL, Goonetilleke N, Margolis DM. 2017. Interval dosing with the HDAC inhibitor vorinostat effectively reverses HIV latency. J Clin Invest.

122. Elliott JH, McMahon JH, Chang CC, Lee SA, Hartogensis W, Bumpus N, Savic R, Roney J, Hoh R, Solomon A, Piatak M, Gorelick RJ, Lifson J, Bacchetti P, Deeks SG, Lewin SR. 2015. Short-term administration of disulfiram for reversal of latent HIV infection: a phase 2 dose-escalation study. Lancet HIV.

123. Gutiérrez C, Serrano-Villar S, Madrid-Elena N, Pérez-Eĺas MJ, Martń ME, Barbas C, Ruipérez J, Muñoz E, Muñoz-Fernández MA, Castor T, Moreno S. 2016. Bryostatin-1 for latent virus reactivation in HIV-infected patients on antiretroviral therapy. AIDS.

124. Rasmussen TA, Tolstrup M, Brinkmann CR, Olesen R, Erikstrup C, Solomon A, Winckelmann A, Palmer S, Dinarello C, Buzon M, Lichterfeld M, Lewin SR, Ostergaard L, Søgaard OS. 2014. Panobinostat, a histone deacetylase inhibitor, for latent virus

reactivation in HIV-infected patients on suppressive antiretroviral therapy: A phase 1/2, single group, clinical trial. Lancet HIV.

125. Søgaard OS, Graversen ME, Leth S, Olesen R, Brinkmann CR, Nissen SK, Kjaer AS, Schleimann MH, Denton PW, Hey-Cunningham WJ, Koelsch KK, Pantaleo G, Krogsgaard K, Sommerfelt M, Fromentin R, Chomont N, Rasmussen TA, Østergaard L, Tolstrup M. 2015. The Depsipeptide Romidepsin Reverses HIV-1 Latency In Vivo. PLoS Pathog.

126. Boucau J, Das J, Joshi N, Le Gall S. 2020. Latency reversal agents modulate HIV antigen processing and presentation to CD8 T cells. PLoS Pathog.

127. Walker-Sperling VE, Pohlmeyer CW, Tarwater PM, Blankson JN. 2016. The Effect of Latency Reversal Agents on Primary CD8+ T Cells: Implications for Shock and Kill Strategies for Human Immunodeficiency Virus Eradication. EBioMedicine 8:217–229.

128. Deng K, Pertea M, Rongvaux A, Wang L, Durand CM, Ghiaur G, Lai J, McHugh HL, Hao H, Zhang H, Margolick JB, Gurer C, Murphy AJ, Valenzuela DM, Yancopoulos GD, Deeks SG, Strowig T, Kumar P, Siliciano JD, Salzberg SL, Flavell RA, Shan L, Siliciano RF. 2015. Broad CTL response is required to clear latent HIV-1 due to dominance of escape mutations. Nature.

129. Blackburn SD, Shin H, Haining WN, Zou T, Workman CJ, Polley A, Betts MR, Freeman GJ, Vignali DAA, Wherry EJ. 2009. Coregulation of CD8+ T cell exhaustion by multiple inhibitory receptors during chronic viral infection. Nat Immunol.

130. Youngblood B, Noto A, Porichis F, Akondy RS, Ndhlovu ZM, Austin JW, Bordi R, Procopio FA, Miura T, Allen TM, Sidney J, Sette A, Walker BD, Ahmed R, Boss JM, Sékaly R-P, Kaufmann DE. 2013. Cutting Edge: Prolonged Exposure to HIV Reinforces a Poised Epigenetic Program for PD-1 Expression in Virus-Specific CD8 T Cells. J Immunol.

131. Fukazawa Y, Lum R, Okoye AA, Park H, Matsuda K, Bae JY, Hagen SI, Shoemaker R, Deleage C, Lucero C, Morcock D, Swanson T, Legasse AW, Axthelm MK, Hesselgesser J, Geleziunas R, Hirsch VM, Edlefsen PT, Piatak M, Estes JD, Lifson JD, Picker LJ. 2015. B cell follicle sanctuary permits persistent productive simian immunodeficiency virus infection in elite controllers. Nat Med.

132. Tateishi H, Monde K, Anraku K, Koga R, Hayashi Y, Ciftci HI, Demirci H, Higashi T, Motoyama K, Arima H, Otsuka M, Fujita M. 2017. A clue to unprecedented strategy to HIV eradication: “Lock-in and apoptosis.” Sci Rep.

133. Fong LE, Sulistijo ES, Miller-Jensen K. 2017. Systems analysis of latent HIV reversal reveals altered stress kinase signaling and increased cell death in infected T cells. Sci Rep.

134. Bohn-Wippert K, Tevonian EN, Lu Y, Huang MY, Megaridis MR, Dar RD. 2018. Cell Size-Based Decision-Making of a Viral Gene Circuit. Cell Rep.

135. Kulkosky J, Nunnari G, Otero M, Calarota S, Dornadula G, Zhang H, Malin A, Sullivan J, Xu Y, DeSimone J, Babinchak T, Stern J, Cavert W, Haase A, Pomerantz RJ. 2002. Intensification and Stimulation Therapy for Human Immunodeficiency Virus Type 1 Reservoirs in Infected Persons Receiving Virally Suppressive Highly Active Antiretroviral Therapy. J Infect Dis.

136. Jamaluddin MS, Hu PW, Jan Y, Siwak EB, Rice AP. 2016. Short Communication: The Broad-Spectrum Histone Deacetylase Inhibitors Vorinostat and Panobinostat Activate Latent HIV in CD4+ T Cells in Part Through Phosphorylation of the T-Loop of the CDK9 Subunit of P-TEFb. AIDS Res Hum Retroviruses.

137. Rasmussen TA, Søgaard OS, Brinkmann C, Wightman F, Lewin SR, Melchjorsen J, Dinarello C, Østergaard L, Tolstrup M. 2013. Comparison of HDAC inhibitors in clinical development: Effect on HIV production in latently infected cells and T-cell activation. Hum Vaccines Immunother 9:993–1001.

138. Blazkova J, Chun T-W, Belay BW, Murray D, Justement JS, Funk EK, Nelson A, Hallahan CW, Moir S, Wender PA, Fauci AS. 2012. Effect of histone deacetylase inhibitors on HIV production in latently infected, resting CD4(+) T cells from infected individuals receiving effective antiretroviral therapy. J Infect Dis 206:765–9.

139. Archin NM, Bateson R, Tripathy MK, Crooks AM, Yang K-H, Dahl NP, Kearney MF, Anderson EM, Coffin JM, Strain MC, Richman DD, Robertson KR, Kashuba AD, Bosch RJ, Hazuda DJ, Kuruc JD, Eron JJ, Margolis DM. 2014. HIV-1 Expression Within Resting CD4+ T Cells After Multiple Doses of Vorinostat. J Infect Dis 210:728–735.

140. Archin NM, Liberty AL, Kashuba AD, Choudhary SK, Kuruc JD, Crooks AM, Parker DC, Anderson EM, Kearney MF, Strain MC, Richman DD, Hudgens MG, Bosch RJ, Coffin JM, Eron JJ, Hazuda DJ, Margolis DM. 2012. Administration of vorinostat disrupts HIV-1 latency in patients on antiretroviral therapy. Nature 487:482–485.

141. Spivak AM, Bosque A, Balch AH, Smyth D, Martins L, Planelles V. 2015. Ex vivo bioactivity and HIV-1 latency reversal by ingenol dibenzoate and panobinostat in resting CD4+T cells from aviremic patients. Antimicrob Agents Chemother 59:5984–5991.

142. Banga R, Procopio F, Cavassini M, Perreau M. 2015. In Vitro Reactivation of Replication Competent and Infectious HIV-1 by HDAC Inhibitors. J Virol 4:JVI.02359-15.

143. Shirakawa K, Chavez L, Hakre S, Calvanese V, Verdin E. 2013. Reactivation of latent HIV by histone deacetylase inhibitors. Trends Microbiol.

144. Park SY, Kim KC, Hong KJ, Kim SS, Choi BS. 2013. Histone deactylase inhibitor SAHA induces a synergistic HIV-1 reactivation by 12-O-tetradecanoylphorbol-13-acetate in latently infected cells. Intervirology 56:242–248.

145. Margolis DM. 2011. Histone deacetylase inhibitors and HIV latency. Curr Opin HIV AIDS 6:25–29.

146. Doyon G, Zerbato J, Mellors JW, Sluis-Cremer N. 2013. Disulfiram reactivates latent HIV-1 expression through depletion of the phosphatase and tensin homolog. AIDS 27.

147. Xing S, Bullen CK, Shroff NS, Shan L, Yang H-C, Manucci JL, Bhat S, Zhang H, Margolick JB, Quinn TC, Margolis DM, Siliciano JD, Siliciano RF. 2011. Disulfiram Reactivates Latent HIV-1 in a Bcl-2-Transduced Primary CD4+ T Cell Model without Inducing Global T Cell Activation. J Virol 85:6060–6064.

148. Bullen CK, Laird GM, Durand CM, Siliciano JD, Siliciano RF. 2014. New ex vivo approaches distinguish effective and ineffective single agents for reversing HIV-1 latency in vivo. Nat Med 20:425–429.

149. McKernan LN, Momjian D, Kulkosky J. 2012. Protein kinase C: One pathway towards the eradication of latent HIV-1 Reservoirs. Adv Virol.

150. Darcis G, Kula A, Bouchat S, Fujinaga K, Corazza F, Ait-Ammar A, Delacourt N, Melard A, Kabeya K, Vanhulle C, Van Driessche B, Gatot JS, Cherrier T, Pianowski LF, Gama L, Schwartz C, Vila J, Burny A, Clumeck N, Moutschen M, De Wit S, Peterlin BM, Rouzioux C, Rohr O, Van Lint C. 2015. An In-Depth Comparison of Latency-Reversing Agent Combinations in Various In Vitro and Ex Vivo HIV-1 Latency Models Identified Bryostatin-1+JQ1 and Ingenol-B+JQ1 to Potently Reactivate Viral Gene Expression. PLoS Pathog 11.

151. Dental C, Proust A, Ouellet M, Barat C, Tremblay MJ. 2017. HIV-1 Latency-Reversing Agents Prostratin and Bryostatin-1 Induce Blood–Brain Barrier Disruption/Inflammation and Modulate Leukocyte Adhesion/Transmigration. J Immunol 198:1229–1241.

152. Spivak AM, Planelles V. 2018. Novel Latency Reversal Agents for HIV-1 Cure. Annu Rev Med 69:annurev-med-052716-031710.

153. Gosselin A, Wiche Salinas TR, Planas D, Wacleche VS, Zhang Y, Fromentin R, Chomont N, Cohen ÉA, Shacklett B, Mehraj V, Ghali MP, Routy J-P, Ancuta P. 2017. HIV persists in CCR6+CD4+ T-cells from colon and blood during antiretroviral therapy. AIDS 31:35–38.

154. Wacleche VS, Chomont N, Gosselin A, Monteiro P, Goupil M, Kared H, Tremblay C, Bernard N, Boulassel MR, Routy JP, Ancuta P. 2012. The colocalization potential of

HIV-specific CD8 + and CD4 + T-cells is mediated by integrin β7 but not CCR6 and regulated by retinoic acid. PLoS One 7.

155. Sadowski I, Lourenco P, Malcolm T. 2008. Factors Controlling Chromatin Organization and Nucleosome Positioning for Establishment and Maintenance of HIV Latency. Curr HIV Res.

156. Ahlenstiel C, Mendez C, Lim STH, Marks K, Turville S, Cooper DA, Kelleher AD, Suzuki K. 2015. Novel RNA duplex locks HIV-1 in a latent state via chromatin-mediated transcriptional silencing. Mol Ther - Nucleic Acids.

157. Pengue G, Caputo A, Rossi C, Barbanti-Brodano G, Lania L. 1995. Transcriptional silencing of human immunodeficiency virus type 1 long terminal repeat-driven gene expression by the Krüppel-associated box repressor domain targeted to the transactivating response element. J Virol.

158. Jin H, Li D, Sivakumaran H, Lor M, Rustanti L, Cloonan N, Wani S, Harrich D. 2016. Shutdown of HIV-1 transcription in T cells by Nullbasic, a mutant tat protein. MBio.

159. Murchie AIH, Davis B, Isel C, Afshar M, Drysdale MJ, Bower J, Potter AJ, Starkey ID, Swarbrick TM, Mirza S, Prescott CD, Vaglio P, Aboul-ela F, Karn J. 2004. Structure-based Drug Design Targeting an Inactive RNA Conformation: Exploiting the Flexibility of HIV-1 TAR RNA. J Mol Biol.

160. Li MJ, Kim J, Li S, Zaia J, Yee JK, Anderson J, Akkina R, Rossi JJ. 2005. Long-term inhibition of HIV-1 infection in primary hematopoietic cells by lentiviral vector delivery of a triple combination of anti-HIV shRNA, anti-CCR5 ribozyme, and a nucleolar-localizing TAR decoy. Mol Ther.

161. Wang Q, Liu S, Liu Z, Ke Z, Li C, Yu X, Chen S, Guo D. 2018. Genome scale screening identification of SaCas9/gRNAs for targeting HIV-1 provirus and suppression of HIV-1 infection. Virus Res.

162. Wang G, Zhao N, Berkhout B, Das AT. 2018. CRISPR-Cas based antiviral strategies against HIV-1. Virus Res.

163. Yin C, Zhang T, Qu X, Zhang Y, Putatunda R, Xiao X, Li F, Xiao W, Zhao H, Dai S, Qin X, Mo X, Young W Bin, Khalili K, Hu W. 2017. In Vivo Excision of HIV-1 Provirus by saCas9 and Multiplex Single-Guide RNAs in Animal Models. Mol Ther.

164. Qu X, Wang P, Ding D, Li L, Wang H, Ma L, Zhou X, Liu S, Lin S, Wang X, Zhang G, Liu S, Liu L, Wang J, Zhang F, Lu D, Zhu H. 2013. Zinc-finger-nucleases mediate specific and efficient excision of HIV-1 proviral DNA from infected and latently infected human T cells. Nucleic Acids Res.

165. Willems L, Gillet NA. 2015. APOBEC3 interference during replication of viral

genomes. Viruses.

166. Refsland EW, Stenglein MD, Shindo K, Albin JS, Brown WL, Harris RS. 2010. Quantitative profiling of the full APOBEC3 mRNA repertoire in lymphocytes and tissues: Implications for HIV-1 restriction. Nucleic Acids Res 38:4274–4284.

167. Rebhandl S, Huemer M, Greil R, Geisberger R. 2015. AID/APOBEC deaminases and cancer. Oncoscience.

168. Smith HC, Bennett RP, Kizilyer A, McDougall WM, Prohaska KM. 2012. Functions and regulation of the APOBEC family of proteins. Semin Cell Dev Biol.

169. Stenglein MD, Burns MB, Li M, Lengyel J, Harris RS. 2010. APOBEC3 proteins mediate the clearance of foreign DNA from human cells. Nat Struct Mol Biol.

170. Mangeat B, Turelli P, Caron G, Friedli M, Perrin L, Trono D. 2003. Broad antiretroviral defence by human APOBEC3G through lethal editing of nascent reverse transcripts. Nature.

171. Liddament MT, Brown WL, Schumacher AJ, Harris RS. 2004. APOBEC3F properties and hypermutation preferences indicate activity against HIV-1 in vivo. Curr Biol.

172. Dang Y, Wang X, Esselman WJ, Zheng Y-H. 2006. Identification of APOBEC3DE as Another Antiretroviral Factor from the Human APOBEC Family. J Virol.

173. Hultquist JF, Lengyel JA, Refsland EW, LaRue RS, Lackey L, Brown WL, Harris RS. 2011. Human and Rhesus APOBEC3D, APOBEC3F, APOBEC3G, and APOBEC3H Demonstrate a Conserved Capacity To Restrict Vif-Deficient HIV-1. J Virol.

174. Doehle BP, Schäfer A, Cullen BR. 2005. Human APOBEC3B is a potent inhibitor of HIV-1 infectivity and is resistant to HIV-1 Vif. Virology.

175. Thielen BK, McNevin JP, McElrath MJ, Hunt BVS, Klein KC, Lingappa JR. 2010. Innate immune signaling induces high levels of TC-specific deaminase activity in primary monocyte-derived cells through expression of APOBEC3A isoforms. J Biol Chem.

176. Harris RS, Liddament MT. 2004. Retroviral restriction by APOBEC proteins. Nat Rev Immunol.

177. Wang Y, Schmitt K, Guo K, Santiago ML, Stephens EB. 2016. Role of the single deaminase domain APOBEC3A in virus restriction, retrotransposition, DNA damage and cancer. J Gen Virol.

178. Bishop KN, Holmes RK, Malim MH. 2006. Antiviral Potency of APOBEC Proteins Does Not Correlate with Cytidine Deamination. J Virol.

179. Iwatani Y, Chan DSB, Wang F, Maynard KS, Sugiura W, Gronenborn AM, Rouzina I, Williams MC, Musier-Forsyth K, Levin JG. 2007. Deaminase-independent inhibition of HIV-1 reverse transcription by APOBEC3G. Nucleic Acids Res.

180. Kobayashi T, Koizumi Y, Takeuchi JS, Misawa N, Kimura Y, Morita S, Aihara K, Koyanagi Y, Iwami S, Sato K. 2014. Quantification of Deaminase Activity-Dependent and -Independent Restriction of HIV-1 Replication Mediated by APOBEC3F and APOBEC3G through Experimental-Mathematical Investigation. J Virol.

181. Yu Q, König R, Pillai S, Chiles K, Kearney M, Palmer S, Richman D, Coffin JM, Landau NR. 2004. Single-strand specificity of APOBEC3G accounts for minus-strand deamination of the HIV genome. Nat Struct Mol Biol.

182. Harris RS, Bishop KN, Sheehy AM, Craig HM, Petersen-Mahrt SK, Watt IN, Neuberger MS, Malim MH. 2003. DNA deamination mediates innate immunity to retroviral infection. Cell.

183. Harari A, Ooms M, Mulder LCF, Simon V. 2009. Polymorphisms and Splice Variants Influence the Antiretroviral Activity of Human APOBEC3H. J Virol.

184. Ara A, Love RP, Follack TB, Ahmed KA, Adolph MB, Chelico L. 2017. Mechanism of Enhanced HIV Restriction by Virion Coencapsidated Cytidine Deaminases APOBEC3F and APOBEC3G. J Virol.

185. Feng Y, Baig TT, Love RP, Chelico L. 2014. Suppression of APOBEC3-mediated restriction of HIV-1 by Vif. Front Microbiol.

186. Desimmie BA, Delviks-Frankenberrry KA, Burdick RC, Qi D, Izumi T, Pathak VK. 2014. Multiple APOBEC3 restriction factors for HIV-1 and one vif to rule them all. J Mol Biol.

187. Smith HC. 2011. APOBEC3G: A double agent in defense. Trends Biochem Sci.

188. Sheehy AM, Gaddis NC, Choi JD, Malim MH. 2002. Isolation of a human gene that inhibits HIV-1 infection and is suppressed by the viral Vif protein. Nature.

189. Ikeda T, Symeonides M, Albin JS, Li M, Thali M, Harris RS. 2018. HIV-1 adaptation studies reveal a novel Env-mediated homeostasis mechanism for evading lethal hypermutation by APOBEC3G. PLoS Pathog.

190. Cuevas JM, Geller R, Garijo R, López-Aldeguer J, Sanjuán R. 2015. Extremely High Mutation Rate of HIV-1 In Vivo. PLoS Biol.

191. Hu WS, Hughes SH. 2012. HIV-1 reverse transcription. Cold Spring Harb Perspect Med.

192. Dapp MJ, Heineman RH, Mansky LM. 2013. Interrelationship between HIV-1 fitness and mutation rate. J Mol Biol.

193. Mansky LM, Temin HM. 1995. Lower in vivo mutation rate of human immunodeficiency virus type 1 than that predicted from the fidelity of purified reverse transcriptase. J Virol.

194. Bleul CC, Wu L, Hoxie JA, Springer TA, Mackay CR. 1997. The HIV coreceptors CXCR4 and CCR5 are differentially expressed and regulated on human T lymphocytes. Proc Natl Acad Sci U S A.

195. McCune JM. 2001. The dynamics of CD4+ T-cell depletion in HIV disease. Nature.

196. Lee B, Sharron M, Montaner LJ, Weissman D, Doms RW. 1999. Quantification of CD4, CCR5, and CXCR4 levels on lymphocyte subsets, dendritic cells, and differentially conditioned monocyte-derived macrophages. Proc Natl Acad Sci U S A.

197. Finzi D, Blankson J, Siliciano JD, Margolick JB, Chadwick K, Pierson T, Smith K, Lisziewicz J, Lori F, Flexner C, Quinn TC, Chaisson RE, Rosenberg E, Walker B, Gange S, Gallant J, Siliciano RF. 1999. Latent infection of CD4+T cells provides a mechanism for lifelong persistence of HIV-1, even in patients on effective combination therapy. Nat Med 5:512–517.

198. Finzi D, Hermankova M, Pierson T, Carruth LM, Buck C, Chaisson RE, Quinn TC, Chadwick K, Margolick J, Brookmeyer R, Gallant J, Markowitz M, Ho DD, Richman DD, Siliciano RF. 1997. Identification of a reservoir for HIV-1 in patients on highly active antiretroviral therapy. Science 278:1295–300.

199. Abner E, Jordan A. 2019. HIV “shock and kill” therapy: In need of revision. Antiviral Res.

200. Eckmann CR, Rammelt C, Wahle E. 2011. Control of poly(A) tail length. Wiley Interdiscip Rev RNA.

201. Fiebig EW, Wright DJ, Rawal BD, Garrett PE, Schumacher RT, Peddada L, Heldebrant C, Smith R, Conrad A, Kleinman SH, Busch MP. 2003. Dynamics of HIV viremia and antibody seroconversion in plasma donors: Implications for diagnosis and staging of primary HIV infection. AIDS 17:1871–1879.

202. Summers MF, Henderson LE, Chance MR, South TL, Blake PR, Perez-Alvarado G, Bess JW, Sowder RC, Arthur LO, Sagi I, Hare DR. 1992. Nucleocapsid zinc fingers detected in retroviruses: EXAFS studies of intact viruses and the solution-state structure of the nucleocapsid protein from HIV-1. Protein Sci 1:563–574.

203. Momany C, Kovari LC, Prongay a J, Keller W, Gitti RK, Lee BM, Gorbalenya a E, Tong L, McClure J, Ehrlich LS, Summers MF, Carter C, Rossmann MG. 1996. Crystal

structure of dimeric HIV-1 capsid protein. Nat Struct Biol 3:763–770.

204. Jurkat, Clone E6-1 ATCC ® TIB-152™ Homo sapiens peripheral b.

205. Finkelshtein D, Werman A, Novick D, Barak S, Rubinstein M. 2013. LDL receptor and its family members serve as the cellular receptors for vesicular stomatitis virus. Proc Natl Acad Sci U S A.

206. Cary DC, Fujinaga K, Peterlin BM. 2016. Molecular mechanisms of HIV latency. J Clin Invest.

207. Rice A, Herrmann C. 2005. Regulation of TAK / P-TEFb in CD4+ T Lymphocytes and Macrophages. Curr HIV Res.

208. Nilson KA, Price DH. 2011. The Role of RNA Polymerase II Elongation Control in HIV-1 Gene Expression, Replication, and Latency. Genet Res Int.

209. Knights HDJ. 2017. A Critical Review of the Evidence Concerning the HIV Latency Reversing Effect of Disulfiram, the Possible Explanations for Its Inability to Reduce the Size of the Latent Reservoir in Vivo, and the Caveats Associated with Its Use in Practice. AIDS Res Treat.

210. Wu G, Swanson M, Talla A, Graham D, Strizki J, Gorman D, Barnard RJ, Blair W, Søgaard OS, Tolstrup M, Østergaard L, Rasmussen TA, Sekaly RP, Archin NM, Margolis DM, Hazuda DJ, Howell BJ. 2017. HDAC inhibition induces HIV-1 protein and enables immune-based clearance following latency reversal. JCI insight.

211. Chatila T, Silverman L, Miller R, Geha R. 1989. Mechanisms of T cell activation by the calcium ionophore ionomycin. J Immunol.

212. Hamid F Bin, Kim J, Shin CG. 2017. Distribution and fate of HIV-1 unintegrated DNA species: A comprehensive update. AIDS Res Ther.

213. Alu Element - an overview | ScienceDirect Topics.

214. Reagent Datasheet Detail: Catalog 3942 - GHOST (3) CXCR4+CCR5+ Cells - NIH AIDS Reagent Program.

215. Bannwarth S, Gatignol A. 2005. HIV-1 TAR RNA: The Target of Molecular Interactions Between the Virus and its Host. Curr HIV Res.

216. Rice AP. 2017. The HIV-1 Tat Protein: Mechanism of Action and Target for HIV-1 Cure Strategies. Curr Pharm Des.

217. Rice AP. 2019. Unexpected mutations in HIV-1 that confer resistance to the tat inhibitor Didehydro-Cortistatin A. MBio.

218. Battivelli E, Migraine J, Lecossier D, Yeni P, Clavel F, Hance AJ. 2011. Gag Cytotoxic T Lymphocyte Escape Mutations Can Increase Sensitivity of HIV-1 to Human TRIM5 , Linking Intrinsic and Acquired Immunity. J Virol.

219. Draenert R, Le Gall S, Pfafferott KJ, Leslie AJ, Chetty P, Brander C, Holmes EC, Chang SC, Feeney ME, Addo MM, Ruiz L, Ramduth D, Jeena P, Altfeld M, Thomas S, Tang Y, Verrill CL, Dixon C, Prado JG, Kiepiela P, Martinez-Picado J, Walker BD, Goulder PJR. 2004. Immune Selection for Altered Antigen Processing Leads to Cytotoxic T Lymphocyte Escape in Chronic HIV-1 Infection. J Exp Med.

220. Brumme ZL, John M, Carlson JM, Brumme CJ, Chan D, Brockman MA, Swenson LC, Tao I, Szeto S, Rosato P, Sela J, Kadie CM, Frahm N, Brander C, Haas DW, Riddler SA, Haubrich R, Walker BD, Harrigan PR, Heckerman D, Mallal S. 2009. HLA-associated immune escape pathways in HIV-1 subtype B Gag, Pol and Nef proteins. PLoS One.

221. Dahabieh MS, Battivelli E, Verdin E. 2015. Understanding HIV Latency: The Road to an HIV Cure. Annu Rev Med 66:407–421.

Appendices

Appendix 1- Primers and Probes

Table 2 Primer and Probe Sequences

Primer/Probe Name	5’-3’ Sequence
Actin Probe	56TAM-CCCTGTACGCCTCTGGCCGTACCACTGGC-3IABRQ
LTR R REGION Probe	5YAKYEI-CTTTATTGAGGCT+TAAG+C+AG+T+G+GGT-3IABKFQ (IDT)
Actin 1	CATGTACGTTGCTATCCAGGC
Actin 2	CTCCTTAATGTCACGCACGAT
Alu1 Primer	TCCCAGCTACTGGGGAGGCTGAGG
Alu2 Primer	GCCTCCCAAAGTGCTGGGATTACAG
Lambda R Rev 2	GTTTCGCTTACGTGGCATCAGACGG
Lambda R U5 Rev 1	AGTTTCGCTTACGTGGCATCAGACGGGCACACACTACTTTGAGCAC
Late U3 For	GCTACATATAAGCAGCTGCTTTTTGCCTGTAC
NL4 Pre XhoI For	AATGAGACGAGCTGAGCCAG
NL4 Post XhoI Rev	TGCTTGTGCCTGGCTAGAAG
NL4 3’LTR Rev	CTCACTGCAACCTCTACCTC

Appendix 2- Concentrations of Latency Reversing Agents Tested

Table 3 Concentrations of Latency Reversing Agents

Latency Reversing Agent	Concentration used on HEK 293T Cells	Concentration used on Jurkat Cells	Concentration used on U87 Cells
ATRA	10nM	10nM	
Bryostatin-1	10nM	1nM	
Disulfiram	10uM	10uM	
Panobinostat	50nM	50nM	
PMA + Ionomycin	PMA: 10ng/mL I: 1uM	PMA: 10ng/mL I: 1uM	PMA: 5ng/mL I: 0.5uM
Romidepsin	500nM	500nM	
Valproic Acid	40uM	40uM	
Vorinostat	1uM	10uM	

Appendix 3- Creation of Latency Prone Viruses by Cindy Lam

Cell culture

HEK 293T cells were maintained in complete DMEM. Cells were propagated in T-75 culture flasks (Corning Inc., Tewksbury, Massachusetts, USA) at 37 °C in a 5% CO_2 incubator (Forma Series II Water Jacket CO_2 Incubator) (Thermo Scientific Inc., Burlington, Ontario, Canada).

Initial Plasmids

The viral vector encoding single-round HIV-1 (pNL4.3-Δenv-eGFP) was obtained through the NIH AIDS Reagent Program (Catalog #11100). The *Env* gene of this vector has been disrupted with an enhanced green fluorescent protein (eGFP) reporter gene and rendered non-functional. Our lab further manipulated this vector by inactivating the *Vif* gene via two stop codons introduced by site-directed mutagenesis (SDM), herein referred to as pNL4-3-Δenv-eGFPΔVif. VSVG envelope plasmid used to pseudotype single-round HIV-1 infections was obtained through Addgene (Cambridge, Massachusetts, USA). The human APOBEC2, APOBEC3G, and APOBEC3F expression plasmids have been described previously (Langlois *et al.,* 2009; Takeda *et al.,* 2008; Bélanger *et al.,* 2013).

Transfection and Infections

HEK 293T cells were used to produce the infectious VSVG-pseudotyped HIV-1 viral particles with packaged APOBEC3 proteins in co-transfections. 3.0 x 10^5 cells were seeded per well of a 6-well plate in 2 mL of complete DMEM and incubated for approximately 24 hours until they reached 80% confluency. Prior to transfection, the media was replaced with 3 mL of fresh complete DMEM. Co-transfections were performed with 500ng of pNL4-3-Δenv-eGFPΔVif plasmid, 200ng of VSVG and 150ng of either APOBEC3G or APOBEC3F plasmid.

Expression vectors were mixed with GeneJuice transfection reagent (EMD Millipore Corp., Billerica, Massachusetts, USA) and used to transfect the HEK 293T producer cells according to the manufacturer's specifications. The cells were then incubated for 48 hours to allow for production of infectious virus and packaged APOBEC3 protein.

24 hours prior to infection, 3.0 x 10^5 HEK 293T cells were seeded per well of a 6 well plate in 2 mL of DMEM and incubated until they reached 50-60% confluency. Prior to infection, the media was replaced with 3 mL of fresh DMEM plus polybrene (Sigma-Aldrich Canada Co., Oakville, Ontario, Canada) at a final concentration of 8 μg/mL. 48 hours post-transfection, virus-containing supernatants from HEK 293T producer cells were collected and cleared by centrifugation at 2000rpm for 10 minutes in a Sorvall ST40R centrifuge (Thermo Scientific). The HEK 293T target cells were infected with equal volumes of the viral supernatants by spinoculation at 900g for 1 hour and then incubated at 37 °C. At 48 hours post-infection, infectivity was analyzed by monitoring expression of the integrated eGFP reporter gene by flow cytometry using the CyAN ADP9 flow cytometer (Beckman Coulter, Inc., Brea, California, USA).

PCR

In addition to flow cytometry analysis on the infected HEK 293T target cells, a portion of the cells was collected and lysed for genomic DNA (gDNA) extraction. The gDNA was extracted using the Wizard Genomic DNA Purification Kit (Promega Corp., Madison, Wisconsin, USA) according to manufacturer's specifications. Following gDNA extraction, a semi-nested polymerase chain reaction (PCR) was performed on the gDNA to specifically amplify both the 5' and 3' LTRs of the integrated proviruses. All PCR reactions were performed in a total

reaction volume of 50 µL with (final) 1U PrimeSTAR HS DNA polymerase (TaKaRa), 1X PrimeSTAR buffer (Mg^{2+}), 200 µM dNTPs, 200 nM of each forward and reverse primers, and 10 ng of gDNA template for the first round (2 µL of a 1:25 dilution of the 1st round PCR products for the second round). The primers used to specifically amplify the 5' LTR were HIV LTR FWD deg 2 and HIV LTR REV 1 for the first round, and HIV LTR FWD deg 2 (and HIV LTR REV 3 deg for the second round (Lam et al, Table A1). The primers used to specifically amplify the 3' LTR were HIV 3' LTR FWD 1 and HIV 3' LTR REV deg for the first round, and HIV 3' LTR FWD 2 deg and HIV 3' LTR REV deg for the second round (Lam et al, Table A1). The second round primers for both LTRs were designed to include restriction endonuclease sites (*AseI* and *NheI*) for downstream cloning applications. All primers were ordered from Sigma-Aldrich. The cycling conditions were as follows: an initial denaturation at 98 °C for 1 minute, followed by 32 cycles of denaturation at 98 °C for 10 seconds, annealing at 56 °C for 15 seconds (58 °C for 30 seconds for the second round), elongation at 72 °C for 1.5 minutes (1 minute for the second round), and a final elongation at 72 °C for 2 minutes. All PCRs were performed in an Eppendorf mastercycler Pro S series thermocycler.

Cloning

PCR products were resolved on 1% (w/v) agarose gels containing 1% ethidium bromide and visualized under UV light using the AlphaImager MINI Gel Imaging System (Alpha Innotech Corp., San Jose, California, USA) and accompanying software. The correct-sized bands (639 bp prior to digestion) were excised and gel purified using the Wizard SV Gel and PCR Clean-Up System (Promega) according to manufacturer's specifications. The purified PCR products were then digested with the enzymes *AseI* and *NheI* (New England Biolabs Ltd. (NEB), Whitby,

Ontario, Canada) for 6 hours at 37 °C, column purified, and phosphorylated with T4 polynucleotide kinase (NEB) according to manufacturer's specifications. The peGFP-C3 expression vector was digested with the same enzymes as the PCR insert and dephosphorylated using Antarctic phosphatase (NEB) according to manufacturer's specifications prior to gel purification. Using T4 DNA ligase (NEB) according to manufacturer's specifications, the digested and phosphorylated PCR inserts were ligated in the place of the Cytomegalovirus (CMV) promoter upstream of the eGFP reporter gene of the similarly digested and dephosphorylated peGFP-C3 vector at varying ligation ratios (commonly 1:1, 1:3, and 1:5 vector:insert ratios). The ligations were performed in a total reaction volume of 10 µL and incubated at 16 °C or 4 °C overnight. The next day, the ligation reactions were mixed with 100 µL of DH5α competent *E. coli* cells, incubated on ice for 30 minutes prior to heat-shocking in a 42 °C water bath for 1.5 minutes and incubated on ice for 3 minutes. 900 µL of Luria Bertani (LB)-only broth was added to each of the transformation tubes and grown for at least one hour with shaking at 37 °C. The transformations were lightly pelleted at 1000 RPM for 5 minutes in a Sorvall Legend Micro 17 microcentrifuge (Thermo Scientific), resuspended in the remaining broth after decanting, and plated onto LB-Agar plates supplemented with 30 mg/mL kanamycin (KAN) for selection and incubated overnight at 37 °C.

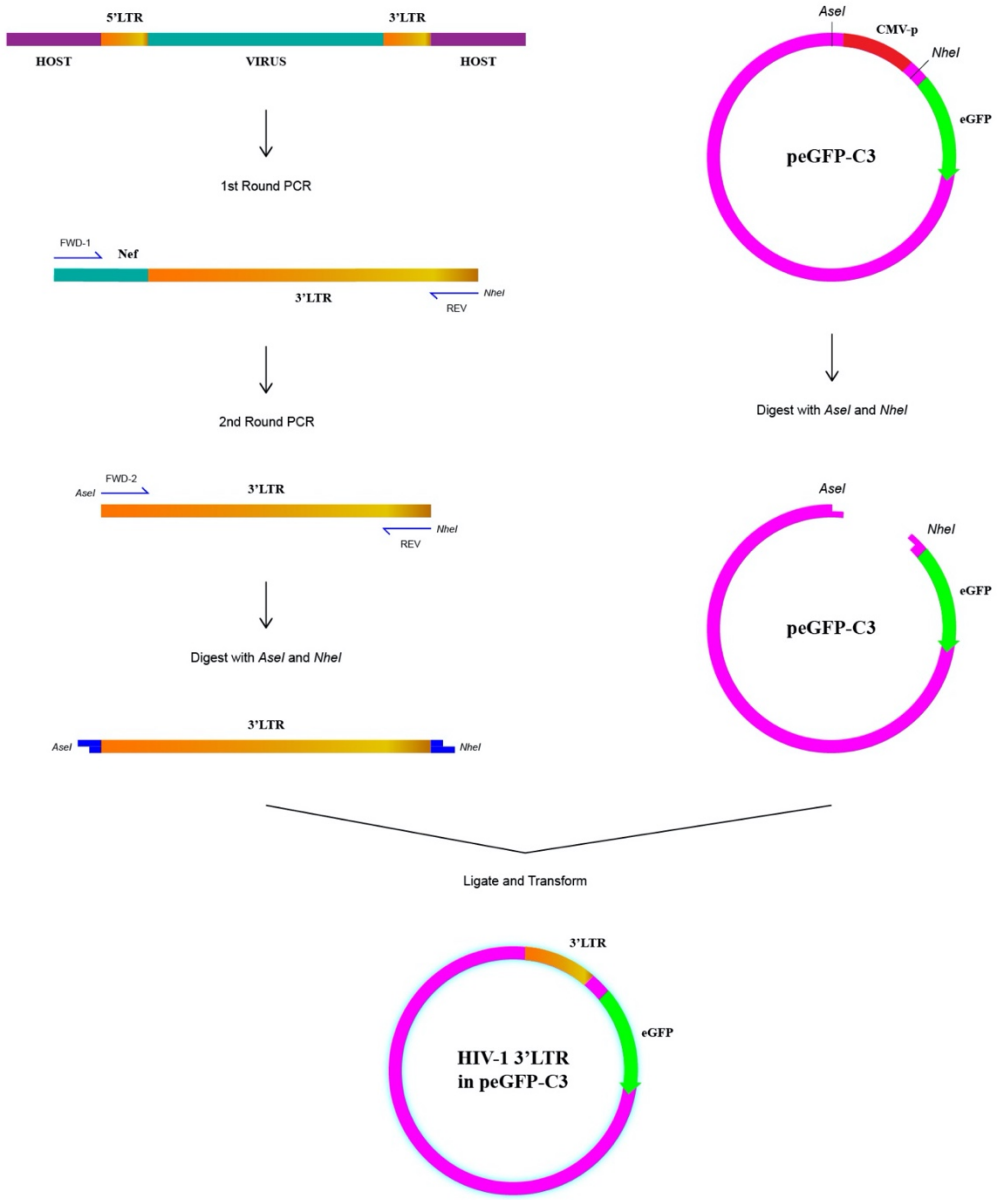

Figure 21 Initial Cloning Strategy for LTR-eGFP Reporter Constructs

High Resolution Melt (HRM)

Individual colonies from the transformations were diluted in 250 µL of sterile water in 96-well plates. 8 µL of each colony dilution was added to another 96-well plate containing (final) 1X MeltDoctor HRM Master Mix (AmpliTaq Gold 360 DNA Polymerase, MeltDoctor HRM Dye, dNTP blend, Mg^{2+}, buffer) (Applied Biosystems, Life Technologies Corp., Burlington, Ontario, Canada), 0.3 µM of each Seq peGFP-C3 LTR FWD and Seq peGFP-C3 LTR REV primers (Lam et al, Table A1), and topped up to 20 µL with sterile water. The reaction plate was briefly centrifuged at 2000 RPM for 2 minutes in a Sorvall centrifuge to bring all contents to the bottom of the plate. The cycling conditions for the real-time PCR (qPCR) reaction were as follows: an initial denaturation at 94 °C for 2 minutes, followed by 40 cycles of denaturation at 95 °C for 30 seconds, annealing at 55 °C for 45 seconds, and extension at 72 °C for 1 minute. Following the qPCR reaction, the samples underwent a melting curve analysis whereby each amplicon was heated up from 72 °C to 95 °C and fluorescence of the intercalated dye was measured in increments of 0.025 °C. The melting curves were aligned and samples that appeared to the left of the unmutated control curves were selected for Sanger sequencing to confirm G-to-A mutations. All HRM reactions were performed in a ViiA 7 real-time PCR system (Applied Biosystems).

Sequencing

The wells of the 96-well plate that contained the colony dilutions corresponding to the samples of interest from the HRM reaction were resuspended and each added to 1.5 mL of LB broth supplemented with kanamycin (minipreps). The minipreps were grown overnight for approximately 16-20 hours at 37 °C in a shaking incubator. The next day, the minipreps

were processed using the Wizard Plus SV Minipreps DNA Purification System (Promega) according to manufacturer's specifications. 8 µL of each purified prep was sent out to the Nanuq Sequencing Facility at McGill University and Genome Quebec Innovation Centre for Sanger sequencing along with 10 µL of the forward and reverse sequencing primers, Seq peGFP-C3 LTR FWD and Seq peGFP-C3 LTR REV, respectively at 5.0 µM (Table A1). Upon receiving the sequencing results back from the facility, the sequences were aligned using Sequencher 4.10.1 software (Gene Codes Corp., Ann Arbor, Minnesota, USA) and analyzed for G-to-A mutations in an APOBEC3 deamination context using the wildtype (wt) pNL4-3-Δenv-eGFPΔVif LTR (5' or 3' as applicable) sequence as a reference.

Functional Assays with LTR-eGFP Reporter Constructs

Uniquely-mutated clones as analyzed by sequencing were selected to generate a library of APOBEC3-mutated LTR-eGFP reporter constructs. HEK 293T cells were seeded at 1.0 x 10^5 cells per well of a 24-well plate in 0.5 mL of complete DMEM 24 hours prior to transfection until they reached approximately 80% confluency. Prior to transfection, the media was replaced with 1 mL of fresh DMEM. The cells were transfected with 100 ng of each clone alone as well as co-transfected with 100 ng of the Tat expression plasmid using GeneJuice transfection reagent according to manufacturer's specifications. 48 hours post-transfection, the cells were harvested and the functionality of the mutated promoters was assessed by measuring the expression and fluorescence intensity of the eGFP reporter gene using flow cytometry on a CyAN ADP9 flow cytometer.

HIV-1 Vector Backbone

A fragment of the viral vector pNL4-3-Δenv-eGFPΔVif was PCR amplified using (final) 2.5U Bestaq DNA polymerase (Applied Biological Materials Inc. (abm), Richmond, British Columbia, Canada), 1X PCR buffer (Mg^{2+}), 200 µM dNTP mix, 200 nM of each of the primers pNL4-3 XhoI 3' LTR FWD and pNL4-3 NaeI-SacII 3' LTR REV (Table A1), 20 ng of template, and topped up to 50 µL with sterile water. The reverse primer incorporated an additional restriction endonuclease site (*SacII*) and spacer within the viral sequence for downstream cloning. The PCR conditions were as follows: an initial denaturation at 94 °C for 3 minutes, followed by 30 cycles of denaturation at 94 °C for 10 seconds, annealing at 58 °C for 30 seconds, extension at 72 °C for 30 seconds, and a final extension at 72 °C for 5 minutes. The amplicon was then digested with the restriction enzymes *XhoI* and *NaeI* (NEB), phosphorylated, and ligated into another pNL4-3-Δenv-eGFPΔVif vector previously digested with the same restriction enzymes and dephosphorylated. The ligations were transformed on LB-Agar plates supplemented with 100 mg/mL ampicillin (AMP) and minipreps were grown in LB+AMP broth and processed as previously described. This intermediate vector was further digested with the restriction enzymes *SacII* and *NaeI* (NEB) and dephosphorylated in order to create the HIV-1 vector backbone in which the heavily mutated LTRs from the eGFP reporter library would be reconstituted. This HIV-1 vector backbone was sent for Sanger sequencing to confirm successful ligation of the intermediate fragment using the primer Seq HIV int-mut 3' LTR FWD.

Heavily Mutated LTR Inserts

The heavily mutated LTRs from the LTR-eGFP reporter library were PCR amplified using the same PCR reagents and conditions as above with the exception of the primers used (peGFP-C3 SacII 3' LTR FWD deg and peGFP-C3 NaeI 3' LTR REV deg (Lam et al, Table A1)) and the extension time during cycles (45 seconds). The amplicons were then digested with the restriction enzymes *SacII* and *NaeI*, phosphorylated, and ligated into the HIV-1 vector backbone generated previously. The clonings were processed as described previously and successful reconstitution was confirmed through Sanger sequencing with the primers Seq HIV mut 3' LTR FWD and Seq HIV mut 3' LTR REV (Lam et al, Table A1) using each heavily mutated LTR from the eGFP reporter constructs as references for the reconstituted clones.

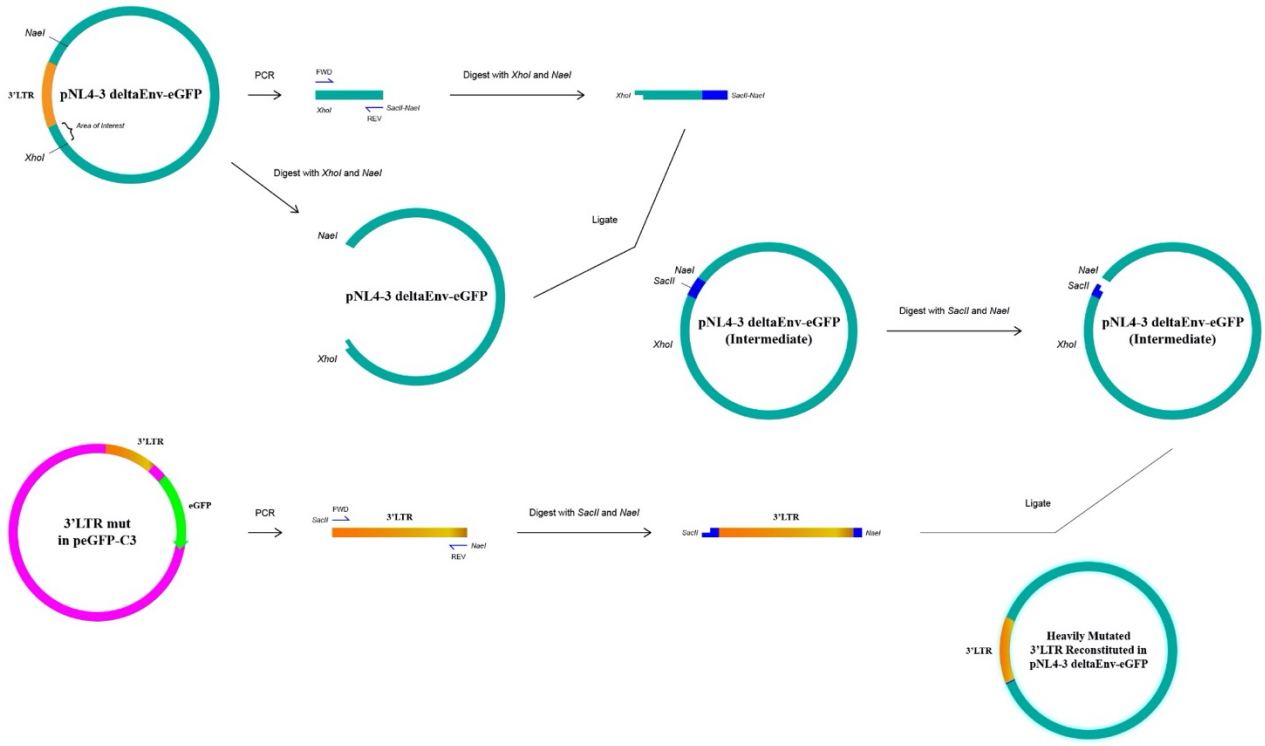

Figure 22 Cloning Strategy for Reconstituted Latency Prone Viral Plasmids and Heavily Mutated Clones.

Appendix 4- Propagation of Antibodies for p24 ELISA

Hybridoma cells were thawed and centrifuged at 300g for 5 min to remove freezing medium. Cells were resuspended in 10mL complete RPMI and cultured in T75 flask (Sigma-Aldrich #CLS430641, Oakville, ON, Canada). When confluent, cells were centrifuged at 300g for 5 min in a 50mL tube, washed with 1X PBS+5mM EDTA, resuspended in 20mL complete RPMI media and placed in T175 flask (Sigma-Aldrich #CLS431080, Oakville, ON, Canada). This expansion was repeated every 2 days until 8 T175 confluent flasks were obtained.

Once enough flasks were obtained, cells were collected, centrifuged at 300g for 5 min, and washed with 1X PBS+ 5mM EDTA. Cells were then resuspended in 37^{o}C warmed CD Hybridoma Media (Thermo Fisher #11279023, Waltham, MA, USA) supplemented with100U/mL penicillin and 100ug/mL streptomycin (P/S) and 8mM L-glutamine. Cells were placed in T175 flasks containing 50mL of complete media each. Once confluent, another 50mL of warmed complete hybridoma media was added to each flask before flasks were allowed to grow out for 2 weeks.

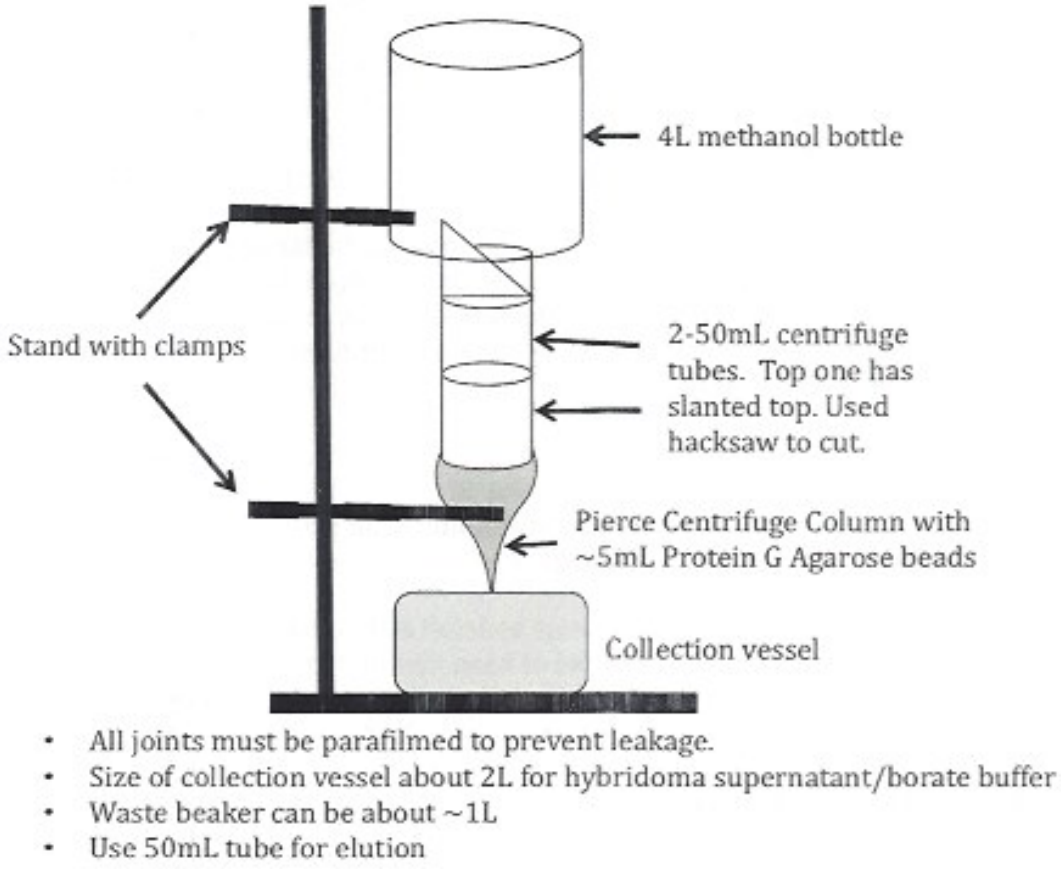

Figure 23 Column Setup for Antibody Purification

After 2 weeks cells and supernatant was collected and centrifuged in 50mL tubes at 3500rpm for 1-2 hours at 4°C. While cellular debris was pelleting from supernatant, column was prepared as seen in Figure X with 5mL of Protein G Agarose Beads (Exalpha #X1198, Shirley, MA, USA). The 50% slurry of beads was transferred to a centrifuge column and then centrifuged at 500g for 5 min to collect beads before the solution was pipetted out and replaced with borate buffer (38.1g sodium borate decahydrate in 2L of Mili-Q water, brought to pH 8 with 36g of boric acid). Post spin supernatant was extracted, 0.2um filtered and combined with borate buffer to a ratio of 1L hybridoma supernatant : 2L borate buffer. Once supernatant + borate solution was ready, the bottom of the centrifuge column containing

the agarose beads and borate buffer was broken, and borate buffer was allowed to flow out into a waste beaker. 100mL of borate buffer was then added and allowed to flow through. After borate buffer finished flowing, the waste beaker was replaced with a 2L collection beaker, and all supernatant + borate solution was allowed to flow through the column, followed by 100mL of borate buffer to wash column (the last 100mL of borate buffer can go into the waste beaker). When only 1mL of buffer remained in the column, a 50mL tube containing 3mL of Neutralization buffer (242.28g of Tris base in 1L sterile Mili-Q water, pH 9.5) was placed underneath column. 12mL of Elution buffer (8.92g citric acid, 1.04g sodium citrate dehydrate, 1L sterile Mili-Q water, pH 2.6) was placed into the top of the column and allowed to flow through the column and into the neutralization tube, followed by an additional 12mL of elution buffer. Neutralization tube was removed after flow through was complete, inverted gently to mix, and kept at 4^{o}C as 'Elution #1'. 50mL of borate buffer was then run through into the waste beaker to wash the column. When borate wash was near completion (<2mL remaining), the collected hybridoma + borate mixture once again was added to the column. The collection of the hybridoma+borate mixture, elution and wash steps was repeated 3-4 more times. To check yields of the antibody in neutralized elution mixtures, a nanodrop was used with a blanking on a solution of 1mL neutralization buffer to 5mL elution buffer.

Once the entire elution buffer containing antibody had been collected, samples were concentrated using a 30KDa centrifugal columns (Millipore-Sigma #UFC903008, Burlington, MA, USA). Centrifugation occurred at 3500rpm for 5 minutes until all liquid had been added to a column, followed by a resuspension in 1mL of 1X PBS per concentrating tube. All tubes

containing the same antibody were then combined, with 1X PBS added until a concentration of 1ug/mL was achieved. Aliquots of 1mL were created in 1.7mL eppendorf tubes and kept at -20^{o}C for long-term storage or 4^{o}C for short-term storage between ELISAs.

The biotinylation of p24 antibody 31-90-25 was achieved by using the EZ-Link Sulfo-NHS-LC-Biotin Kit (Thermo Scientific, #21335, Waltham, MA, USA). A 20 fold molar excess of biotin to IgG was used according to kit instructions. After an 2 hour incubation on ice, solution was reconcentrated using the same centrifugal column as above to clear unreacted biotin from solution. Btn-IgG was resuspended once again in 1X PBS, nanodropped and kept at 4^{o}C for ELISA use.

Appendix 5 – Statistical Analysis of Number of LPV Mutations vs Baseline Transfection and Infection Values

Transfections were quantified by both a p24 in house ELISA on the resulting transfection supernatants as well as through the expression of eGFP within transfected cells detected through flow cytometry acquisition. These values for each LPV were then normalized by setting the wild-type pNL4 value to 100. To determine if there was a correlation between the normalized transfection results and the quantity of LTR mutations that each LPV contained, a linear and exponential correlation was performed on GraphPad Prism (Version 6.0b). A linear and exponential line of best fit was performed between the number of mutations and either the normalized ELISA or flow cytometry-acquired values (Figure 24). All R2 values for both the linear and exponential lines of best fit were under 0.2, and therefore it was determined that there was no correlation between the number of LTR mutations that each LPV contained and their relative viral output post transfection.

Next, both a linear and exponential line of best fit was performed between the number of mutations within each LPV and the mean number of cells expressing eGFP post-infection (without LRA stimulation) (Figure 25). This was performed for both HEK 293T and Jurkat cell infection data using Graphpad Prism (Version 6.0b). It was determined that within the subset of LPVs that were tested, there was a much stronger exponential correlation between mutation count and baseline infectivity as compared to a linear correlation. This was true in both HEK 293T cells (R^2 of 0.7614 compared to 0.4192) and Jurkat cells (R^2 of 0.7609 compared to 0.3606).

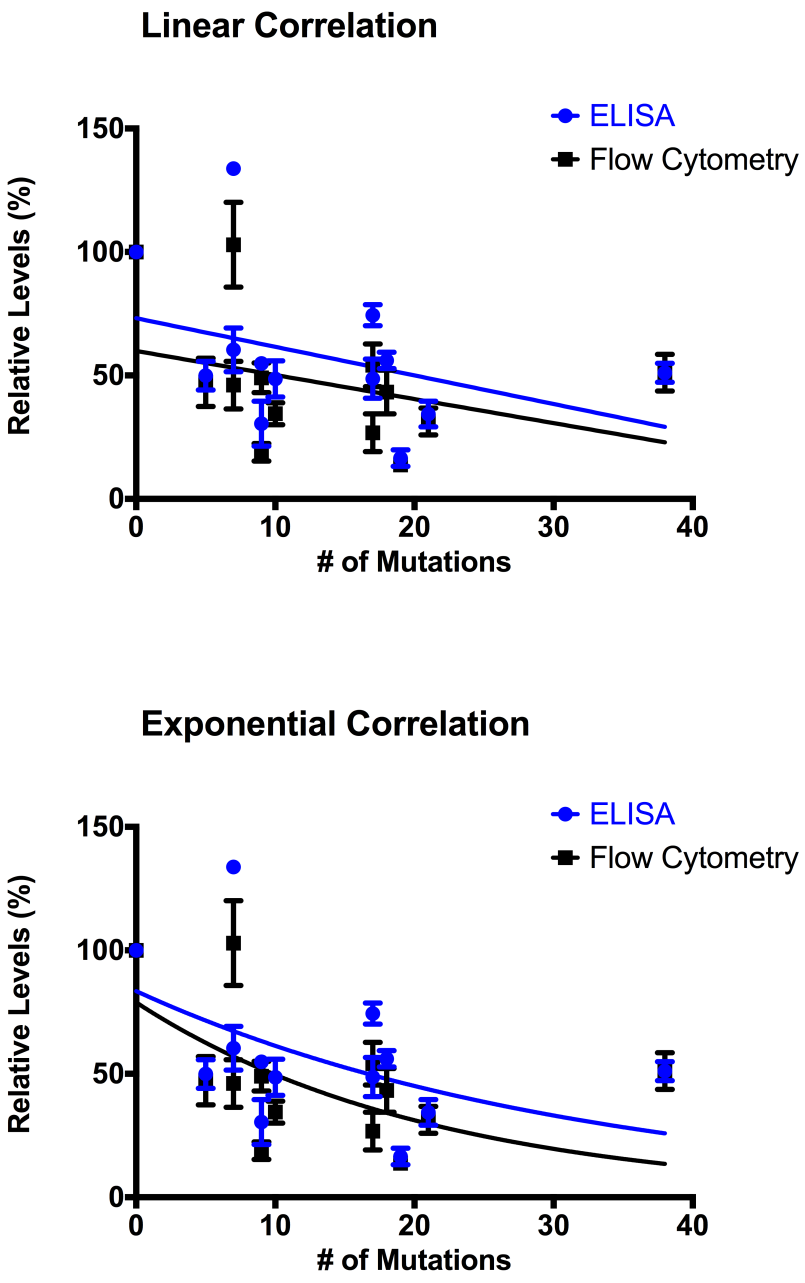

Figure 24 Number of LPV Mutations vs Normalized Transfection Values Correlational Analysis. *The number of mutations within each LPV was confirmed by Sanger Sequencing and aligned from least mutations to most mutations. The number of cells expressing eGFP post-transfection was determined by flow cytometry acquisition while the estimated p24 quantifications were provided my an in house ELISA and standard p24 curve. Both were normalized to wild-type pNL4=100. Linear and exponential growth correlations were separately performed between the number of LPV mutations and either the normalize transfection ELISA values or the normalized p24 supernatant values. The linear correlation provided an R^2 value of 0.1301 for the ELISA quantification vs mutation count and 0.1048 for the transfection quantification vs mutation count. The exponential growth correlation provided an R^2 value of 0.1749 for the ELISA quantification vs mutation count and 0.1946 for the transfection quantification vs mutations count.*

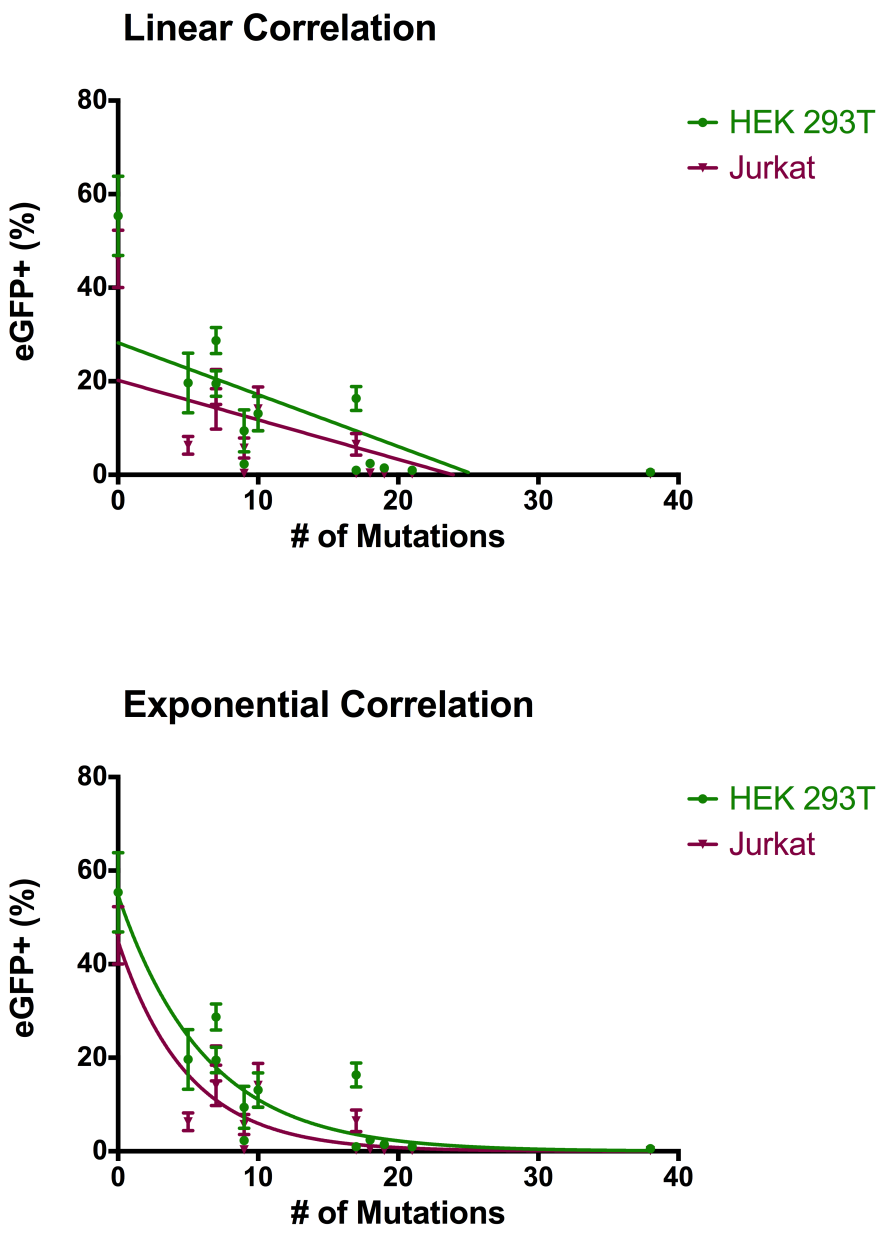

Figure 25 Number of LPV Mutations vs Baseline Infectivity Correlational Analysis. *The number of mutations within each LPV was confirmed by Sanger Sequencing and aligned from least mutations to most mutations. The number of cells expressing eGFP was determined by flow cytometry acquisition. A linear correlation was determined for each cell type by creating a linear line of best fit between all points. HEK 293T R^2 = 0.4192 and Jurkat R^2 =0.3606. An exponential line of correlation was determined for each cell type by creating a growth exponential curve between all points. HEK 293T R^2 = 0.7164 and Jurkat R^2 = 0.7609.*

CV

Matthew Greig

EDUCATION

September 2018-Current	**MSc in Biochemistry Microbiology and Immunology** University of Ottawa, Ottawa, ON • CGPA 10.0/10
September 2013 – April 2018	**Honours Bachelor of Science in Biomedical Science** University of Ottawa, Ottawa, ON • CGPA (5 years): 8.76/10
September 2009 - June 2013	**Ontario Secondary School Diploma** Sacred Heart Catholic High School

SCHOLARSHIPS, AWARDS AND BURSARIES

May 8, 2019	• Mark Wainberg Fund Travel Award o $2500 for travel to CAHR 2019 Conference
May 2, 2019	• BMI Graduate Departmental Poster Day o 3rd place Award for Masters Poster Presentation
Sept 2018-August 2020	• University of Ottawa Graduate Admissions Scholarship o $7500 received per year for total of $15000
Sept 2013-June 2018	• University of Ottawa Undergraduate Admission Scholarship o $3000 received for 1st, 3rd, and 4th years for a total of $9000

HONOURS AND AWARDS

Dean's Honour List

- 2013-2014
- 2015-2016
- 2016-2017

RESEARCH EXPERIENCE

September 2018-Current

MSc Candidate

Dr. Marc-Andre Langlois Lab, University of Ottawa, Department of Biochemistry, Microbiology and Immunology

- MSc Project: Characterization of HIV-1 Proviral Latency Induced through APOBEC3 Mutagenesis and Reverse Transcriptase Error
- Advanced my current research project on HIV latency induced through APOBEC3 mutagenesis.

- Aided in the research and development of serological immunoassays used for SARS-CoV-2 antibody detection within Ottawa
- Laboratory techniques used included viral transfections and infections, tissue culture work, western blotting, PCR, qPCR, ELISAs, cellular staining and flow cytometry
- Attended seminars and University symposiums to broaden my scientific knowledge
- Attended and presented research at the 2019 Canadian Conference of HIV/AIDS Research (CAHR). Attended a New Researchers Workshop at CAHR to develop skills in presentations, scholarship applications, and professionalism.
- Completed one Masters level course on Infectious diseases and Immunology followed by one PhD level course on Advanced Virology. Finished both classes with an A+ grade

July 2019 – June 2020

Hepatitis Clinic Research Data Entry

Dr Curtis Cooper, The Ottawa Hospital/Ottawa Hospital Research Institute

- Part-time work as a data entry assistant at The Ottawa Hospital viral hepatitis clinic
- Inputting patient data, bloodwork, and medications into clinical research databases
- Learned how to handle treatment plans, patient confidentiality and consent

May 2018- July 2018

Laboratory Summer Research Student

Dr. Marc-Andre Langlois Lab, University of Ottawa, Department of Biochemistry, Microbiology and Immunology

- Continued to advance my work on HIV latency induced through APOBEC3 mutagenesis. Experiments included viral transfections, CD4+ T cell isolations, CD4+ T cell infections and molecular cloning.
- Spent two months training a future honours project student in the lab. Training included techniques such as Westerns, PCR and qPCR, viral transfections and infections, and flow cytometry.

September 2017- April 2018

Honours Research Project

Dr. Marc-Andre Langlois Lab, University of Ottawa, Department of Biochemistry, Microbiology and Immunology

- 8 month research project involving the activation of HIV latency prone viruses by various latency reversing agents
- Planned and conducted experiments from start to finish, employing a variety of laboratory techniques such as tissue

culture, creation of virus by transfection, infection of cells, western blotting, gDNA extractions, sandwich ELISA analysis, examination of cells under flow cytometry, PCR and qPCR.

- Began work in cell lines before moving into T cells which employed the use of the following additional techniques: Ficoll-Paque extraction of peripheral blood mononuclear cells (PBMCs) and CD4+ T cell extraction, activation and infection.
- With only 1 class requirement, was able to work full time and experience the work level of a masters student (approximately 45 hours per week)
- Developed necessary skills in time management and experimental scheduling
- Gained valuable research experience working individually with minimal necessary supervision
- Will culminate in an honours thesis and poster (April 2018)

Laboratory Summer Research Student

May 2017 – August 2017

Dr. Marc-Andre Langlois Lab, University of Ottawa, Department of Biochemistry, Microbiology and Immunology

- Completed a 4 month summer student work term
- Worked to identify the integration sites of murine retroviruses in the genomes of bovine samples
- Planned and executed experiments that developed skills in tissue culture, viral transfection and infection, gDNA extractions, cell staining and flow cytometry, PCR on plasmids and extracted gDNA, western blotting, PAGE, bacterial transformations, and site directed mutagenesis of plasmids

September 2013 – April 2017

Relevant Laboratory + Class Experiences and Knowledge

University of Ottawa

- 3rd year Molecular Biology Laboratory which developed skills in restriction site mapping, western blotting, SDS-PAGE and PCR
- 4th year Immunology class that taught various fundamentals of immunology such as antigen recognition and response, leukocyte development and differentiation, and principles of self-tolerance.
- 4th year Bacteriology class that covered relevant topics including biofilms, host defense mechanisms against bacterial infections, and antibiotic resistance.
- 4th year Virology class that focused on the genetic classification of viruses, viral entry patterns, and the transcriptional and translational differences between various viral categories.

Medical Volunteer Experience

September 2019-December 2019	**Physiotherapy Clinic Shadowing** Sports Medicine Centre, Ottawa • 4 hours per week • Shadowing physiotherapists to learn how to best interact with patients, diagnose injuries and schedule treatment plans

PUBLICATIONS AND PRESENTATIONS

PUBLICATIONS: N/A

ORAL PRESENTATIONS:

Greig M, McBane J, Langlois MA. **Characterization of HIV-1 Proviral Latency Induced by APOBEC3 and Reverse Transcriptase Mutagenesis**

Presented at

- Canadian Association for HIV/AIDS Research (CAHR) 2019 Conference. May 8-12 2019. Saskatoon, Saskatchewan

POSTERS:

Greig M, McBane J, Langlois MA. **Characterization of HIV-1 Proviral Latency Induced by APOBEC3 Mutagenesis, 2018, Ottawa, ON.**

Presented at

- University of Ottawa 2018 Department of Biology Undergraduate Honours Poster Day
- University of Ottawa 2018 BMI Department Symposium
- University of Ottawa 2018 Flow Cytometry Symposium

Greig M, McBane J, Renner T, Langlois MA. **Characterization of HIV-1 Proviral Latency Induced by Reverse Transcriptase Error and APOBEC3 Mutagenesis**, 2019, Ottawa, ON.

Presented at

- University of Ottawa 2019 BMI Departmental Poster Day
    - Awarded 3rd place in poster competition as judged by departmental professors.

SKILLS AND TRAINING

Teamwork skills	• Experience working under senior lab members, alongside other lab members, as well as independently. • Coordinate experiments with other lab members in order to obtain the most efficient data acquisition for an experiment.
Communication	• Experience presenting research within groups to graduate students and university researchers. • Experience creating presentations for graduate level courses

	• Experience putting together short progress updates for lab meetings. • Experience training multiple undergraduate lab members and new trainees in important laboratory techniques • Experience effectively working remotely from other members of the team
Organizational skills	• Maintain an up-to-date, detailed lab book and keep experiment data files organized. • Able to efficiently plan experiments in order to obtain the most results possible without delay. • Able to coordinate simultaneous experimental timelines
Laboratory training	• University of Ottawa Lab Safety, Workplace Hazardous Material Information System (WHMIS) – for laboratory workers and Principles of Biosafety workshops.
Computer	• Proficient with Microsoft Office, Excel, Prism, FlowJo, BD FACSDiva

Permission to Use Figures

SPRINGER NATURE LICENSE
TERMS AND CONDITIONS

Jun 18, 2020

This Agreement between 451 Smyth Rd ("You") and Springer Nature ("Springer Nature") consists of your license details and the terms and conditions provided by Springer Nature and Copyright Clearance Center.

License Number	4852020104065
License date	Jun 18, 2020
Licensed Content Publisher	Springer Nature
Licensed Content Publication	Journal of NeuroVirology
Licensed Content Title	HIV-1 transcriptional regulation in the central nervous system and implications for HIV cure research
Licensed Content Author	Melissa J. Churchill et al
Licensed Content Date	Jul 25, 2014
Type of Use	Thesis/Dissertation
Requestor type	academic/university or research institute
Format	electronic
Portion	figures/tables/illustrations

Number of figures/tables/illustrations	1
Will you be translating?	no
Circulation/distribution	1 - 29
Author of this Springer Nature content	no
Title	Characterization of HIV-1 Proviral Latency Induced Through APOBEC3 Mutagenesis and Reverse Transcriptase Error
Institution name	University of Ottawa
Expected presentation date	Aug 2020
Portions	Figure 1: Structure of the HIV-1 LTR
Requestor Location	451 Smyth Rd 451 Smyth Rd Ottawa, ON K1H 8L1 Canada Attn: 451 Smyth Rd
Total	0.00 CAD
Terms and Conditions	

ELSEVIER LICENSE
TERMS AND CONDITIONS

Jul 03, 2020

This Agreement between 451 Smyth Rd ("You") and Elsevier ("Elsevier") consists of your license details and the terms and conditions provided by Elsevier and Copyright Clearance Center.

License Number 4852020733621

License date Jun 18, 2020

Licensed Content PublisherElsevier

Licensed Content Publication. Canadian Journal of Cardiology

Licensed Content Title Lipid Abnormalities in Persons Living with HIV Infection

Licensed Content Author David D. Waters,Priscilla Y. Hsue

Licensed Content Date Mar 1, 2019

Licensed Content Volume 35

Licensed Content Issue 3

Licensed Content Pages 11

Start Page	249
End Page	259
Type of Use	reuse in a thesis/dissertation Portion
Number of figures/tables/illustrations	1
Format	electronic
Elsevier article?	
Will you be translating?	No
Title	Characterization of HIV-1 Proviral Latency Induced Through APOBEC3 Mutagenesis and Reverse Transcriptase Error
Institution name	University of Ottawa
Expected presentation date	Aug 2020
Portions	Figure 1: Targets of antiretroviral therapy
	451 Smyth Rd 451 Smyth Rd

Requestor Location. 451 Smyth Rd, Ottawa ON, K1H 8L1 Canada

Publisher Tax ID	GB 494 6272 12
Total	0.00 USD

Terms and Conditions

ELSEVIER LICENSE
TERMS AND CONDITIONS

Jul 03, 2020

This Agreement between 451 Smyth Rd ("You") and Elsevier ("Elsevier") consists of your license details and the terms and conditions provided by Elsevier and Copyright Clearance Center.

License Number	4852030054327
License date	Jun 18, 2020
Licensed Content Publisher	Elsevier
Licensed Content Publication	Cell Host & Microbe
Licensed Content Title	Getting the “Kill” into “Shock and Kill”: Stra Latent HIV
Licensed Content Author	Youry Kim,Jenny L. Anderson,Sharon R. Lewin
Licensed Content Date	Jan 10, 2018
Licensed Content Volume	23
Licensed Content Issue	1
Licensed Content Pages	13

Start Page	14
End Page	26
Type of Use	reuse in a thesis/dissertation
Portion	figures/tables/illustrations
Number of figures/tables/illustrations	1
Format	electronic
Elsevier article?	
Will you be translating?	No
Title	Characterization of HIV-1 Proviral Latency APOBEC3 Mutagenesis and Reverse Transc
Institution name	University of Ottawa
Expected presentation date	Aug 2020
Portions	Figure 2 Classes of LRAs

	451 Smyth Rd 451 Smyth Rd
Requestor Location	
	Ottawa, ON K1H 8L1 Canada Attn: 451 Smyth Rd
Publisher Tax ID	GB 494 6272 12
Total	0.00 USD

ELSEVIER LICENSE
TERMS AND CONDITIONS

Jul 03, 2020

This Agreement between 451 Smyth Rd ("You") and Elsevier ("Elsevier") consists of your license details and the terms and conditions provided by Elsevier and Copyright Clearance Center.

License Number 4852030976593

License date Jun 18, 2020

Licensed Content Publisher. Elsevier

Licensed Content Publication. Virology

Licensed Content Title APOBECs and virus restriction

Licensed Content Author Reuben S. Harris, Jaquelin P. Dudley

Licensed Content Date May 1, 2015

Licensed Content Volume 479

Licensed Content Issue n/a

Licensed Content Pages	15
Start Page	131
End Page	145
Type of Use	reuse in a thesis/dissertation
Portion	figures/tables/illustrations
Number of figures/tables/illustrations	1
Format	electronic
Elsevier article?	
Will you be translating?	No
Title	Characterization of HIV-1 Proviral Latency APOBEC3 Mutagenesis and Reverse Transc
Institution name	University of Ottawa
Expected presentation date	Aug 2020
Portions	Figure 2 Model of HIV-1 Restriction

	451 Smyth Rd 451 Smyth Rd
Requestor Location	
	Ottawa, ON K1H 8L1 Canada Attn: 451 Smyth Rd
Publisher Tax ID	GB 494 6272 12
Total	0.00 USD